Study of Heavy Minerals from the Beach Sands of Keri (Querim), Goa, West Coast of India

A Dissertation for

Course code and Course Title: MSC 617 Discipline Specific Dissertation

Credits: 16

Submitted in partial fulfilment of Master's Degree

M.Sc. in Marine Sciences

by

LAKSHMI RAMESH VAIDYA

Seat Number: 22P0400013

ABC ID: 351-423-133-035

PRN: 202200075

Under the Supervision of

Ms. MANJUSHA MADKAIKAR

School of Earth, Ocean and Atmospheric Sciences

Marine Sciences

GOA UNIVERSITY

APRIL 2024

Examined by:

Seal of the School

To My Parents

DECLARATION BY STUDENT

I hereby declare that the data presented in this Dissertation report entitled, "Study of Heavy Minerals from the Beach Sands of Keri (Querim), West Coast of India" is based on the results of investigations carried out by me in the discipline of Marine Sciences at the School of Earth, Ocean, and Atmospheric Sciences, Goa University under the Supervision of Ms. Manjusha Madkaikar and the same has not been submitted elsewhere for the award of a degree or diploma by me. Further, I understand that Goa University or its authorities will not be responsible for the correctness of observations / experimental or other findings given in the dissertation. I hereby authorize the University authorities to upload this dissertation on the dissertation repository or anywhere else as the UGC regulations demand and make it available to any one as needed.

Lvaidya

Lakshmi Ramesh Vaidya

Seat Number: 22P0400013

Date: 26/04/2024

Place: Goa University, Taleigao, Goa-403206

COMPLETION CERTIFICATE

This is to certify that the dissertation report **"Study of Heavy Minerals from the Beach Sands of Keri (Querim), West Coast of India"** is a bonafide work carried out by **Ms. Lakshmi Ramesh Vaidya** under my supervision in partial fulfilment of the requirements for the award of the degree of **Master of Science** in the Discipline of Marine Sciences at the School of Earth, Ocean, and Atmospheric Sciences, Goa University.

26/04/24

Ms. Manjusha Madkaikar

Assistant Professor

Dept. of Marine Sciences

Goa University

Goa- 403206

Date:

SEOAS, GOA UNIVERSITY
TALEIGAO PLATEAU GOA

School Stamp

29/4/24.

Sr. Prof. Sanjeev C. Ghadi

Senior Professor and Dean

Marine Sciences

School of Earth, Ocean and Atmospheric Sciences

Date:

Place: Goa University, Taleigao, Goa-403206

PREFACE

The topic of heavy minerals has been an intriguing one because of the scientific importance it holds in investigating their source, transportation history and the post-depositional aftermath. It unfolds the mystery of the formation and dynamics of the earth's surface by indicating the type of rocks present in the hinterland, how they formed, the type and rate of weathering they are undergoing and the path of the river that has carried and deposited them along the beach.

Not only are they scientifically important but also hold a great deal of economic importance due to their industrial demand thereby promoting a country's economic growth. This makes it highly necessary to explore these resources gifted by the mother nature.

Since there have been scanty studies conducted for heavy minerals along the state of Goa, the topic attracted my attention and motivated me to conduct my research on the same.

ACKNOWLEDGEMENT

I am highly indebted to Ms. Manjusha Madkaikar, Assistant Professor, Department of Marine Sciences, School of Earth, Ocean, and Atmospheric Sciences, Goa University, Goa for her guidance and valuable suggestions for the successful completion of the dissertation. I am grateful to the Dean, Sr. Prof. S. C. Ghadi, the Former Dean, Dr. C. U. Rivonker and the Programme Director, Dr. M. R. Nasnodkar, Department of Marine Sciences, School of Earth, Ocean, and Atmospheric Sciences, Goa University, Goa for providing me with the opportunity and facility of working on this research topic.

I would like to thank my friend, Chetan Puntambekar for accompanying me on the fieldwork and helping me during the various stages of the dissertation. I am also thankful to the laboratory assistants for their help with the instruments and equipment during the laboratory work.

Special thanks to the Chemistry Department, School of Chemical Sciences, Goa University, Goa for analysing my samples in the X-Ray Diffractometer Laboratory and providing the data of the same.

Last but not least, I would like to take this opportunity to express my gratitude and love to my parents for their constant moral support and encouragement.

Lakshmi Vaidya

CONTENTS

TABLES

FIGURES

ABBREVIATIONS USED

Entity	Abbreviation
Backshore	BS
Banded Hematite Quartzite	BHQ
Banded Magnetite Quartzite	BMQ
Foreshore	FS
Fraction 1	F1
Fraction 2	F2
Fraction 3	F3
Geological Survey of India	GSI
Heavy Minerals	HM
Indian Meteorological Department	IMD
Magnetic Heavy Minerals	MHM
Non-magnetic Heavy Minerals	NHM
Poly Vinyl Chloride	PVC
Total Heavy Minerals	THM
Total Light Minerals	TLM
X-Ray Diffraction	XRD

ABSTRACT

The study was conducted to investigate the distribution and provenance of heavy minerals along the 2 km long Keri Beach located in North Goa, India. The heavy mineral concentration ranges from 6.20% to 46.20%. The concentration was higher in the backshore samples than in the foreshore samples. It was also observed that the ratio of heavy to light minerals increased with a decrease in grain size. X-ray diffraction studies revealed the presence of actinolite, ilmenite, hematite, magnetite, and pyrite. The non-magnetic minerals were identified under a stereo-zoom microscope. The non-magnetic suite consists of apatite, epidote, garnet, rutile, sillimanite, staurolite, tourmaline, and zircon. The presence of fresh and altered minerals indicates the reworking of the sediments. The literature survey suggests that the minerals have a heterogeneous origin. The minerals have been transported to the beach via the Terekhol River as well as the northward longshore current flowing locally in the area. The presence of high concentrations of the heavies makes the location a promising area for sustainable exploitation in future.

Keywords: Heavy minerals; Goa; Provenance; X-Ray Diffraction; Beach placers

INTRODUCTION

CHAPTER-1: INTRODUCTION

1.1 BACKGROUND

As we all know, a mineral is a naturally occurring, inorganic, homogenous solid substance, with a definite chemical composition and possessing an ordered unit atomic structure. Heavy minerals are those which have a specific gravity of 2.89 or higher **(Morton,1978)**. The specific gravity of minerals is determined by their density, which is influenced by the atoms that make up the mineral as well as their packing and atomic structure. A closely packed lattice results in higher density, while a loosely packed one leads to lower density. An example of this is Diamond and graphite. Both are made up of carbon atoms. But diamond shows a tight packing whereas graphite is loosely packed in hexagonal close packing forming sheets (Figure 1.1). As a result, graphite is very soft and is used as a lubricant and diamond, on the other hand, is the hardest mineral on earth with a hardness of 10 on Moh's Scale of Hardness and is used as an abrasive. Metallic minerals, such as magnetite, are heavier than non-metallic ones, such as quartz, since metal atoms have a higher atomic mass than non-metallic atoms. However, orthoclase containing a metal (potassium) is still considered a light mineral because potassium is an alkali metal, lighter than other transition metals. Heavy minerals are comparatively smaller than light minerals owing to their closer packing.

Some common heavy minerals include rutile, ilmenite, zircon, garnet, and magnetite. These minerals are formed along with other minerals during the processes of rock formation. Weathering of the rocks leads to their liberation and then are transported through various media such as water and glaciers, eventually causing their

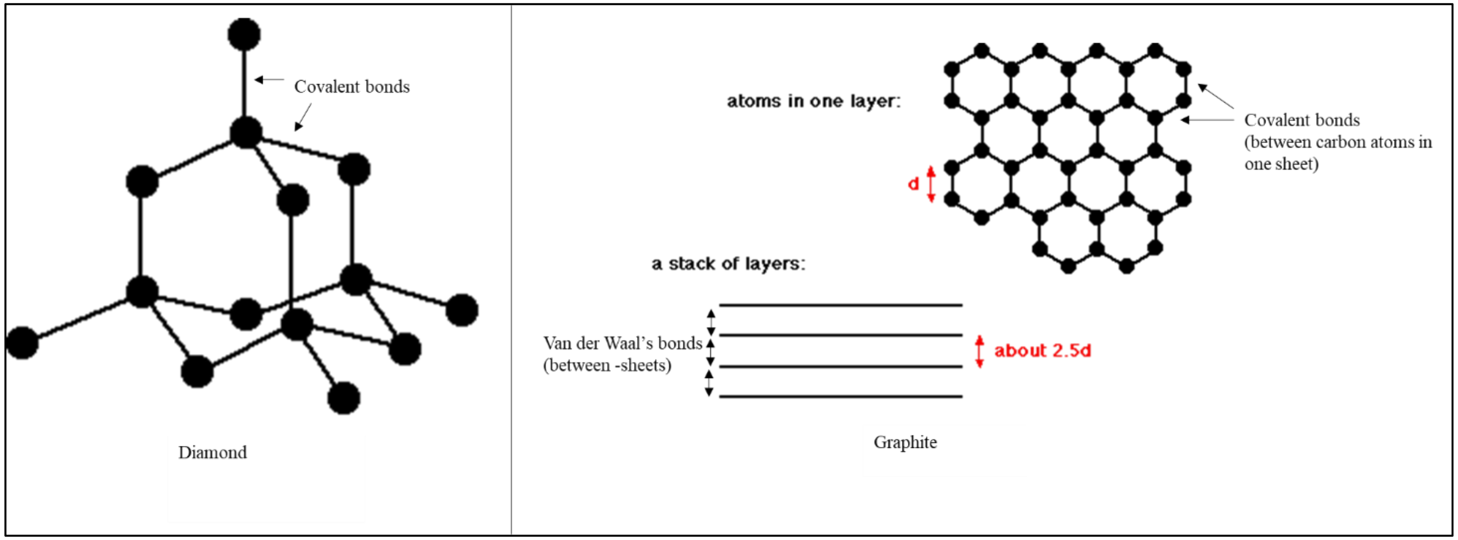

Figure 1.1 Structure of Diamond and Graphite **(obtained from the website:**

https://chem.libretexts.org/Bookshelves/Inorganic_Chemistry/Map:_Inorganic_Chemistry_(Housecroft)/14:_The_Group_14_Elements/14.04:_Allotropes_of_Carbon/14.4A:_Graphite_and_Diamond_-_Structure_and_Properties)

deposition in a basin such as a beach. They are present in all types of rocks. Table 1.1 shows examples of a few rock types and some of the common heavies associated with them. **Emery and Noakes (1968)**, classified heavy minerals into 3 types, namely, heavy-heavy minerals (sp. gr. 6.8-21) such as gold and platinum, light-heavy minerals (sp. gr. 4.2-5.3) such as magnetite, ilmenite, rutile, and zircon, and gemstones (sp. gr. 2.9-4.1) such as diamond and ruby.

These minerals are more stable as compared to lighter ones and therefore undergo lesser alteration and survive longer transportation. These minerals have a scientific significance. Since they tend to occur in specific types of rocks, this property helps determine their origin, transportational history, and depositional environments.

A tropical climate is ideal for setting heavy minerals free from the rocks as it accelerates the process of weathering by several mechanisms. Once they are removed from the rocks, they are incorporated into a medium of transportation which carries them from the hinterland to the depositional basin. In the tropics, rivers and streams are the most effective agents of transportation for heavy minerals and sediments in general. In fact, heavy minerals are a part of the sediments. Geologically speaking, sediments are loose, broken-down rock material of varying sizes. **Wentworth (1922)** classified rock materials into various categories based on their size, ranging from boulders (> 256 mm) to clay (<0.004 mm). However, on their journey to the sink through the rivers or even in the depositional basin, other materials like organic matter may also get incorporated into them. Organic matter can be in the form of living organisms such as microbes, dead and decayed remains of plants and animals as well

Table 1.1 Rock types and associated heavy minerals **(Mitchell, 1975)**

Rock type	**Associated heavy minerals**
Granite	Mica, tourmaline, topaz, sphene, rutile
Pegmatite	Tourmaline, rutile, zircon
Diorite	Hornblende, augite, zircon
Gabbro	Olivine, pyroxene, amphibole, magnetite, ilmenite, spinel
Basalt	Olivine, pyroxene
Peridotite	Olivine, pyroxene, chromite, magnetite, ilmenite
Sandstone	Zircon, tourmaline, rutile
Laterite	Hematite, magnetite, goethite
Schist	Mica, hornblende, actinolite, tremolite, garnet, sillimanite
Gneiss	Staurolite, sillimanite, mica

as excreta. In recent times, sediments in areas impacted by human activities have been found to contain pollutants such as heavy metals, pesticides, industrial chemicals, and other contaminants. These sediments may be transported by the river by the process of traction, saltation, suspension, or solution depending on their grain size and chemical composition. Typically, the upper reaches of the river contain coarse material such as boulders and cobbles, whereas the mouth of the river where it meets the sea contains fine materials such as sand, silt, and clay. This is because the sediments undergo abrasion and attrition due to the hydraulic action of the river as they travel long distances, resulting in smaller particle sizes.

The hydraulic action of the river also causes sorting and rounding of the sediment grains. The longer the transportation, the more sorted and rounded the sediments are. It is well documented that the concentration of heavy minerals is higher in well-sorted sediments than in poorly sorted ones. It is also observed that their concentration is higher in finer sediments than in the coarser ones. This may be due to the deposition of the coarser heavy minerals as fluvial placers due to their weight while the rest of the coarser sediments being lighter than them is carried forward. Continuation of such a process leads to loss of the heavies from the coarser fraction. Since the finer sediments undergo such a process at a much lesser intensity, it leads to a concentration of heavy minerals in them.

A sedimentary basin is a location which effectively acts as a sink for sediment deposition. As the river loses its speed in the lower reaches, it is unable to hold the sediments leading to their deposition. This deposition can occur at the river's mouth in the form of deltas, along the beaches and even in the deep ocean basins. The ocean basins are the largest sink for the sediments.

A coast is a broad transitional environment between land and sea. Coasts are highly populated as they provide fertile land, food, transportation, a means of livelihood in the form of fishery and tourism and economic minerals. A beach is a part of the coast dominantly consisting of loose sand with varying amounts of silt and clay and extends between the shoreline and the permanent vegetation. It acts as a buffer zone between land and ocean and is unstable as waves, nearshore currents, and the wind constantly shift about the sediments **(Komar, 1977)**. The morphology of a coast depends on whether it is an eroding or an accreting one. Erosional coasts show features such as wavecut platforms, sea caves, sea arches, sea stacks and coastal straightening whereas a depositional one will show sand spits, tombolo, barrier islands etc.

The morphology of the coast will influence the characteristics of the sediments. The morphology of the coast depends on the various processes shaping it which include wind action, waves, erosion, deposition etc. The wind is responsible for the generation of waves and in the formation of sand dunes along the beaches. It can also cause erosion of the beach by blowing off the sediments. Wind also plays an important role of bringing in the monsoon. During monsoons, the rivers bring a lot of sediments in, causing the volume of the beach to swell. Heavy minerals are comparatively more concentrated during the monsoonal months as a result of a high-energy environment **(Nayak, 1993)**. The waves help in the selective sorting of sediments. It causes the lighter sediments to get washed off leaving behind heavy minerals which leads to their concentration, forming deposits. Waves also cause the finer grains to get deposited more landward than the coarser ones which accumulate closer to the shoreline. This is the reason why foreshore regions are associated with higher concentrations of coarser and lighter sediments as compared to the backshore region which has a high concentration of finer and denser materials. Hence, we can observe high concentrations of heavy minerals in features like berms and dunes which are associated with lower energy and calmer environments than in the intertidal region where wind-driven processes can sort and concentrate them. Biological activity also plays an important role in the distribution of sediments. Burrowing organisms such as crabs cause the reworking of sediments with their movement through the sediments while on the other hand, vegetation causes the stabilization of dunes preventing their erosion. This also facilitates the formation of placers in them. All these processes, either directly or indirectly facilitate the formation of beach placers. Phenomena like storms, cyclones and tsunami are devastating and can cause erosion and redistribution of sediments, retreat or complete loss of beaches and alteration of beach morphology. This will also alter the placer deposits. The beach placers form as laminae of black sands alternating with the white sand (Figure 1.2). The process of their formation is a slow one and depends on the rates of weathering, transport, and sedimentation.

In order to study these minerals, they are first separated from the sand in a separating funnel using heavy liquids like bromoform, tetrabromoethane, tribromoethane, methylene iodide, and polytungstate liquids. The heavy minerals sink to the bottom as they are heavier than these liquids and are separated by opening the knob of the funnel. Magnetic separation is carried out next using a hand magnet, in

Figure 1.2 Laminae of light and heavy minerals exposed in a pit dug at Keri Beach, Goa

which the magnetic minerals are separated out from the non-magnetic heavy minerals. X-ray diffraction studies are conducted for the identification of magnetic minerals. In X-ray diffraction, the X-rays produced in the X-ray tube are bombarded onto the sample. The sample acts as planes along which the X-rays diffract at different angles depending on which mineral and mineral face are present and at different intensities depending on the orientation of the sample. These angles and intensities are detected by the detector which are seen on the graphs as peaks. Every mineral will have its own 2θ signatures and will show peaks at those angles only. Depending on the peak position the minerals and their faces are identified. The non-magnetic minerals are identified under the microscope on the basis of their physical properties like colour, habit, lustre, fracture and grain surface features. The physical properties of a few minerals have been listed in Table 1.2.

1.2 SCOPE

Apart from being highly useful in solving scientific problems, heavy minerals are also in demand due to their strategic and commercial use. In the present times, they also form a major component (blue minerals) in the paradigm of Blue Economy and hence a detailed study is needed of their morphological features, composition, formation, and economic importance **(Gujar et al., 2021)**. They are also easy for exploitation compared to land deposits where mining involves a lot of expenditure **(Gujar, 2007)**.

Magnetite is the chief source of the metal Iron, which has countless applications. Rutile and Ilmenite are significant sources of the metal Titanium, which is used in

Table 1.2. Physical properties of transparent heavy minerals **(obtained from the websites: https://webmineral.com/, https://www.mindat.org/)**

Mineral	**Properties**
Actinolite	Colour- Green, green black, gray green, black Crystal System- Monoclinic Luster- Vitreous Habit- Bladed, Prismatic Fracture- Splintery Surface Features- Absent
Apatite	Colour- white, yellow, red, green, blue Crystal System- Hexagonal Luster- Vitreous Habit- Tabular Fracture- Conchoidal Surface Features- Absent
Augite	Colour- Black, light brown, dark brown, brown green, green Crystal System- Monoclinic Luster- Vitreous to Resinous Habit- Prismatic Fracture- Conchoidal Surface Features- Absent
Diopside	Colour- Blue, colourless, green, gray, brown Crystal System- Monoclinic Luster- Vitreous

	Habit-Prismatic Fracture- Conchoidal Surface Features- Absent
Epidote	Colour- Yellowish-green, green, brownish-green, black Crystal System- Monoclinic Luster- Vitreous Habit- Prismatic Fracture- Irregular/Uneven Surface Features- Absent
Garnet (pyrope)	Colour- Blood red, orange red, pink, black red, purple red Crystal System- Isometric Luster- Vitreous Habit- Crystalline/ granular Fracture- Conchoidal Surface Features- Absent
Hornblende	Colour- Green, greenish brown, black Crystal System- Monoclinic Luster- Vitreous to pearly Habit- Prismatic Fracture- Sub-conchoidal Surface Features- Absent
Hypersthene	Colour- Greyish white Crystal System- Orthorhombic Luster- Vitreous, Silky Habit- Massive

	Fracture- Uneven Surface Features- Absent
Kyanite	Colour- Blue, white, light gray, green, rarely yellow, orange, pink Crystal System- Triclinic Luster- Vitreous, Sub-Vitreous, Greasy, Pearly Habit- Bladed Fracture- Splintery Surface Features- Absent
Rutile	Colour- Blood red, brownish yellow, brown-red, yellow, greyish-black, black, brown, bluish, or violet Crystal System- Tetragonal Luster- Adamantine, Metallic Habit- prismatic, often slender to acicular Fracture- Irregular/Uneven, Conchoidal, Sub-Conchoidal Surface Features- Absent
Sillimanite	Colour- Colourless, white, yellow, brown, green, blue, gray Crystal System- Orthorhombic Luster- Sub-Vitreous, Greasy, Silky Habit- Fibrous Fracture- Irregular/Uneven Surface Features- Absent
Staurolite	Colour- Dark brown, brownish-black, red-brown Crystal System- Monoclinic Luster- Sub-Vitreous, Resinous Habit- Prismatic crystals

	Fracture- Sub-Conchoidal Surface Features- Absent
Tourmaline (schorl)	Colour- Bluish-black to black, sometimes brownish-black, rarely greenish-black Crystal System- Trigonal Luster- Vitreous, Resinous Habit- Prismatic to acicular Fracture- Irregular/Uneven, Conchoidal Surface Features- Striations
Tremolite	Colour- White, brown, colourless, grey, light green, green, light yellow, pink-violet Crystal System- Monoclinic Luster- Vitreous, Silky Habit- Elongated, stout prismatic, bladed Fracture- Splintery Surface Features- Absent
Zircon	Colour- Colourless, yellow, grey, reddish-brown, green, brown, black Crystal System- Tetragonal Luster- Adamantine, vitreous, greasy Habit- Long prismatic crystals Fracture- Conchoidal Surface Features- Absent

industries such as paint and aerospace. Zircon is used in various applications, such as ceramics, refractories, and as a gemstone. Garnet is widely used as an abrasive due to its hardness and is also considered a semi-precious gemstone. Monazite-rich black sands are being mined from Kerela, India for their use in nuclear power plants as they contain the radioactive element, Thorium. This can be a better alternative to fossil fuels. Green energy helps in the global transition towards a more sustainable energy future.

The Indian coastline, both east and west, hosts some of the largest and richest beach placer sand deposits in the World. The Atomic Minerals Directorate has proved nearly 640 million tons of heavy minerals, including about 350 million tons of ilmenite **(Ali et al., 2001)**. Some of the significant deposits from the world include Murray Basin in and the Tiwi Islands in Australia, the coast of the Eastern Cape and the KwaZulu-Natal provinces in South Africa, along the Atlantic and Gulf coasts of Florida, Georgia, and Virginia in the United States and in the states of Bahia and Rio Grande do Norte in Brazil.

Numerous studies have been undertaken along the coasts of Kerela, Karnataka, Maharashtra, Tamil Nadu, and Orissa for their reserves of heavy minerals. Kerala has the richest deposits of heavy minerals in India. The Indian Rare Earths (IRE) Limited has started exploring and mining in the states of Kerela (Alappuzha and Kollam district), Tamil Nadu (Kanyakumari district), Andhra Pradesh (Srikakulam and Visakhapatnam districts) and some areas in Odisha in a limited extent. However, not enough studies have been done on the beaches of Goa. Gujar et al. (2021) are the pioneers to present a generalized study on the beach placers of Goa. There is a need to study the individual beaches in detail to gain information on the concentration, distribution, and reserve potential of heavy minerals so that they can also be exploited sustainably in future.

1.3 AIM AND OBJECTIVES OF THE STUDY

1.3.1 Aim

To study heavy minerals from the beach sands of Keri (Querim), Goa, west coast of India

1.3.2 Objectives

1. To study the distribution of heavy minerals along Keri Beach.
2. Identification of the different heavy minerals present in the samples.
3. To study the provenance of the minerals.

1.4 STUDY AREA

1.4.1 Location, Climate and Physiology

Goa is a state located along the west coast of India. It has a coastline of approximately 105 km and contributes to 1.4% of the country's coastline. Despite being small, it is one of India's most important coasts in terms of tourism and fishery. It is part of the Konkan Coast and is blessed with thick mangroves and beautiful beaches which are intervened by rivers, creeks and headlands. It is classified as a submerged coast indicated by geomorphological features such as the drowned river valleys. It experiences a tropical monsoon-type of climate with an average annual rainfall of 3000 mm **(Pradhan, 2016)**. Since it is closer to the sea, the temperatures remain relatively stable throughout the year with high levels of humidity. It experiences semi-diurnal tides with spring and neap tides 15 days apart. Numerous studies have been undertaken along the Goan beaches for their biodiversity, productivity, morphology, beach dynamics and pollution assessments. However, not enough studies have been conducted on the valuable heavy minerals present in their sediments.

For the present study, a beach in the Querim (also known as Keri) village of Pernem taluka in North Goa was selected. It is located south of Tiracol and north of Arambol, 55 km away from Panjim. The beach is approximately 2 km long and extends from 15°43'11.85"N to 15°42'16.51"N. Terekhol River bounds it to the north, Arabian Sea to the west, and a headland to the south. The beach has a few outcrops of laterites. It is a straight/linear beach with sand spit on the riverine side of the beach, and a small creek becomes functional during the monsoonal months. The beach has been altered by human intervention, as evidenced by the presence of tetrapods and a seawall built at the centre which disrupts its natural ecosystem. A ferry operates across the Terekhol River, connecting Keri and Tiracol. The beach provides opportunities for fishing and tourism.

1.4.2 Regional Geology

The study area consists of the rocks of Goa group (Figure 1.4). Goa is the north-western extension of the Western Dharwar Craton with the Peninsular Gneissic Complex (Archean) as the basement for the Supracrustals. The supracrustals i.e. Goa Group of rocks (Archean to lower Proterozoic) are divided into two groups i.e. Barcem Group and Ponda Group. The Barcem Group consists of the Barcem Formation while the Ponda Group is further divided into three formations viz. Sanvordem, Bicholim and Vageri. They are intruded by mafic-ultramafic complexes and intrusive granitoids. Deccan traps (upper Cretaceous to Eocene) are exposed at the eastern border of the state and laterite forms capping for the rocks towards the Arabian. Beach sands are the recent deposits along the coast. The detailed stratigraphy and lithology of the Goa Group of Rocks is given in Table 1.3.

The rocks of the Sanvordem formation, particularly the metagreywackes and metaconglomerates are well exposed between Bati and Keri south of river Tiracol. The river Terekhol flows through the rocks of Bicholim and Vageri formations. The Bicholim formation consists of ferruginous and manganiferous phyllites, banded hematite and magnetite quartzites and quartz-chlorite-amphibole schists. Banded Hematite Quartzites at some places are intercalated by pyritiferous carbonaceous shale. The Vageri Formation is made up of metagreywackes and metabasalts **(Dessai, 2018)**.

The Terekhol River originates in the western ghats in the environs of Manohargad Fort in Kudal and flows NE-SW through the Sindhudurg District before entering Goa.

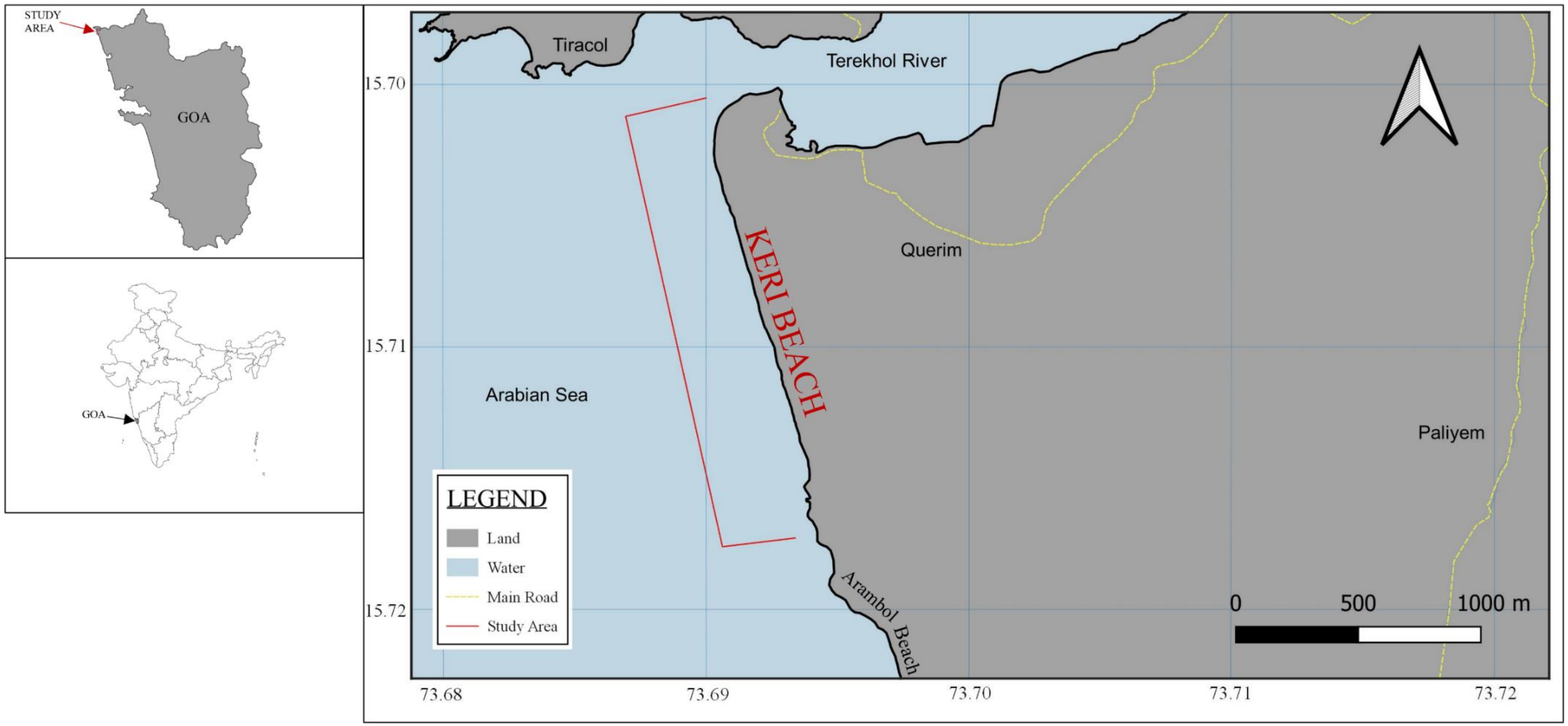

Figure 1.3 Study Area

The river flows over a vast metamorphic and igneous terrain consisting of schists, amphibolites, pyroxenites, quartzite, granite, pegmatite, dolerites, and basalts **(Gujar, 2021)**.

The Sindhudurg mainly consists of the Pre-Cambrian Dharwar Group, Granites/Gneisses, Proterozoic Kaladgi Group, Upper Cretaceous to Lower Eocene Deccan Traps and Pleistocene to sub-recent Laterites (Figure 1.5). The detailed stratigraphy of different parts of Sindhudurg district is given in Tables 1.4 and 1.5.

From Figure 1.5 and 1.6, it can be observed that the river Terekhol predominantly flows through the rocks of the Dharwar Supergroup. The Dharwar Craton is a granite-greenstone terrain trending NNW-SSE and is divided into two parts i.e. western and eastern parts along the Closepet Shear Zone (Figure 1.8). The Dharwarian rocks exposed in Sindhudurg are the north-western extension of the Western Dharwar Craton (WDC). The supracrustal rocks of the Dharwar System have been classified into the older 'Sargur Group' and a younger 'Dharwar Supergroup' **(Sen et al., 2012)**. The stratigraphy and lithology of the same are given in Table 1.6.

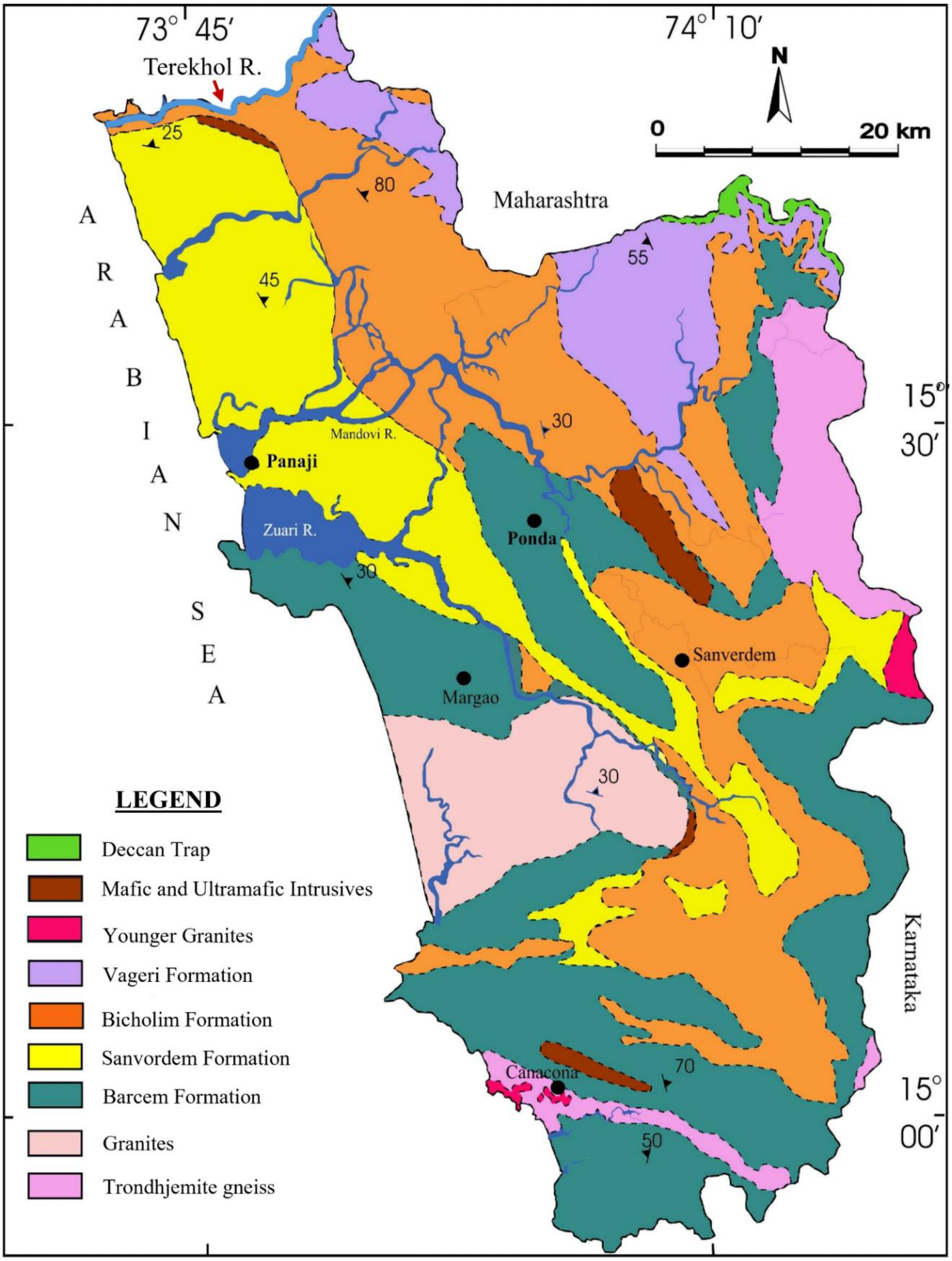

Figure 1.4 Geological Map of Goa **(Desai 2011 and Gujar et al., 2021)**

Table 1.3 Lithostratigraphic sequence of Goa Group **(modified after Desai, 2011)**

Rocks	Age/Formation	Lithology
Residual Rocks		Laterites
Basic Intrusives (late)	65-56 Ma	Dolerites
Deccan Traps	67-64 Ma	Basalts
Basic Intrusives		Metadolerites
Bondla Mafic-ultramafic layered complex		Dunite-peridotite-gabbro and equivalents
Ponda Group	**Vageri Formation**	Metabasalts, Argillites and metagreywackes
	Bicholim Formation	Banded ferruginous quartzite, Manganiferous chert breccia, Limestone, Ferruginous phyllite, Quartz-chlorite amphibolite schist
	Sanvordem Formation	Metagreywacke, Argillite, Quartzite, Para-conglomerate
Unconformity		
Barcem Group	**Barcem Formation**	Metagabbro, Peridotite, talc-chlorite schist, Quartzite, Phyllite, Quartz Porphyry, Massive, schistose and vesicular Metabasalt
Unconformity		
Canacona Granite	2979+4 Ma	Porphyritic potassic granite
Chandranath Granite Gneiss	2900-2700 Ma	Granodiorite
Basement: Anmode Ghat Trondhjemite Gneiss	3400-3300 Ma	Tonalite-Trondhjemite-Granodiorite (TTG) Gneiss

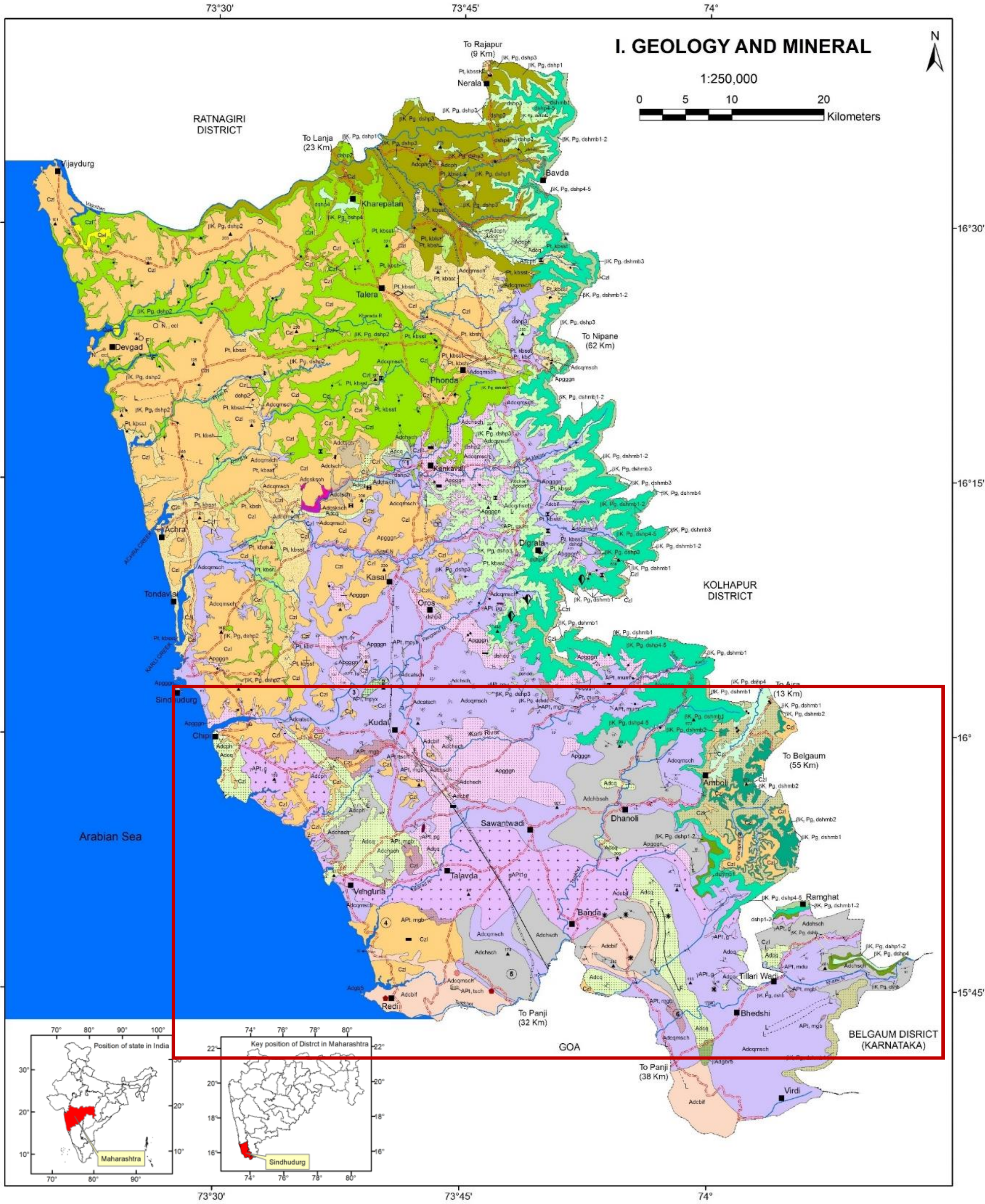

Figure 1.5 Geological Map of Sindhudurg by **GSI, 2021** (Refer to Figure 1.7 for the legend. Close up of the area marked in red is given in Figure 1.6)

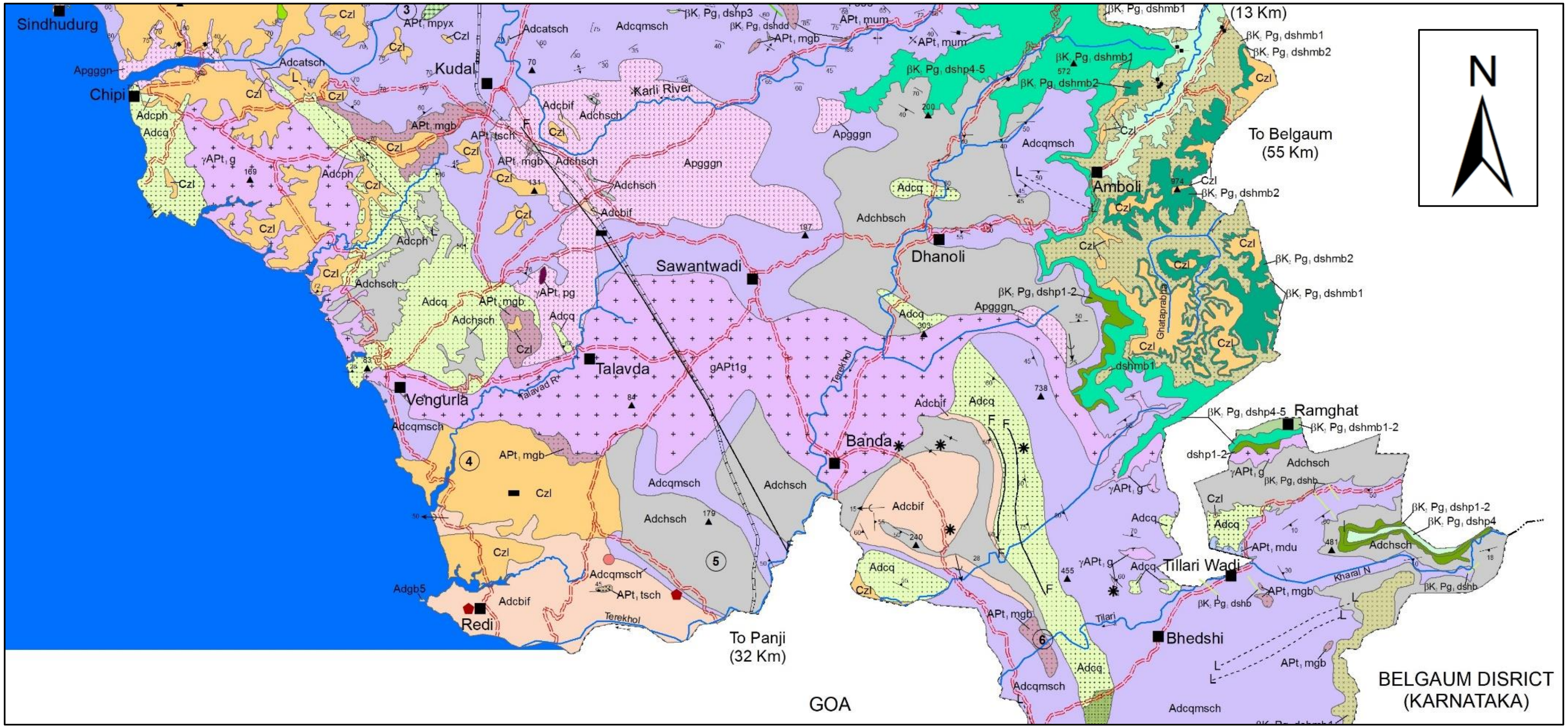

Figure 1.6 Close up of the area marked in red in Figure 1.5

(Refer to Figure 1.7 for the legend)

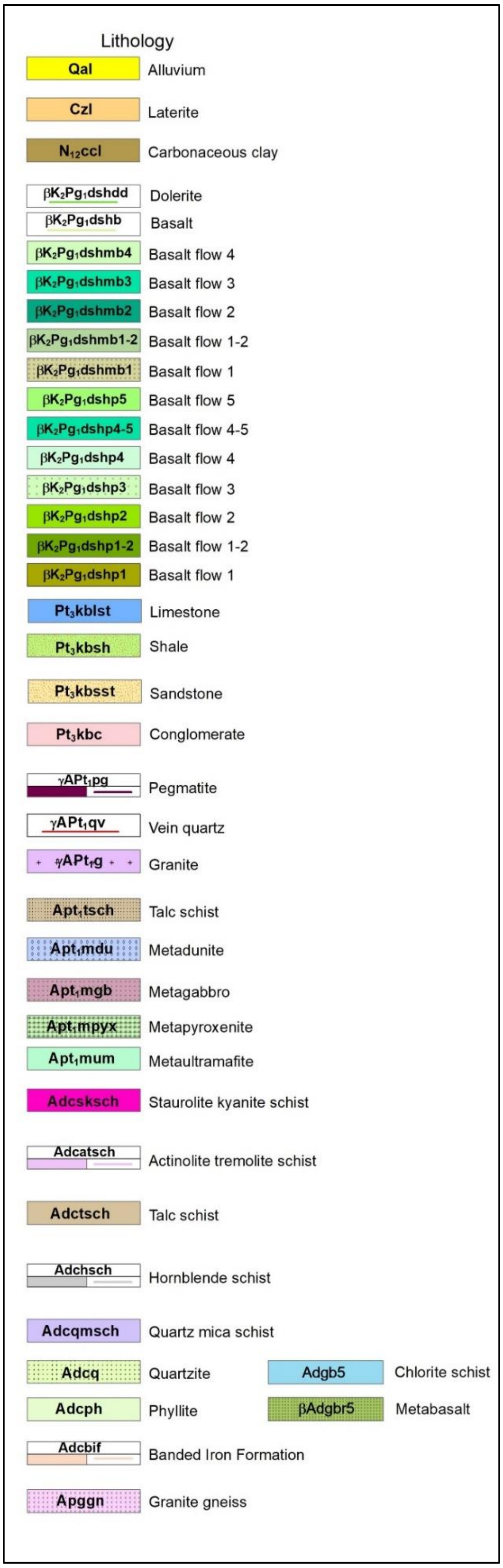

Figure 1.7 Legend for Figures 1.5 and 1.6

Table 1.4 Stratigraphic succession of Sindhudurg area **(Kamble et al., 1987)**

Deccan Trap	Soil and laterite spread Laterite Sparsely to moderately porphyritic basalt (with development of pillows at few localities)
Unconformity	
Kaladgi	Quartzite Grey to brown shale/ clayey shale Ferruginous quartzite, at places grading to Grit Conglomerate
Unconformity	
Late Intrusives **Acid rocks** **Metabasic/Ultrabasic** **Metasedimentaries**	Basic to ultrabasic intrusive (dolerite, gabbro, pyroxenite, serpentinite, etc.) Granite/granite gneisses, pegmatite, alpites and quartz veins Hornblende schist Asrondi quartzite, quartz-biotite-garnet schist, quartz-muscovite-garnet schist, quartz-biotite-garnet-staurolite+kyanite schist Banded magnetite quartzite
Basement unknown	

Table 1.5 Lithostratigraphy of Sindhudurg in parts of 47H/16, 48E/09 and 13 **(Sen et al., 2012)**

<table>
<tr><td colspan="2">Fluvio-Marine deposit
Laterite</td><td>Tertiary to Recent</td></tr>
<tr><td>Deccan Trap</td><td>Basalt (Lava flows and intrusives)</td><td>Cretaceous to Eocene</td></tr>
<tr><td colspan="3" align="center">Unconformity</td></tr>
<tr><td align="center">Intrusives</td><td>Dolerite/basalt dykes
Syenite/pegmatite/quartz-vein
Gabbro/diorite plutons
Pat granite (?)
Metagabbro/metadolerite</td><td rowspan="3">Equivalents of the Ponda Group of Goa ≡ the Chitradurga Group in WDC
(Archean to Meso-Proterozoic)</td></tr>
<tr><td colspan="2" align="center">Intrusive contact</td></tr>
<tr><td align="center">Supracrustals</td><td>BHQ
Metapelites
Metabasalt/actinolite schist/hornblende schist
Quartzite (with intra-formational metaconglomerate)</td></tr>
<tr><td colspan="3" align="center">Tectonic contact (?)</td></tr>
<tr><td rowspan="3" align="center">Basement Gneissic Complex</td><td>Granite Gneiss (Sawantwadi and Zarap-Mangaon plutons)</td><td rowspan="3">Peninsular Gneissic Complex (Archean)</td></tr>
<tr><td align="center">Intrusive contact</td></tr>
<tr><td>Biotite gneiss/migmatite gneiss with enclaves of amphibolite/amphibole schist, ultramafics and BIF (mainly BMQ)</td></tr>
</table>

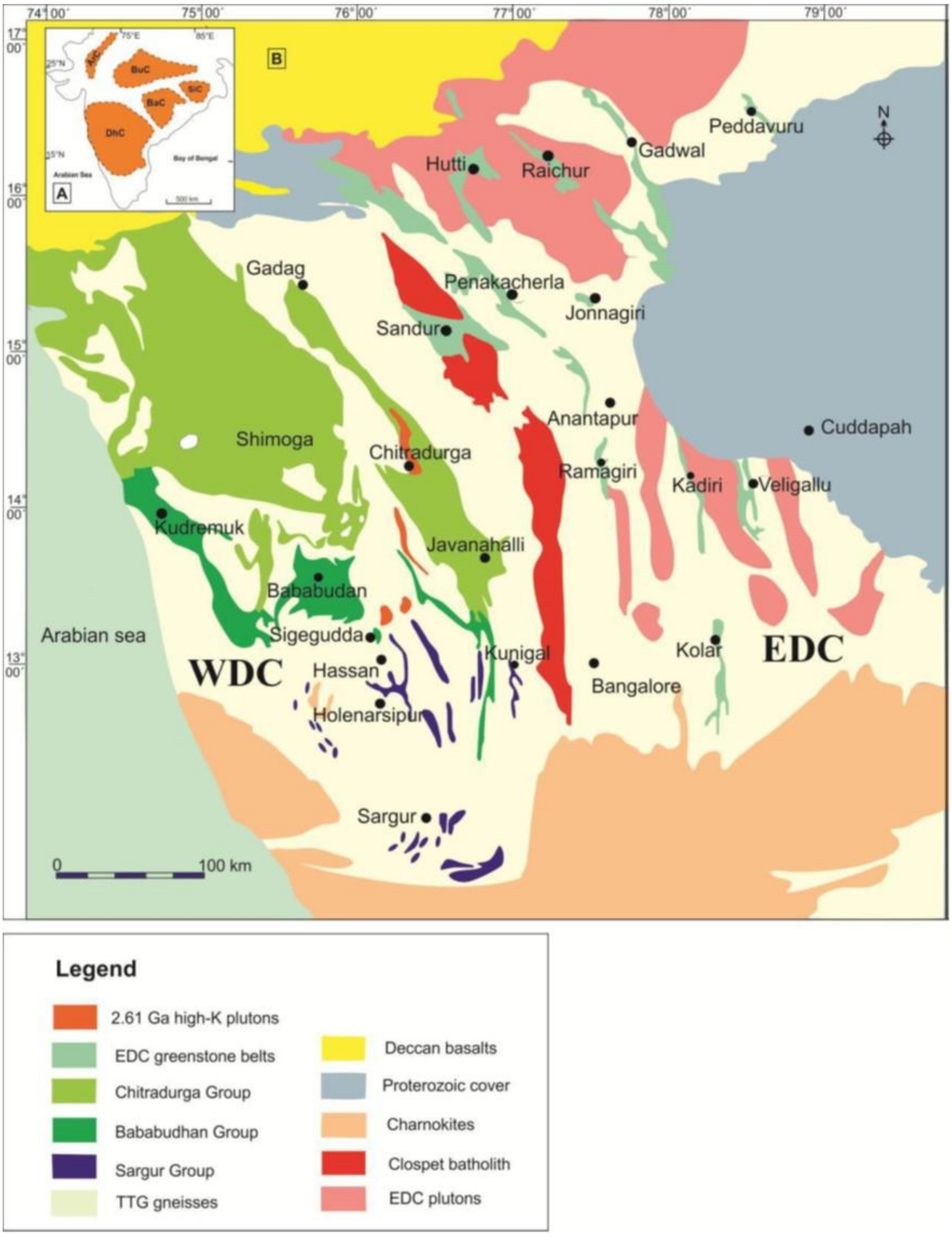

Figure 1.8 Geological Map of Dharwar Craton **(Swami Nath and Ramakrishnan, 1981)**

Table 1.6 Stratigraphic sequence of Western Dharwar Supergroup **(Swami Nath and Ramakrishnan, 1981)**

<table>
<tr><td colspan="5">Proterozoic mafic dykes
Charnokites (2.5-2.6 Ga)
Younger Granites (2.6 Ga)</td></tr>
<tr><td rowspan="6">Dharwar Supergroup (2.6-2.8 Ga)</td><td rowspan="2">Chitradurg Group</td><td>Ranibennur Subgroup</td><td colspan="2">Greywackes with BIF, polymict conglomerate, mafic felsic volcanics</td></tr>
<tr><td>Vanivilas Subgroup</td><td>Mafic-felsic volcanics with BIF, phyllites (basin centre)</td><td>Manganese and iron formations, stromatolitic carbonates, biogenic cherts, pelites, quartzites and polymictic conglomerates. (Basin margin)</td></tr>
<tr><td rowspan="4">Bababudan Group</td><td>Muliangiri Formation</td><td colspan="2">BIF with phyllites and rare ultramafic- mafic sills</td></tr>
<tr><td>Santaveri Formation</td><td colspan="2">Metabasalts, felsic volcanic (Galipuje felsite), Ultramafic schists, layered basic complexes, siliceous phyllites, crossbedded quartzite (Kaimara, Tanigebail)</td></tr>
<tr><td>Allampura Formation</td><td colspan="2">Metabasalts, Gabbros, Ultramafic schists,
local BIF, phyllites, cross-bedded quartzite
(Lakya)</td></tr>
<tr><td>Kalaspura Formation</td><td colspan="2">Metabasalts, Gabbros, Ultramafic schists, phyllites, quartzites, basal quartz pebble conglomerate (Kartikere conglomerate)</td></tr>
<tr><td rowspan="6"></td><td colspan="4">Deformed angular unconformity</td></tr>
<tr><td colspan="4">Peninsular Gneiss with Trondhjemite-Granodiorite plutons (>3.0 Ga)</td></tr>
<tr><td colspan="4">Intrusive/Tectonic contact</td></tr>
<tr><td rowspan="2">Sargur Group (3.1-3.3 Ga)</td><td colspan="3">Ultramafic-mafic layered complexes, tholiitic amphibolites,komatiites,BIF
Quartzite, pelites, marbles and calc-silicate rocks</td></tr>
<tr><td colspan="3">Intrusive/Tectonic contact</td></tr>
<tr><td colspan="4">Gorur Gneiss (3.3-3.4 Ga)</td></tr>
</table>

LITERATURE REVIEW

CHAPTER-2: LITERATURE REVIEW

Chavadi and Nayak (1990) studied the spatial and seasonal distribution of heavy minerals between Loliem and Arge. There was a large variation in the distribution on heavy minerals in this small narrow strip. The different minerals were magnetite, ilmenite, garnet, hornblende, epidote, sphene etc. Their concentration was high near the mouth of Kali River. All the minerals come from the catchment rocks of the river and the coastal cliffs.

Dinesh et al. (2015) studied the occurrence and distribution of heavy minerals in the beach sediments between Dandi and Daman in Gujarat. The heavy minerals dominantly consist of ilmenite and magnetite along with minor quantities of rutile, pyroxene, monazite, zircon, and sillimanite. Their concentration was highest in fine and very fine sand fractions, and it is lower in the silt fraction in both beach and dune samples. The highest concentration of the heavy minerals was found in the samples collected from near the mouth of Par River.

Gandhi et al. (2022) discusses the properties of sediments and the provenance of heavy minerals from Chinnavilai and Erayumanthurai beach of the Kanyakumari District, Tamil Nadu, India. The sediments in the area are medium-grained, moderately well-sorted, unimodal, occasionally bimodal, mesokurtic, leptokurtic, and platykurtic. The heavy mineral assemblage consists of ilmenite, magnetite, garnet, zircon, rutile, sillimanite, monazite, kyanite, etc. The opaque minerals are dominant over the non-opaque minerals. The mineral assemblage and the grain characteristics of the heavy minerals suggest that they originate from an admixture of medium to high-grade metamorphic rocks, reworked sediments, charnockite, and granite gneisses.

The study by **Ghosal et al. (2022)** reports on the distribution, mineralogy, and provenance of heavy minerals along the southwestern coastal part of Odisha. The study area is present in the Charnockite-Migmatite Zone of the Eastern Ghat Mobile Belt (EGMB). Other rock types in the adjacent area consist of Khondalites and Granites. The study focuses on the Thorium, Uranium and Rare Earth Element (REE) concentrations present in monazite and zircon. Geochemical studies show high silica content of the beach sands indicating acidic source rock. The average concentration of REEs in the beach sands is in the order from high to low as Ce > La > Nd > Pr > Sm > Gd > Dy > Er > Yb > Tb. The concentration of Thorium is high in the beach sands as compared to Uranium and Potassium concentrations. Monazite shows high concentrations of Thorium and Cerium while Zircon contains low concentrations of Uranium and REE. The monazite grains are elongated and rounded indicating nearby source and abrasion activity during the transportation. Zircon is also elongated and rounded. The other minerals present in the area are magnetite, ilmenite, rutile, and garnet. Chemical Index of Alteration (CIA) and Plagioclase Index of Alteration (PIA) were calculated to study the intensity of weathering in the study area and their high values suggest that the area experiences a high degree of chemical weathering. The comparison of REE and Radioactive element concentrations with the rocks from the surrounding area suggests Charnockite to be the source rock for the beach sands. Rushikulya River, whose entire catchment lies in the Charnockite-Migmatite Zone, is the major supplier of the sediments to the study area.

Various studies have been done along the coast of South Maharashtra for its heavy mineral deposits. **Gujar et al. (2007) and Gujar et al. (2022)** studied the distribution, mineralogy and reserve potential of heavy mineral placers in South Maharashtra from Vijaydurg to Redi. The heavy mineral composition consisted of opaques, rutile, tourmaline, kyanite, zircon etc. The concentration of heavies was higher in the berm and dune region as compared to the intertidal region. It was concluded that the minerals were derived from mixed source rocks of igneous, high-grade metamorphic types as well as the recycled Kaladgi sediments. High reserves of ilmenite, magnetite and chromite were obtained.

Gujar et al. (2010) investigated the heavy minerals from the beach sediments of South Maharashtra between the rivers Achara and Gad. The heavy minerals observed in the area are magnetite, ilmenite, chromite, zircon, tourmaline, garnet, kyanite, olivine, pyroxene, and amphiboles. They are the pioneers to report the presence of Chromite in the beach placers of South Maharashtra. The concentration of heavy minerals is higher in the backshore sediments as compared to the foreshore sediments. The concentration of heavy minerals is higher in the finer sediments as compared to coarser sediments. There is a trend of increase in the concentration from North to South of the Study Area. The dominant grain size is fine sand hence contains good reserves of opaques. Ilmenite and Magnetite are concluded to have undergone short transportation as the grains show signs of mechanical breaking in the form of cracks, openings, fractures, and impact V-marks. Therefore, their origin is considered to be from the nearby Kaladgi Sandstones. Chromite, on the other hand, has undergone longer transportation and originates from the chromite lenses and associated ultra-basic rocks in the Kankavali region in the upper reaches of the Gad River. The transparent minerals have a mixed source from igneous, metamorphic and re-worked sediments of Kaladgi.

Another study by **Gujar et al. (2010)** provides a detailed understanding of the formation and deposition of chromite placers along the South Maharashtra coast. They have also studied the grain characteristics and chemistry. There are two types of chromites present int the study area, namely, ferro-chromite and magnesio-chromite. ICP-OES analysis of the chromite grains reveals appreciable Cr_2O_3 content. The chromite from the lenses present in the upper reaches of the Gad River (Janoli and Wagda mines) was also studied and it was found out to be comparable to the placer chromite suggesting that it has been derived and transported from these sources.

Gujar et al. (2021) are the pioneers to study the heavy mineral placers along the coast of Goa. The study provides a general understanding on the distribution of the heavy minerals along the beaches of Goa. The heavy minerals present in the area are ilmenite, magnetite, garnet, hornblende, pyroxene, epidote, staurolite, tourmaline, zircon, and rutile. The rivers draining in the area originate in the Western Ghats and flow through a variety of rocks such as schists, amphibolites, pyroxenites, granite, gneisses, pegmatites, dolerites and basalts which are the sources of the heavy minerals. This is also confirmed by the thin-section study of the rock samples collected from the hinterland. Sediments from North Goa are finer than those from South Goa indicating that the sediments from North Goa have undergone longer transportation. The highest concentration of the heavy minerals was in Vagator Beach in North Goa. The backshore environments, especially the dunes, have the highest concentration of heavies. The bimodal nature of X-ray diffraction peaks confirms the presence of fresh and altered opaques which are of moderate grade.

Hegde et al. (2006) studied the heavy mineral assemblage, geochemistry, and provenance with special reference to ilmenite from Honnavar Beach, Karnataka. The heavy minerals obtained in the area include ilmenite, magnetite, zircon, epidote, hornblende, augite, kyanite, staurolite and garnet. EPMA studies showed that the ilmenite is rich in TiO_2 and MnO while it is poor in iron oxide contents. Mn/Mg ratios as well as Ni, Cr, V and Co contents were used as an indicator of source rock. The heavies have a mixed origin from hinterland brought by the Sharavati River and a minor ephemeral stream as well as from the palaeo-beach.

Nallusamy et al. (2013) provides the distribution of heavy minerals from the Thothapally - Kayamkulam Barrier Island of Kerela, India. The sediments from the study area are dominantly of fine sand size. The area shows a general trend of decrease in the total heavy mineral concentration from south to north. The mineral assemblage consists of ilmenite, sillimanite, zircon, rutile, kyanite, monazite, garnets, sphene, epidote and tourmaline. Ilmenite is the most abundant mineral in all the samples as well as in all the sand fractions. X-Ray Diffraction (XRD) studies and Scanning Electron Microscopy (SEM) were done to study the characteristics of ilmenite. XRD results show the association of rutile and pseudo-rutile with ilmenite. SEM results show surficial features on ilmenite grains resulting from mechanical and chemical weathering such as mechanical and chemical pits, etch-Vs, and grooves. The chemical action on the surface of ilmenite grains gave rise to rutile and pseudo-rutile. Thus, chemical dissolution is intense in this area due to acidic ground water.

Nayak (1997) investigated the distribution of heavy minerals between the rivers Tiracol and Chapora in Goa, west coast of India. The sediment samples were collected from 4 stations along the 22 km stretch during the pre-monsoon, monsoon, and post-monsoon periods. The concentration of heavy minerals was highest in the monsoon period. The minerals identified are magnetite, ilmenite, hornblende, augite, staurolite, hypersthene, epidote garnet, actinolite, and rutile. The sources of the minerals were traced back to the catchment area rocks of the two rivers.

Nayak (2011) reports the occurrence of gold as an inclusion in amphibole grains of hornblendic composition in beach placers of Chavakkad-Ponnani area in Kerela. The inclusion has a size of about 25µm. EPMA was carried out in which the inclusion was analyzed scanned for all elements that were detectable by the spectrometers. Gold is detected to be the major constituent of the grain along with impurities of Si and Fe thus concluding that the inclusion is a grain of native gold. It is believed to have come from the auriferous tracts in Wynad-Nilambur and Attapadi valley which lies in the upper reaches of Ponnani River.

Nayak et al. (2012) studied the distribution of heavy minerals and characteristics of ilmenite grains from the Chavakkad-Ponnani area in Kerela. It is an 18 km long coastal stretch and having the mouth of the Ponnani River. The concentration of the minerals decreases away from the mouth of Ponnani River in both directions. The heavy minerals present in the area are pyriboles, ilmenite, garnet, sillimanite, zircon, rutile and traces of monazite and apatite. Pyriboles are the most abundant in the area. Amphiboles are dominant over pyroxenes and hornblende is the most common amphibole. The Electron Probe Micro Analysis of ilmenite grains shows that hematite is present as intergrowth within the ilmenite grains suggesting that the recovery of quality ilmenite is low. On the other hand, amphiboles contain intergrowths of gold which can be exploited in future.

In the study by **Reddy et al. (2012)** the heavy minerals were analyzed for their assemblage, distribution, abundance, and concentration in different fractions of sand between Nizampatnam and Lankavanidibba in Andhra Pradesh. The study area is divided into 7 sectors. The mineral assemblage is same in all the sectors which in decreasing abundance consists of ilmenite, magnetite, pyriboles, garnets, epidote, sillimanite, zircon, staurolite, kyanite, apatite, spinel, monazite, biotite, topaz, leucoxene, and chlorite. Their concentration is higher in finer sand fraction. Their concentration decreases away from the mouth of River Krishna which indicates that the river is the main source of transportation for the heavy minerals. The alternate layers of heavy and light minerals are due to high and low energy conditions and their thickness indicates the duration of the respective energy condition. The sectors experiencing erosion showed high concentrations of heavy minerals as the wave action caused the washing away of the lighter minerals.

METHODOLOGY

CHAPTER 3: METHODOLOGY

3.1 PREPARATION OF BASE MAP, STUDY AREA MAP AND BEACH PROFILE MAP

The study area was selected after the available literature survey and Survey of India toposheet number 48E/10 and a Google Earth image was used for preparing the base map (Figure 3.1). For this, location pins were marked on Google Earth Pro software. A total of 5 location pins were marked namely, A, B, C, D and E along the Keri beach starting from the mouth of Terekhol River towards the Arabian Sea and ending at the Keri Caves (headland) with an interval of 500m. The coordinates of the location pins were noted down (Table 3.1) and saved on the Mobile Application Google Maps and were accessed during the sampling.

The study area map (Figure 3.2) and a beach profile map (Figure 3.3) showing the sampling locations were prepared using QGIS version 3.8.2.

3.2 FIELDWORK

Sampling of the sediments was done on 4th June, 2023 during the lowest low tide (spring tide, full moon). Sampling was done during the pre-monsoon period (monsoon to hit Kerela on 4th June 2023, IMD). Two samples were collected from each location. 10 cm long cores (Figure 3.4) were collected from the foreshore (low tide mark) with the help of a PVC corer having a diameter of 5 cm and backshore(berm) sediments were collected with the help of a plastic scoop. A total of 9 samples (approx. 500g

Table 3.1 Sampling Location Co-ordinates

Location	Latitude	Longitude
A	15.719897	73.691189
B	15.715689	73.690706
C	15.711347	73.692053
D	15.707086	73.693719
E	15.702950	73.694261

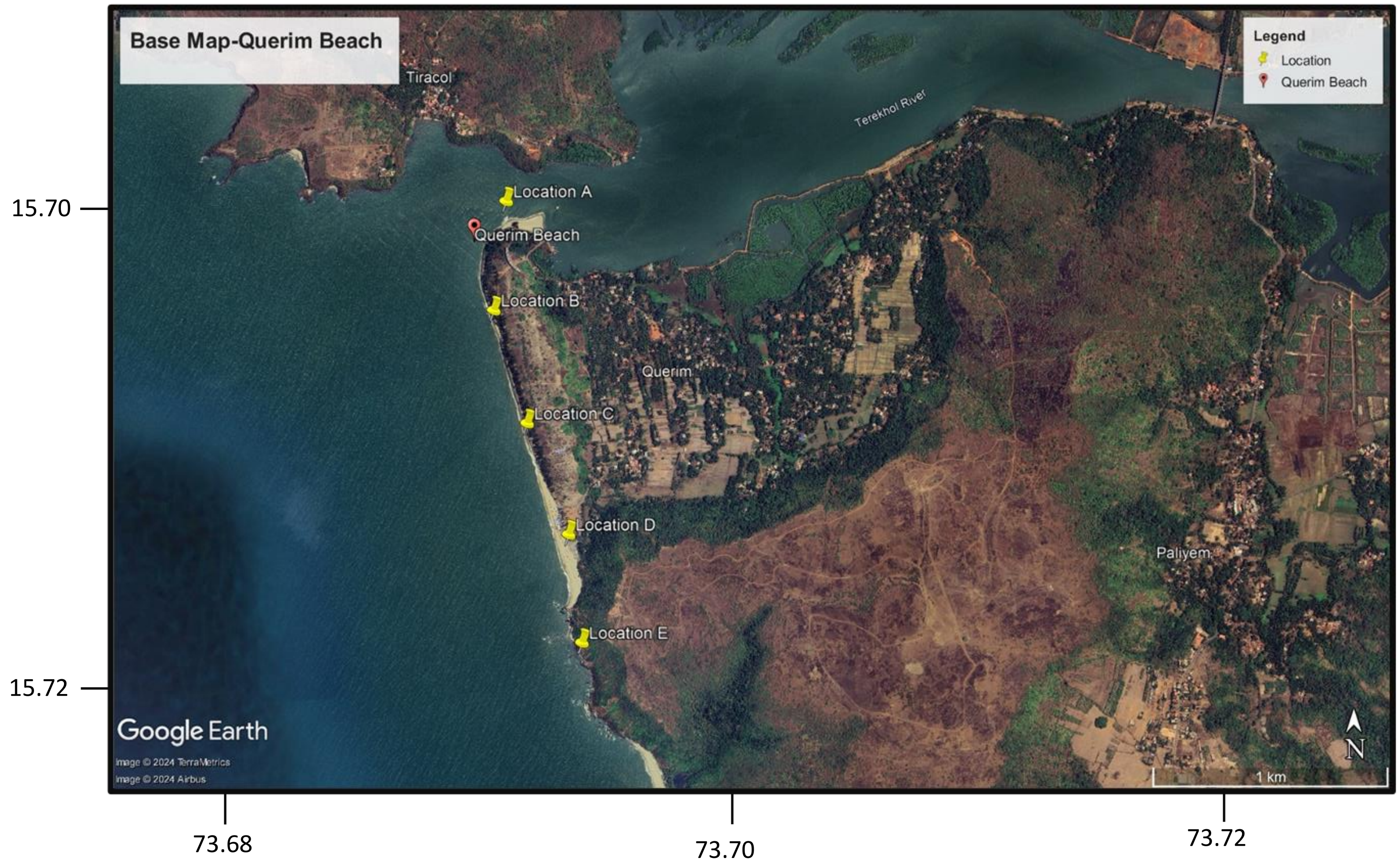

Figure 3.1 Base Map- Keri Beach

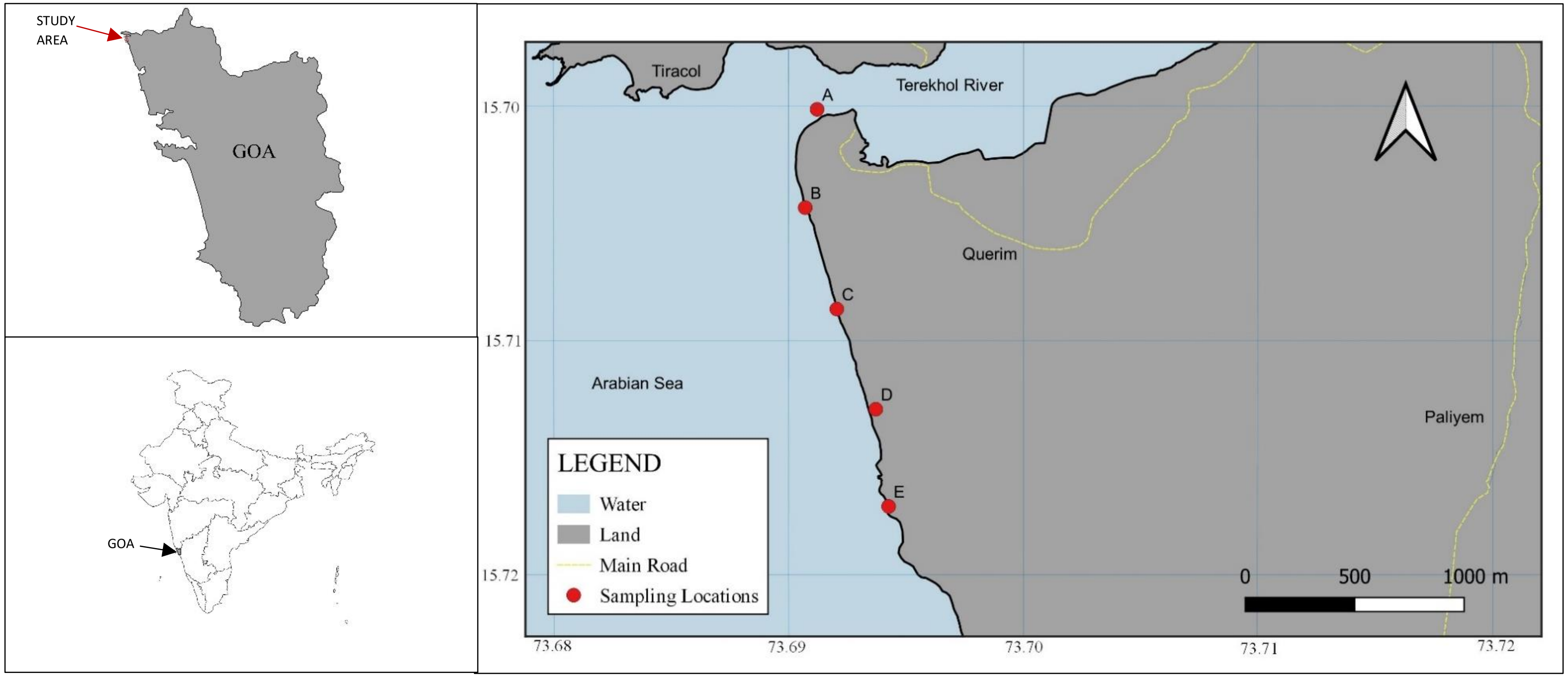

Figure 3.2 Study Area showing sampling locations

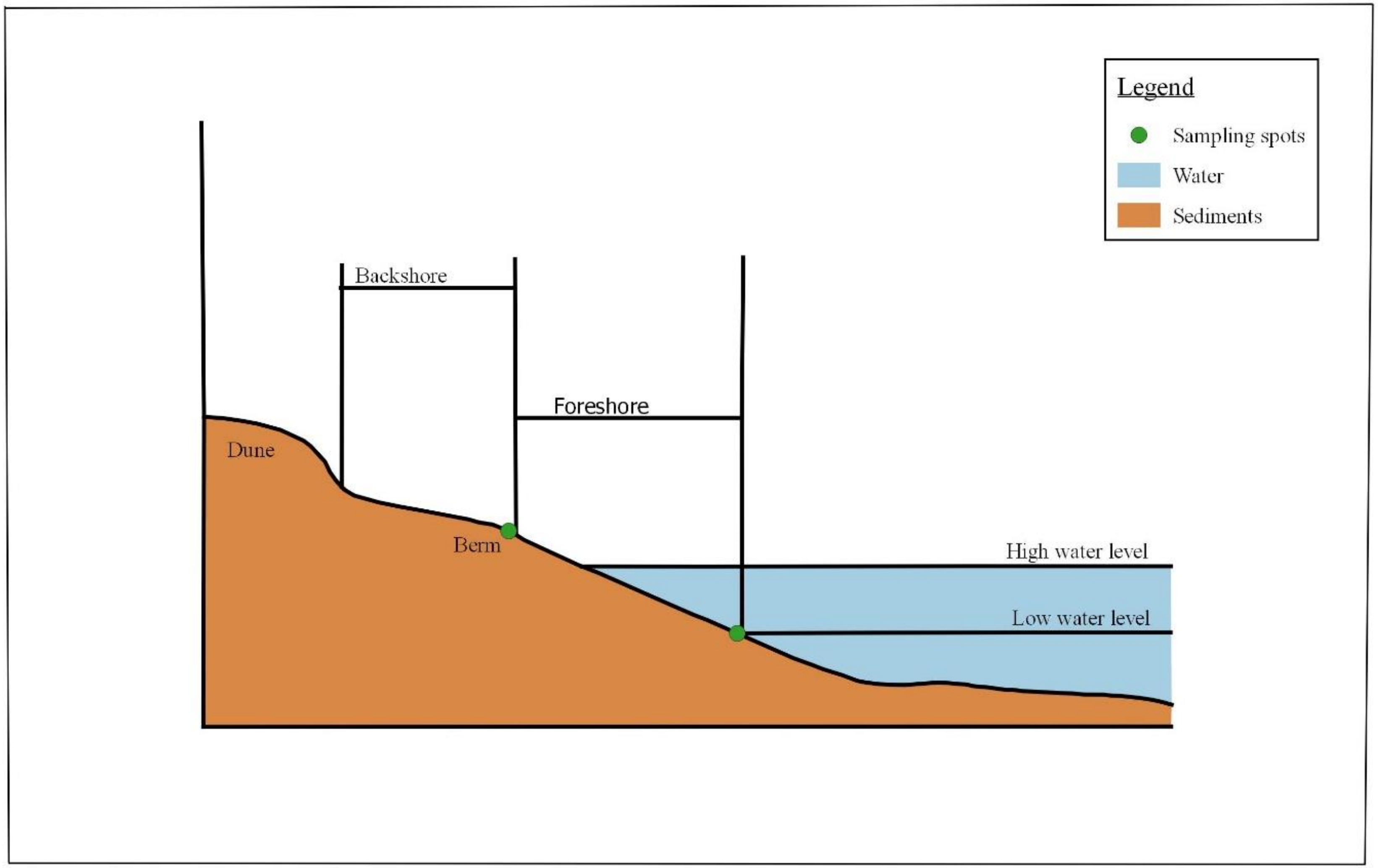

Figure 3.3 Beach profile map showing sampling locations (Not to scale)

each) were collected, labelled, and transported in ziplock bags. Samples S1 and S2 are from the riverine side while samples S3 to S9 are from the seaside. Samples S1, S3, S5, S7 and S8 are from the foreshore (FS) while samples S2, S4, S6 and S9 are from the backshore (BS). The backshore was absent at location D due to the presence of tetrapods and seawall. The samples S8 and S9 are from near the headland at the south of the study area (Table 3.2).

3.3 LABORATORY WORK

3.3.1 Washing and Drying of the Sample

After sampling, the samples were wet sieved to wash away silt, clay, and salinity with the help of a 63μm sieve and tap water. The washed samples were then taken in a petri dish and kept for drying in an oven at 60 ^{0}C until complete dryness. Once dried, coning and quartering were done to homogenise the samples and to remove lumps, if any. Small stones, shells, sticks, and stems were removed with the help of forceps. 50 g of sample was taken from one quarter in a teflon beaker for pre-treatment.

3.3.2 Pre-treatment **(Folk,1968)**

The samples were treated with 40ml, 50% HCl for removing calcareous and ferruginous material for about 10 minutes in the fume hood and 10 mins over the hot plate at 120 ^{0}C. After 10 mins, the acid was decanted, and the samples were washed 3 to 4 times with distilled water to wash away the acid completely taking care that no sediment was lost. For the removal of siliceous cement (authigenic material), the samples were treated with 40ml, 100% KOH (40g of KOH made up to 40ml with

Table 3.2 Sample Locations

Location		**Foreshore**	**Backshore**
A	Riverine side	S1	S2
B	Beach	S3	S4
C	Beach	S5	S6
D	Beach	S7	-
E	Beach, near the headland	S8	S9

Figure 3.4 a. Core sample being collected from the foreshore near the headland (Location E) at Keri Beach

Figure 3.4 b. A core of 10 cm taken from the foreshore at Keri Beach

Figure 3.5 Pit exposing the laminations of heavy and light minerals

Figure 3.6 Sandspit formed at the mouth of the Terekhol River (Location A)

distilled water) for 10 mins in the fume hood. KOH was decanted followed by washing of the samples with distilled water. Lastly, the samples were treated with 40ml, 30% H_2O_2 overnight to remove the organic matter. The following day, H_2O_2 was decanted followed by washing of the samples with distilled water. The samples were then kept for drying in a petri dish in an oven at 60 ºC until completely dry.

3.3.3 Sieving **(Folk, 1968)**

The treated samples were sieved with the help of sieves (ASTM No. 35,60 and 230) and a vibrator sieve shaker (Fritsch analysette 3) for 30 mins at an amplitude of 0.1. The sediments were divided into 3 fractions:

Fraction 1(F1): Coarse sand (>500µm)

Fraction 2(F2): Medium sand (<500µm - >250µm)

Fraction 3(F3): Fine sand (<250µm - >63µm)

3.3.4 Heavy Mineral Separation **(Mueller,1967)**

After sieve analysis, the heavy minerals from all the fractions of each sample were separated using the heavy liquid, bromoform (sp.gr. 2.88). The apparatus was cleaned with distilled water and acetone before use to prevent contamination of the sample. The separating funnel was filled 2/3rd with bromoform. The sample was added to it and stirred vigorously. The heavy minerals were allowed to settle down for about 10 mins. After that, the knob of the separating funnel was opened allowing the heavy minerals to flow out which were collected on a filter paper. The heavy minerals were first washed with ethanol to remove the effect of bromoform and then with acetone to prevent contamination. The filter paper was kept for drying in an oven at 60 ºC until completely dry. The dried heavy minerals were weighed.

3.3.5 Magnetic Separation

The magnetic minerals were separated using a hand-magnet. For the separation, a neodymium magnet covered in tissue paper was moved over the samples. The magnetic heavy minerals (MHM) which got attracted to the magnet were separated out and weighed. The non-magnetic heavy minerals (NHM) left behind were also weighed.

3.3.6 Sample Preparation for X-Ray Diffraction

The magnetic minerals from the finest fraction (F3) from all the samples (S1 to S9) were powdered using agate mortar and pestle to a fine and uniform flour-like size. The powdered samples were then transferred into sterilized vials of 2ml capacity.

3.3.7 X-Ray Diffraction (XRD)

The XRD Analysis was done in the School of Chemical Sciences, Goa University using the instrument PXRD Rigaku Smartlab. The powdered samples from the vials were transferred to alcohol-cleansed XRD slides. The samples were pressed with a glass slide to make the surface smooth and uniform. The samples were then run for 15 minutes within 2-theta range of 20-65. The intensity values obtained were plotted against the 2-theta angles in the Origin 2024 software (License No. KCE635590913F0A0). The peaks were identified with the help of reference data

(obtained from the websites rruff.info and https://rruff.geo.arizona.edu/AMS/amcsd.php). The intensity percentage of the peaks was calculated using the formula:

(Peak intensity/highest peak intensity) *100 (%)

The highest peak's intensity percentage for a given mineral is always considered to be 100% **(obtained from the website http://prism.mit.edu/xray)**.

3.3.8 Identification of Transparent Minerals

The microscopic study was carried out under the stereo zoom microscope (Olympus SZX16) in the School of Earth, Ocean and Atmospheric Sciences, Goa University. Physical properties such as colour, lustre, habit, and surface features are observed, studied, and recorded by microphotography. The finest fractions (F3) of all the samples were used for identifying the minerals as they preserved the habit of the minerals. The minerals identified were classified into four categories, namely, abundant, common, rare, and absent based on their frequency of occurrence in the subsample by visual interpretation/observation. Photographs of the minerals were taken with the help of the camera (Magcam DC 5) connected to the stereo-zoom.

3.4 PROVENANCE

The possible provenance of the identified minerals, opaque and transparent, was established by studying the lithostratigraphy and mineralogy of the hinterland, riverbed, and catchment area rocks from the literature.

RESULTS

CHAPTER 4: RESULTS

4.1 PRE-TREATMENT

The loss in the weight of sediments due to their treatment with hydrochloric acid, potassium hydroxide and hydrogen peroxide to remove calcareous shells and cement, ferruginous cement, siliceous cement, and organic matter varies between 0.68g (1.36%) to 3.83g (7.66%). The reduction is minimal in sample S2 which is from the backshore region of Location A while the maximum loss is in the sediments from sample S7 which is from the foreshore of Location D (Table 4.1).

4.2 SIEVE ANALYSIS

Sieve analysis was done to check the distribution and percentage of various sand types (coarse sand, medium sand, and fine sand) in the sediments of Keri Beach. Medium Sand (250-500 μm) is abundant in all the samples. S1 which is from the mouth region of Terekhol River (sample from the sandspit at Location A) consists of 42% of medium sand and 52% of coarse sand with minor amounts of fine sand (Figure 4.1 a). It is the sample showing the highest coarse sand and lowest fine sand percentage. The coarse sand percentage in the other samples varies between 0.08 to 19. S2 consists of 59% of medium sand and 38% of fine sand (Figure 4.1 b). S3 is dominant in medium sand with a percentage of 49 and consists of 42% of fine sand (Figure 4.1 c). S4 shows 58% of medium sand and 37% of fine sand (Figure 4.1 d). S5 contains 57% of medium sand and 30% of fine sand (Figure 4.1 e). S6 has 38% of medium sand and highest amounts of fine sand (59%) among all the samples (Figure

Table 4.1. Loss of sediments during pre-treatment

Sample No.	**Original weight (g)**	**Post-treatment weight (g)**	**Loss (g)**	**Loss%**
S1	50	49	1	2
S2	50	49.32	0.68	1.36
S3	50	48.05	1.95	3.9
S4	50	48.57	1.43	2.89
S5	50	48.91	1.09	2.18
S6	50	48.46	1.54	3.08
S7	50	46.17	3.83	7.66
S8	50	48.17	1.83	3.66
S9	50	47.94	2.06	4.12

4.1 f). S7 is dominant in medium sand with a percentage of 65% and a low fine sand percentage of 8% (Figure 4.1 g).

S8 has the highest amount of medium sand (66%) among all the samples and a low fine sand content of 12% (Figure 4.1 h). S7 and S8 have higher coarse sand as compared to fine sand. S9 shows 40% of medium sand and 56% of fine sand (Figure 4.1 i). It contains the lowest amount of coarse sand (0.08%) among all the samples.

S1 is dominant in coarse sand. S2, S3, S4, S5, S7, S8 are dominant in medium sand while S6 and S9 are dominant in fine sand. At any given location, the backshore samples have a higher percentage of fine sand and a lower percentage of coarse sand compared to the foreshore samples. This may not be true for Location D as it did not show a berm during the sampling period leading to the absence of a backshore.

4.3 HEAVY MINERAL DISTRIBUTION

The heavy minerals were separated from the light minerals from all the 3 sand fractions from all samples (S1-S9). The percentage of light and heavy minerals in the individual sand fractions from all the samples is given in Table 4.2. In all the samples, light minerals are dominant over heavy minerals (Table 4.3). The total heavy mineral (THM) percentage in the study area varies between 6.2024 and 46.198. It is observed that the ratio of heavy to light minerals increases as the sand size decreases with an exception in samples S3 and S9.

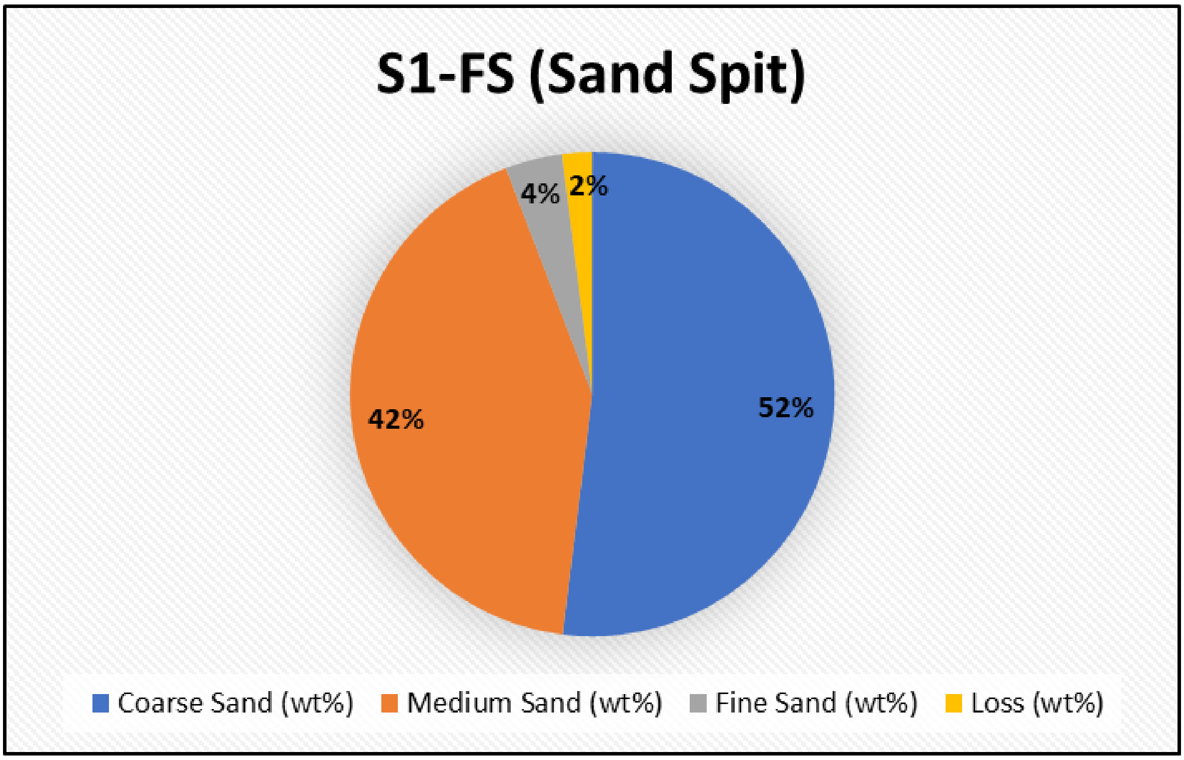

Figure 4.1 a. Distribution of different sand fractions in sample S1-FS (Location A)

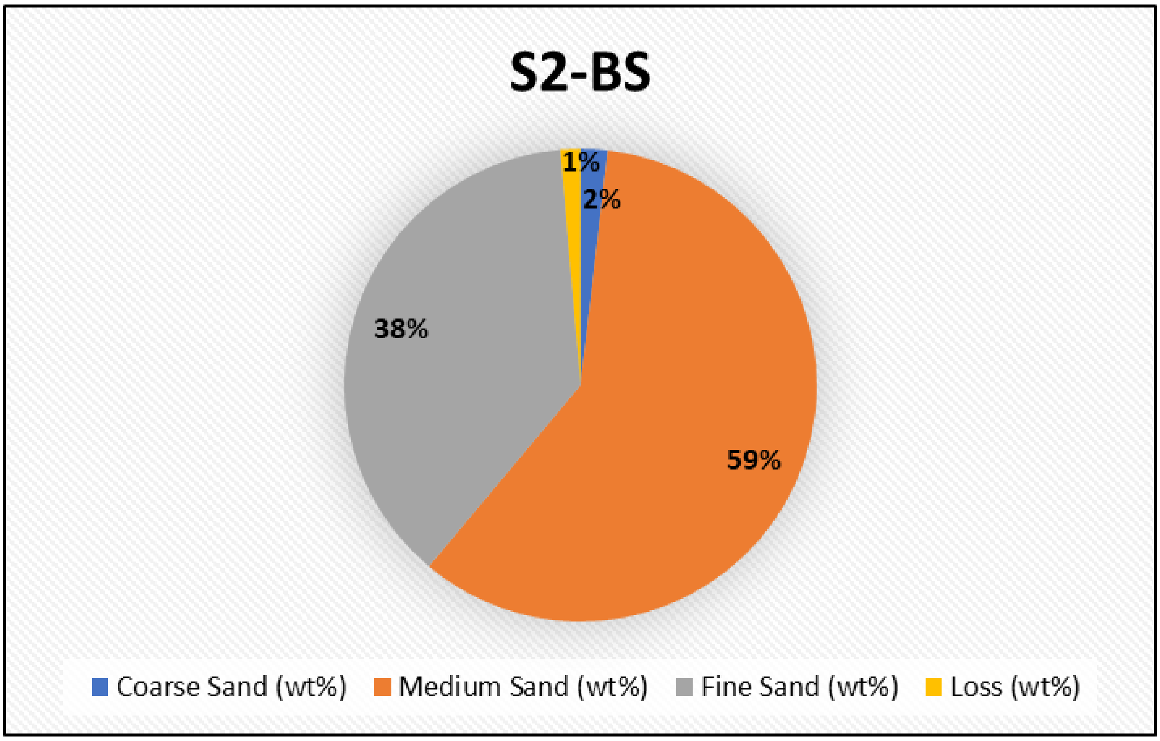

Figure 4.1 b. Distribution of different sand fractions in sample S2-BS (Location A)

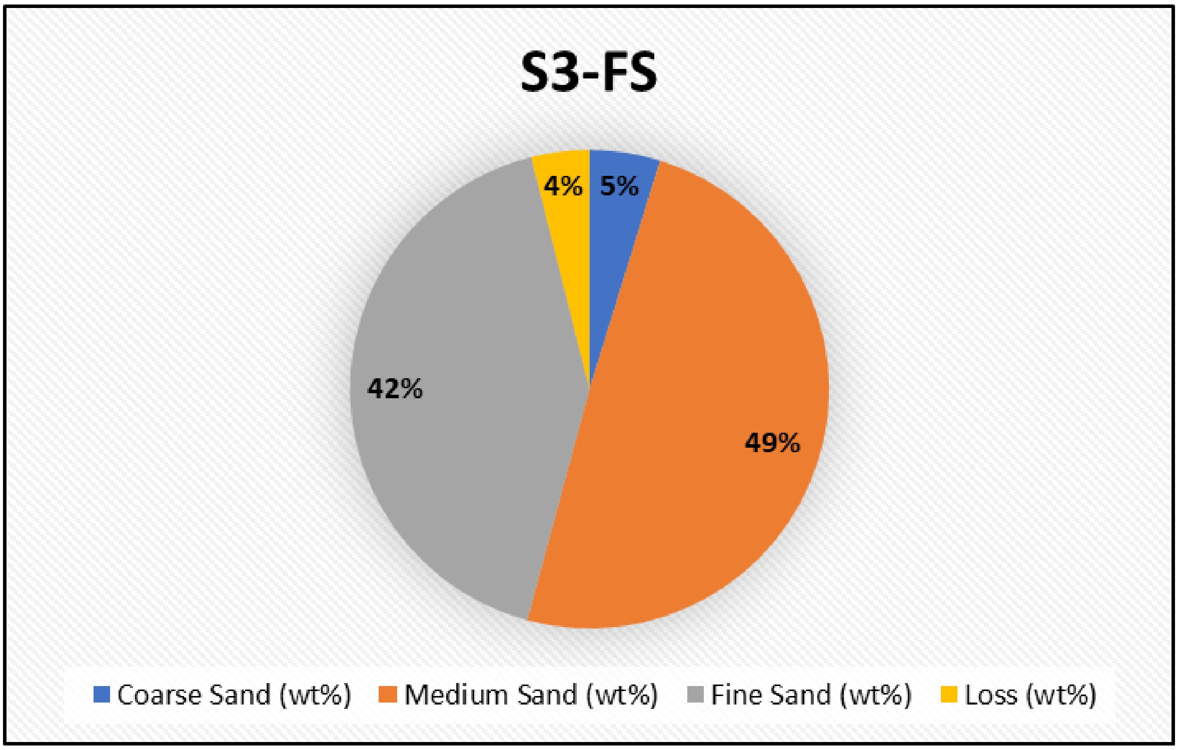

Figure 4.1 c. Distribution of different sand fractions in sample S3-FS (Location B)

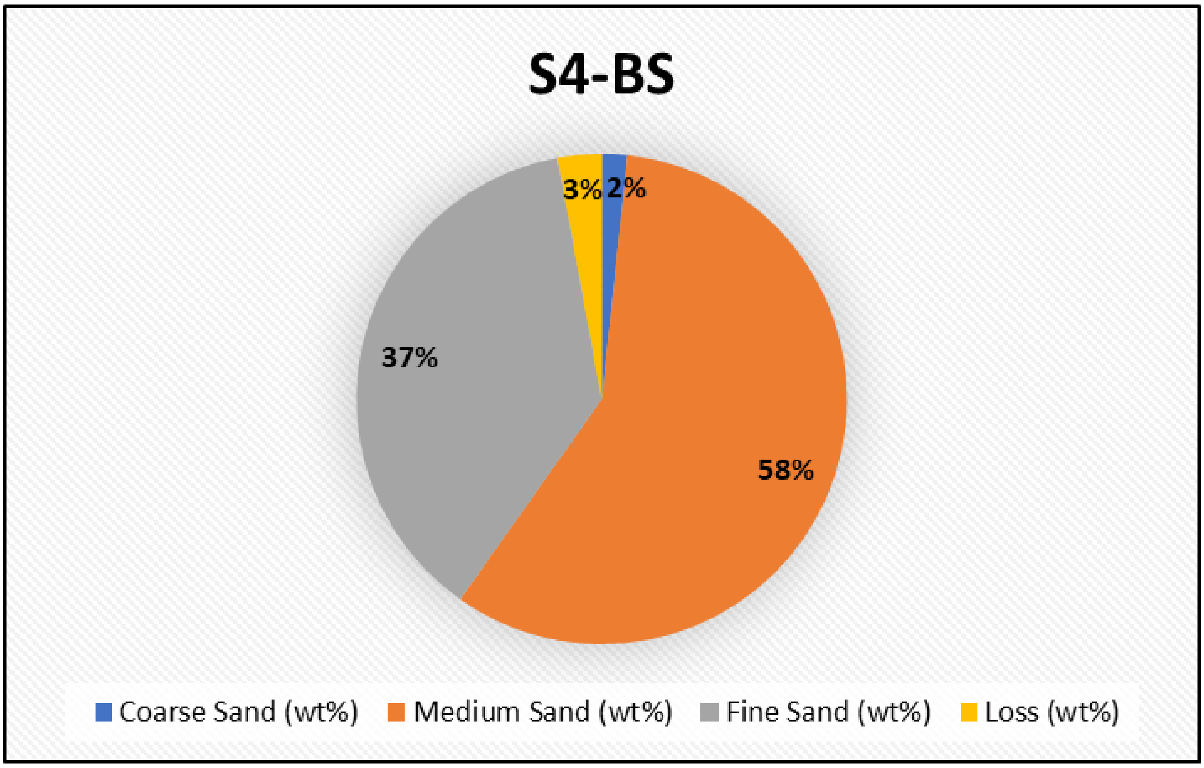

Figure 4.1 d. Distribution of different sand fractions in sample S4-BS (Location B)

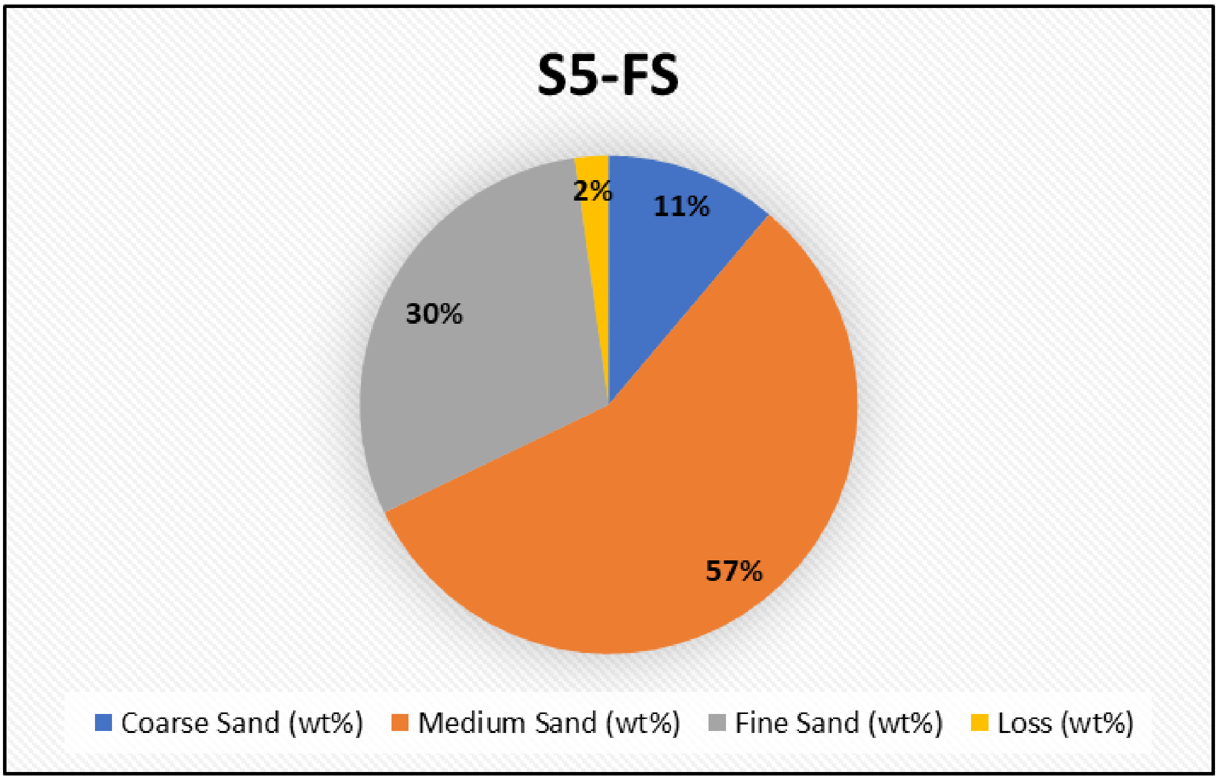

Figure 4.1 e. Distribution of different sand fractions in sample S5-FS (Location C)

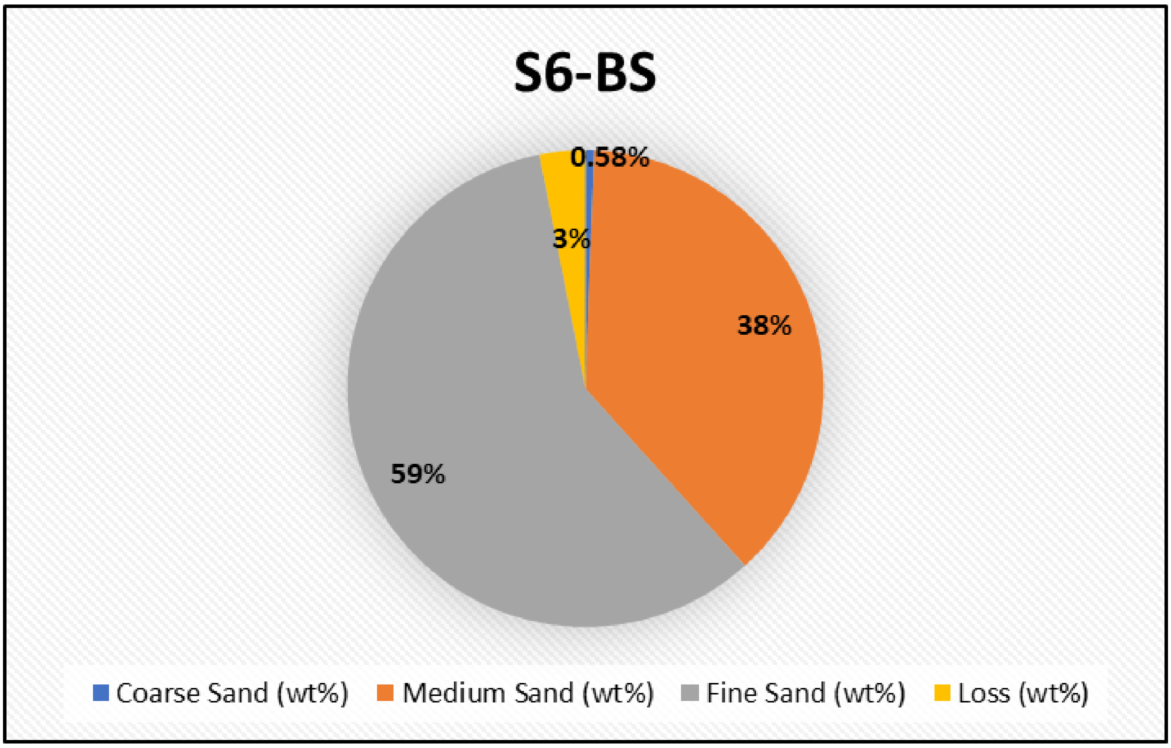

Figure 4.1 f. Distribution of different sand fractions in sample S6-BS (Location C)

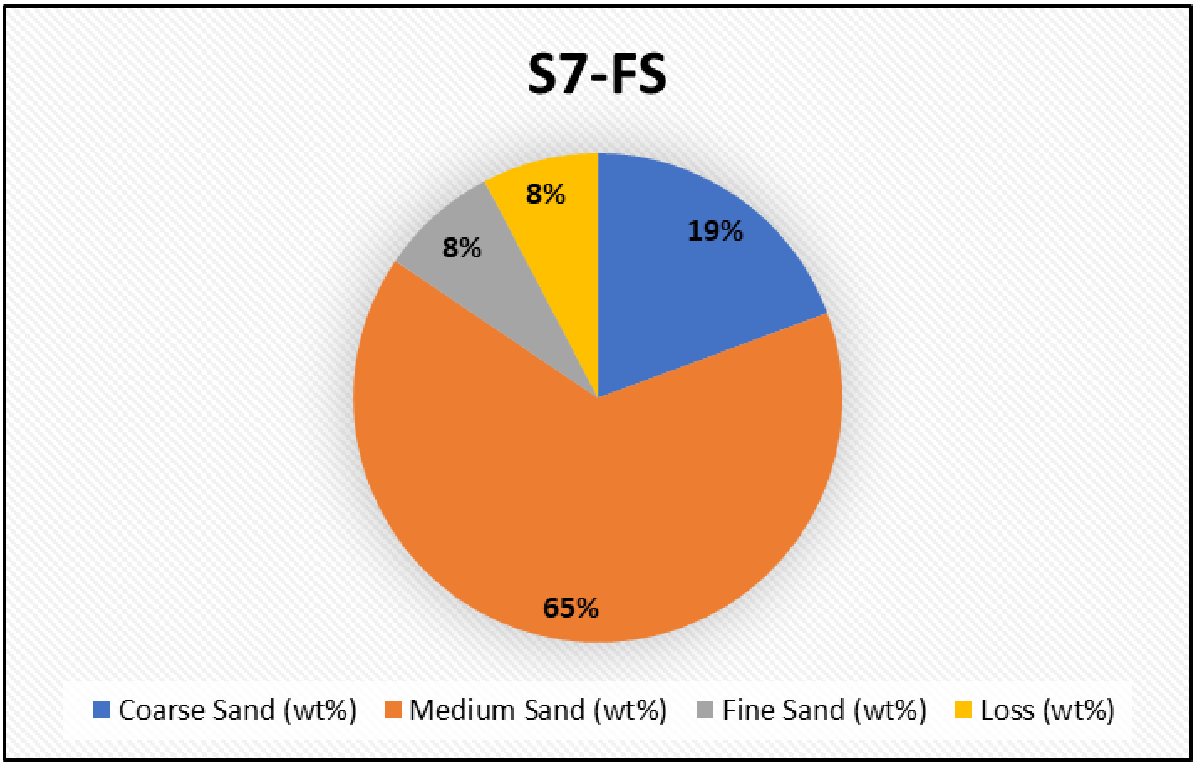

Figure 4.1 g. Distribution of different sand fractions in sample S7-FS (Location D)

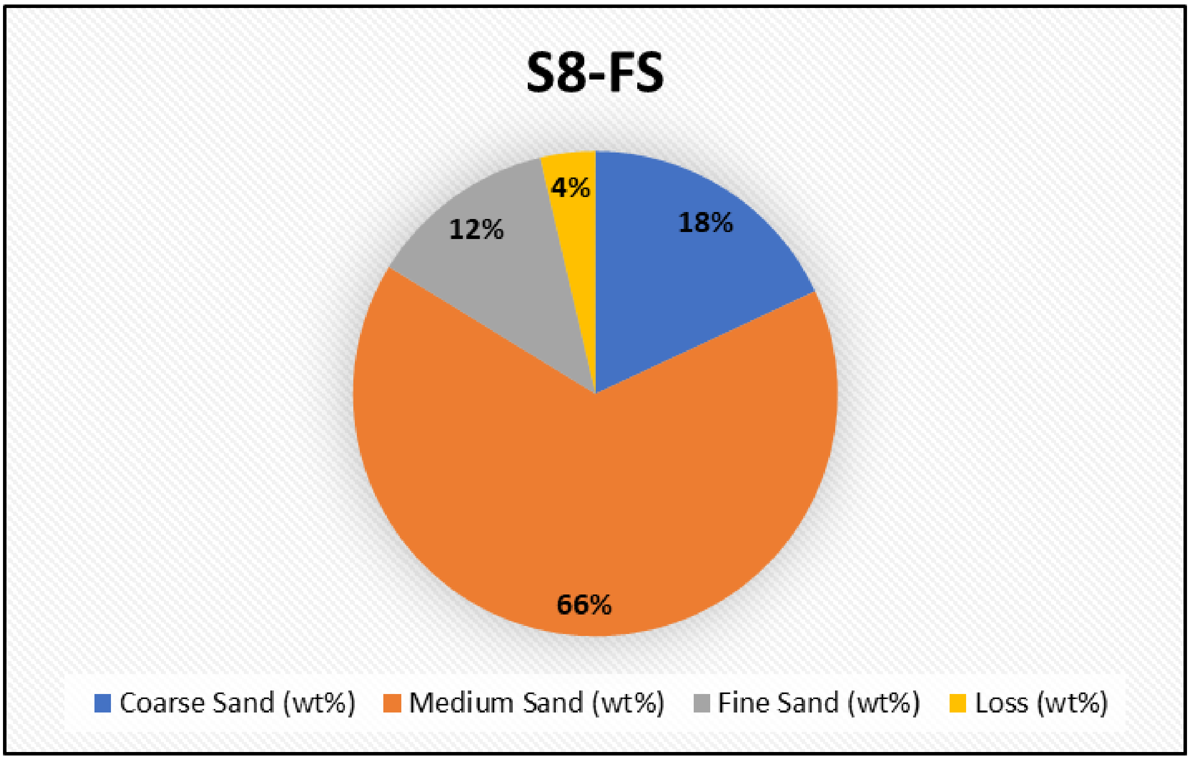

Figure 4.1 h. Distribution of different sand fractions in sample S8-FS (Location E)

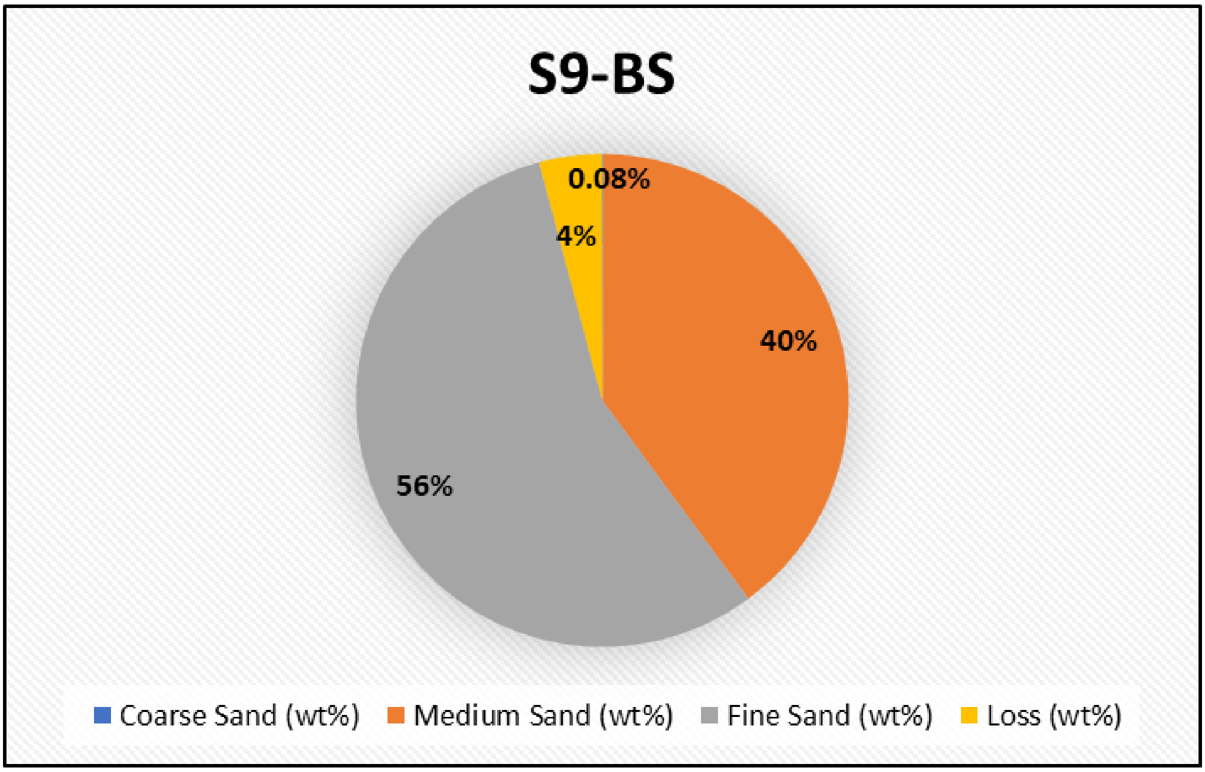

Figure 4.1 i. Distribution of different sand fractions in sample S9-BS (Location E)

Table 4.2 Percentage of heavy and light minerals in individual sand fractions

Sample No.	**Heavy Mineral Percentage (wt. %)**			**Light Mineral Percentage (wt. %)**		
	F1	**F2**	**F3**	**F1**	**F2**	**F3**
S1	3.718	8.514	17.958	96.075	91.321	81.574
S2	9.62	18.825	72.165	88.348	80.921	27.682
S3	4.489	4.163	14.069	91.852	95.74	85.875
S4	5.071	11.99	66.032	94.417	87.857	33.896
S5	2.862	3.757	27.75	97.239	96.053	72.253
S6	6.552	18.001	67.506	91.655	81.839	32.495
S7	4.680	4.685	26.606	95.281	95.14	73.010
S8	4.115	4.181	13.338	95.747	95.734	84.415
S9	16.75	10.31	23.001	82.5	89.483	75.558

Table 4.3 Contribution of heavy minerals (in percentage) by each fraction of sand as calculated for 50 grams of sample

Sample No.	F1	F2	F3	THM (wt.%)	TLM (wt.%)
S1	1.93	3.59	0.6824	6.2024	91.7976
S2	0.177	11.16	27.09	38.427	60.213
S3	0.2128	2.05	5.87	8.1328	87.9672
S4	0.0852	6.95	24.56	31.5952	65.5148
S5	0.3182	2.13	8.28	10.7282	87.0918
S6	0.038	6.76	39.4	46.198	50.722
S7	0.9052	3.05	2.0912	6.0464	86.2936
S8	0.7416	2.74	1.67	5.1516	91.1884
S9	0.0134	4.1	12.85	16.9634	78.9166

From Figure 4.2, it is clear that the backshore samples (S2, S4, S6, S9) have a higher percentage of heavy minerals as compared to the foreshore samples (S1, S3, S5, S7, S8). It is also observed that Location C has the highest concentration of heavy minerals in the study area in both foreshore and backshore regions.

Figures 4.3 b, c, d, e, f and i show that in all the samples, the highest contributor of heavy minerals to the total heavy mineral content in the sample is the fine sand fraction, however, that is not the case in samples S1, S7 and S8 as the total amount of fine sand in these samples is much lower as compared to the other samples. Thus, they do not show the same trend. The highest contributor of heavy minerals to the total mineral content in samples S1, S7 and S8 is medium sand.

Table 4.4 shows that all the samples dominantly consist of magnetic heavy minerals (>86%) while non-magnetic heavy minerals vary between 3.74% to 13.614%.

Just like the heavy minerals a general trend of increase in magnetic minerals and non-magnetic minerals is observed with a decrease in grain size (Table 4.5). S1, S7 and S8 show an exception where the highest contribution of heavy minerals comes from the medium sand fraction.

4.4 MAGNETIC MINERALS

The peaks of the magnetic minerals from the X-ray diffractograms (Figures 4.4 a-i) of all the finest magnetic fractions (S1F3-S9F3) were identified by comparing with the reference data. The magnetic mineral suite consists of actinolite, ilmenite, hematite, magnetite, and pyrite. Tables 4.6 shows the minerals and their faces identified along with the angle of their peaks from all samples. Magnetite in Figure 4.4 d. and Actinolite in Figure 4.4 f. show a bimodal peak indicating that they are fresh as well as altered. Scanty peaks of hornblende and pyroxene (augite) are also present but since the analysis is done within a limited theta range, their presence cannot be confirmed.

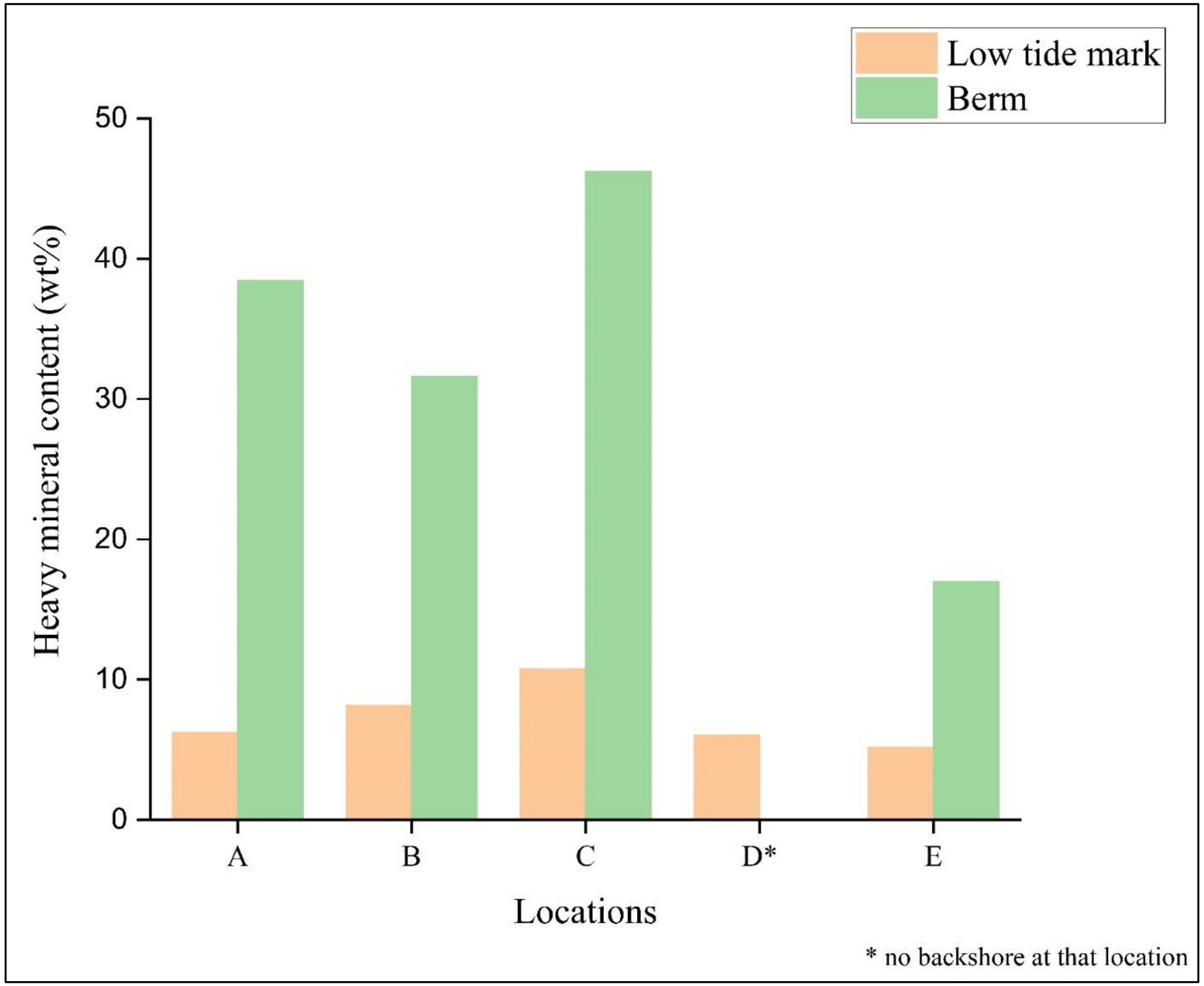

Figure 4.2 Heavy mineral distribution at different physiographic sites at different locations

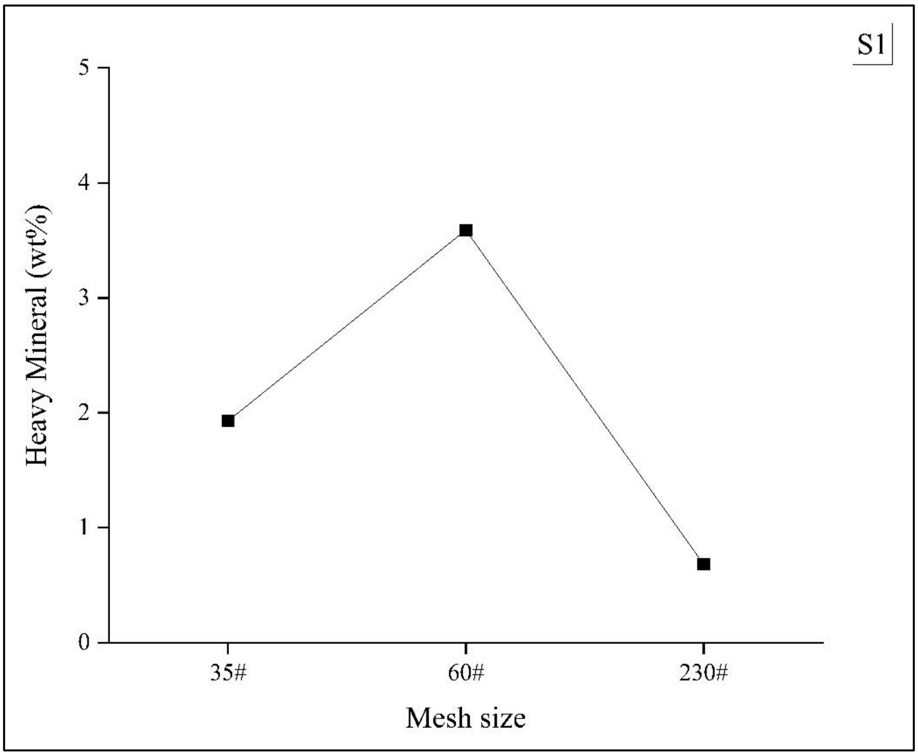

Figure 4.3 a. Heavy mineral distribution in different sand fractions in sample S1-FS

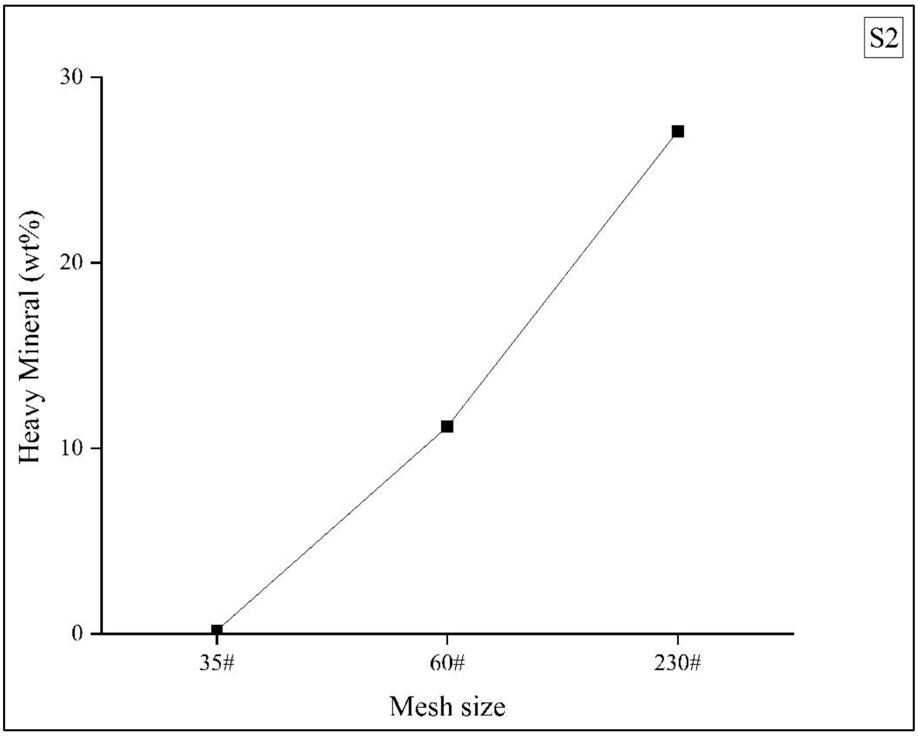

Figure 4.3 b. Heavy mineral distribution in different sand fractions in sample S2-BS

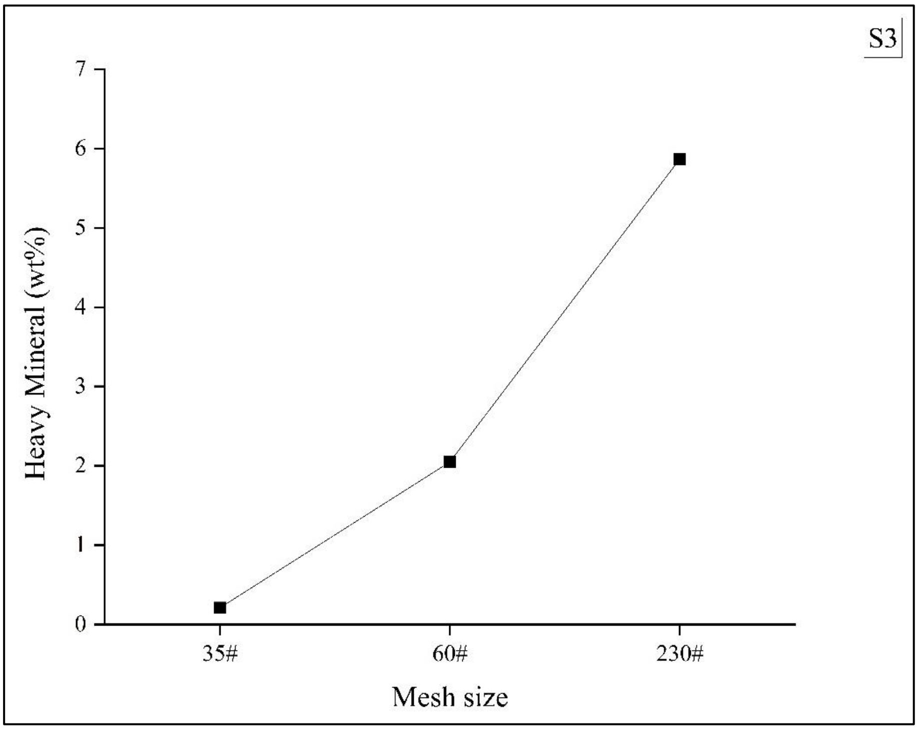

Figure 4.3 c. Heavy mineral distribution in different sand fractions in sample S3-FS

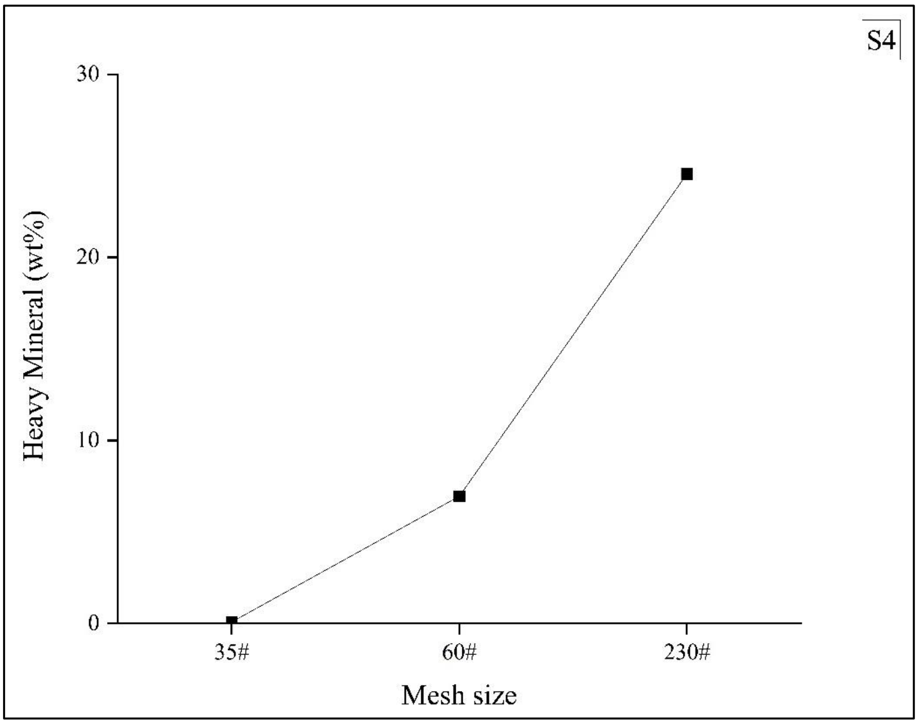

Figure 4.3 d. Heavy mineral distribution in different sand fractions in sample S4-BS

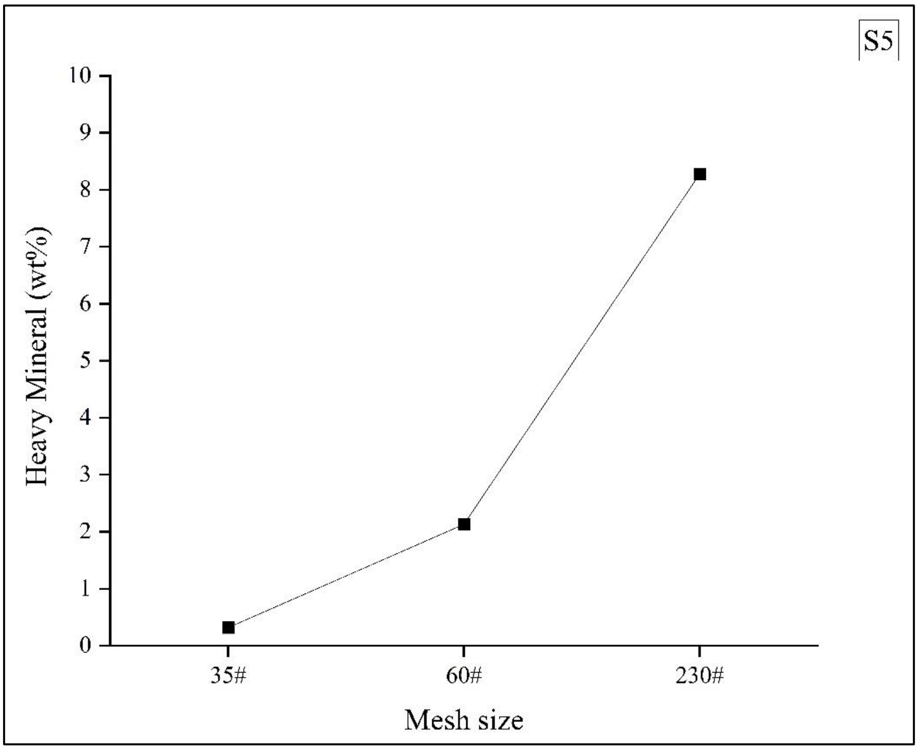

Figure 4.3 e. Heavy mineral distribution in different sand fractions in sample S5-FS

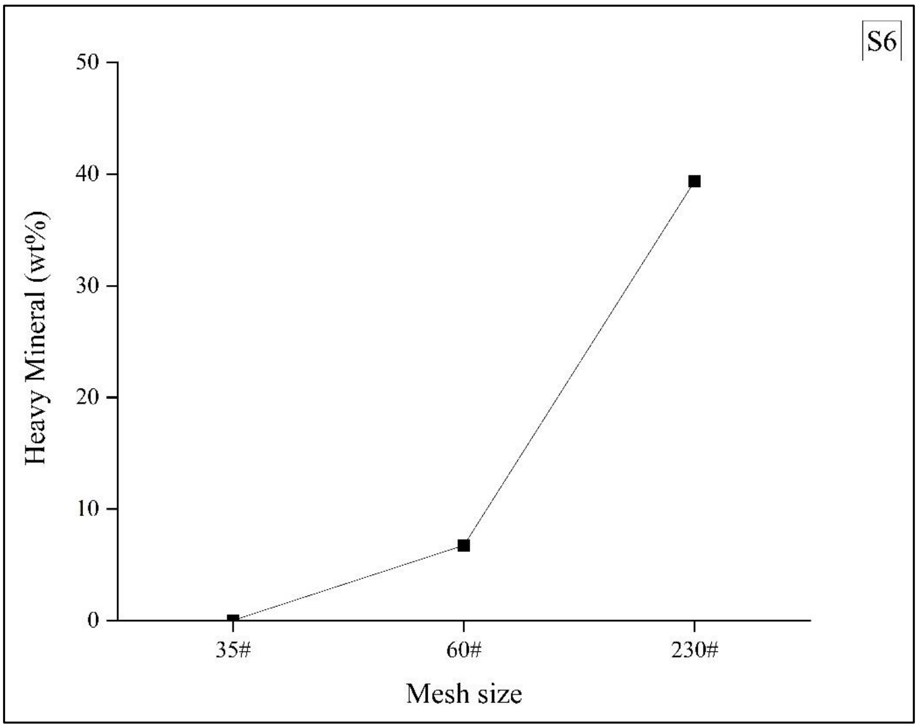

Figure 4.3 f. Heavy mineral distribution in different sand fractions in sample S6-BS

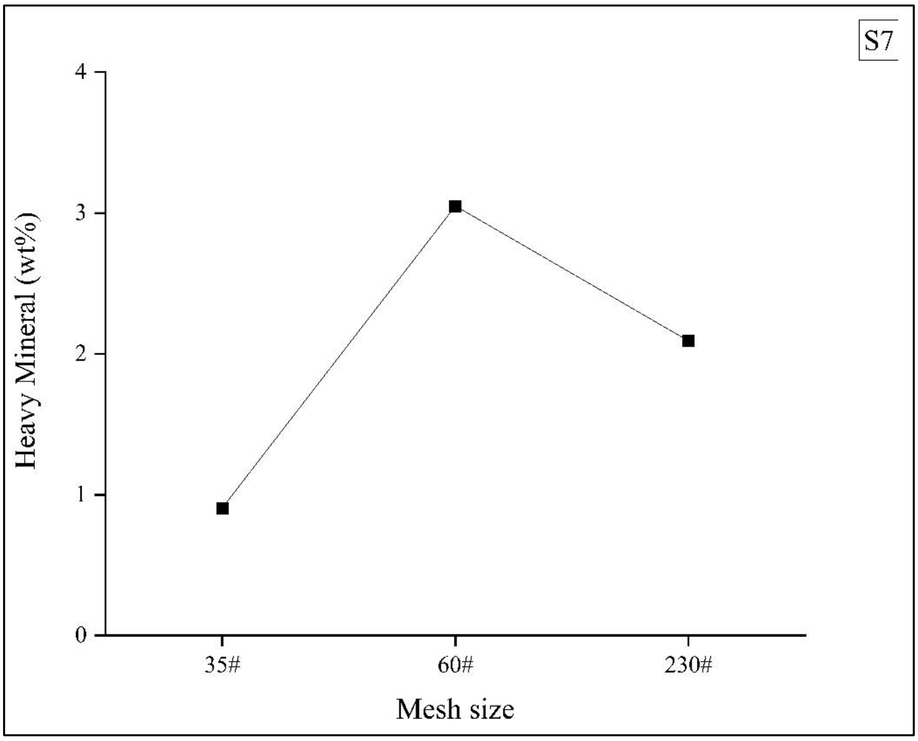

Figure 4.3 g. Heavy mineral distribution in different sand fractions in sample S7-FS

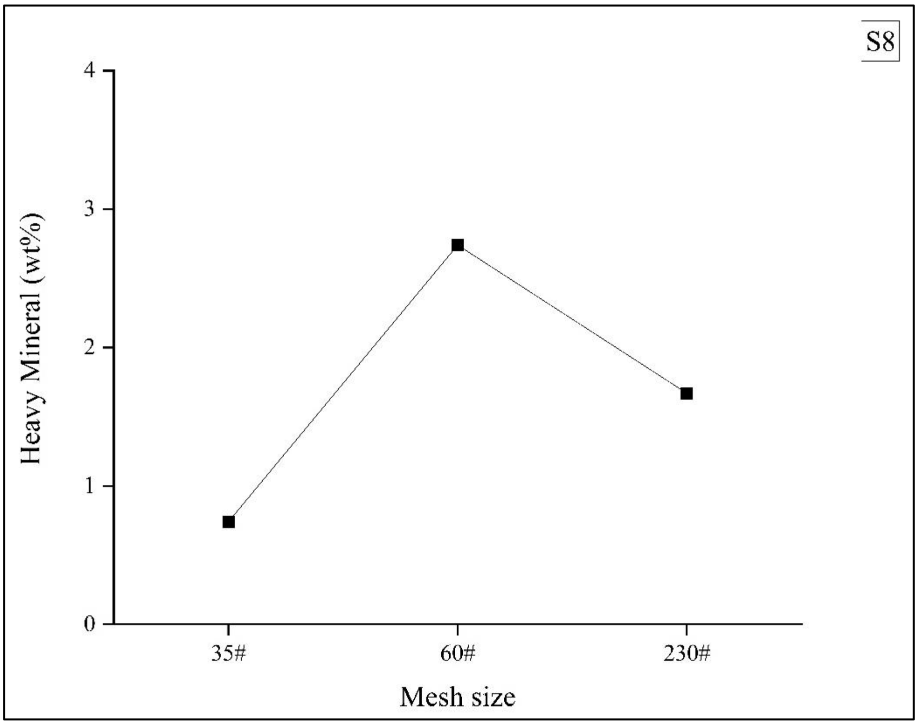

Figure 4.3 h. Heavy mineral distribution in different sand fractions in sample S8-FS

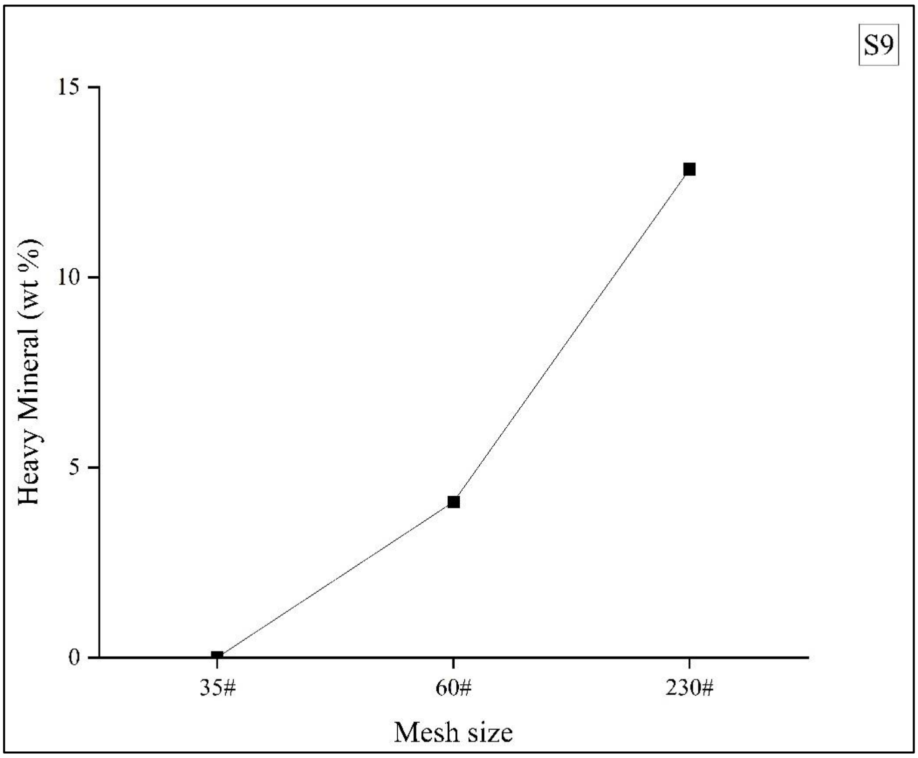

Figure 4.3 i. Heavy mineral distribution in different sand fractions in sample S9-BS

Table 4.4 Percentage of magnetic and non-magnetic heavy minerals in different samples

Sample No.	Total Magnetic Heavy Mineral Percentage (wt%)	Total Non-Magnetic Heavy Mineral Percentage (wt%)
S1	93.589	6.411
S2	95.114	4.886
S3	86.386	13.614
S4	96.256	3.74
S5	93.531	6.469
S6	95.123	4.877
S7	90.055	9.945
S8	88.573	11.427
S9	94.889	5.111

Table 4.5 Contribution of magnetic and non-magnetic minerals (in percentage) by different fractions of sand as calculated for 50 grams of sediment samples

Sample No.	**Magnetic Heavy Minerals (%)**			**Non-magnetic Heavy Minerals (%)**		
	F1	**F2**	**F3**	**F1**	**F2**	**F3**
S1	1.885	3.264	0.665	0.046	0.331	0.018
S2	0.167	9.83	26.263	0.010	1.326	0.828
S3	0.187	1.755	5.077	0.0262	0.294	0.790
S4	0.074	6.445	23.810	0.012	0.502	0.754
S5	0.284	1.938	7.7852	0.034	0.188	0.5
S6	0.031	6.026	38.127	0.007	0.743	1.270
S7	0.745	2.681	1.983	0.16	0.367	0.109
S8	0.601	2.424	1.54	0.141	0.318	0.133
S9	0.013	3.774	12.348	0.0002	0.321	0.500

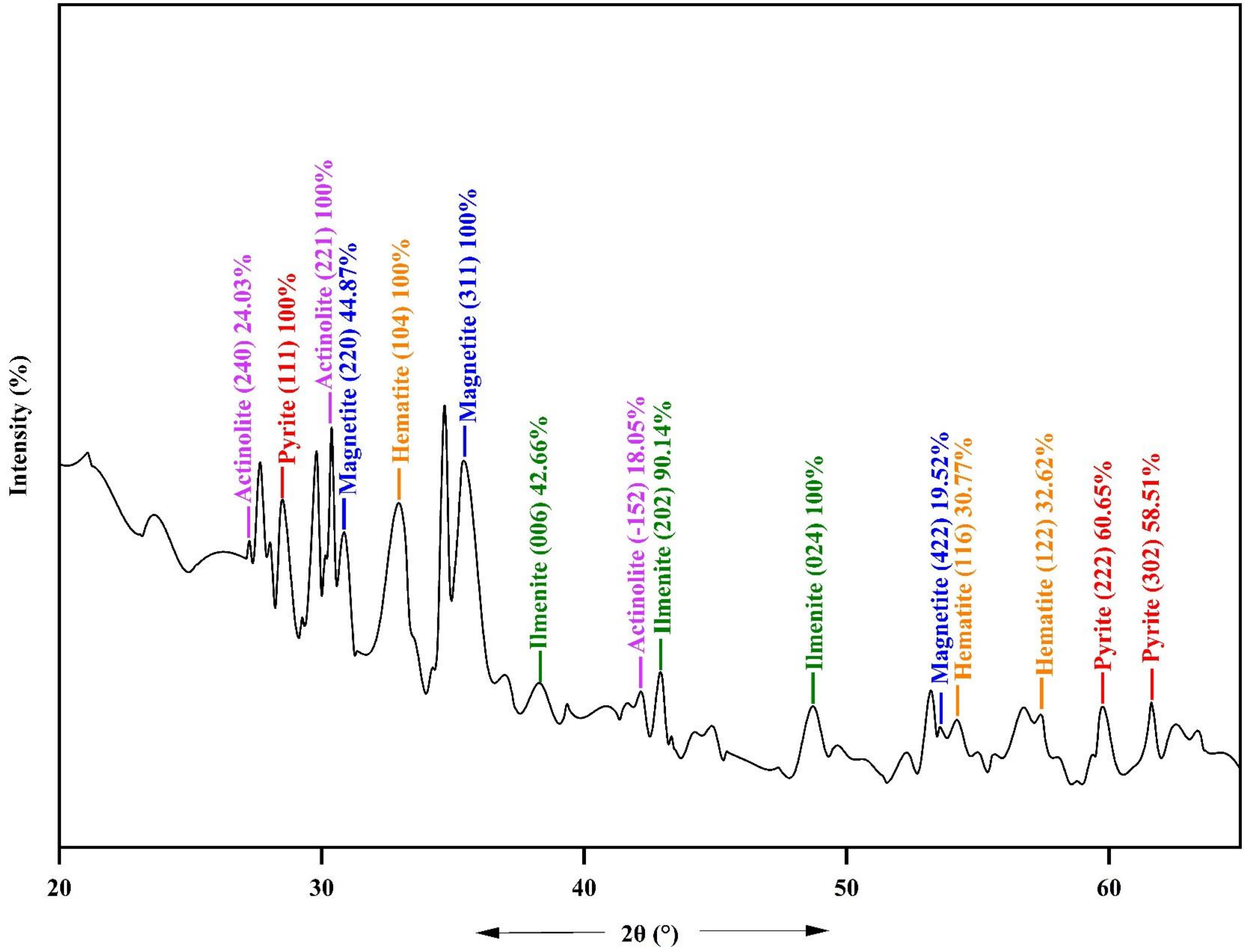

Figure 4.4 a. X-Ray Diffractogram of sample S1F3

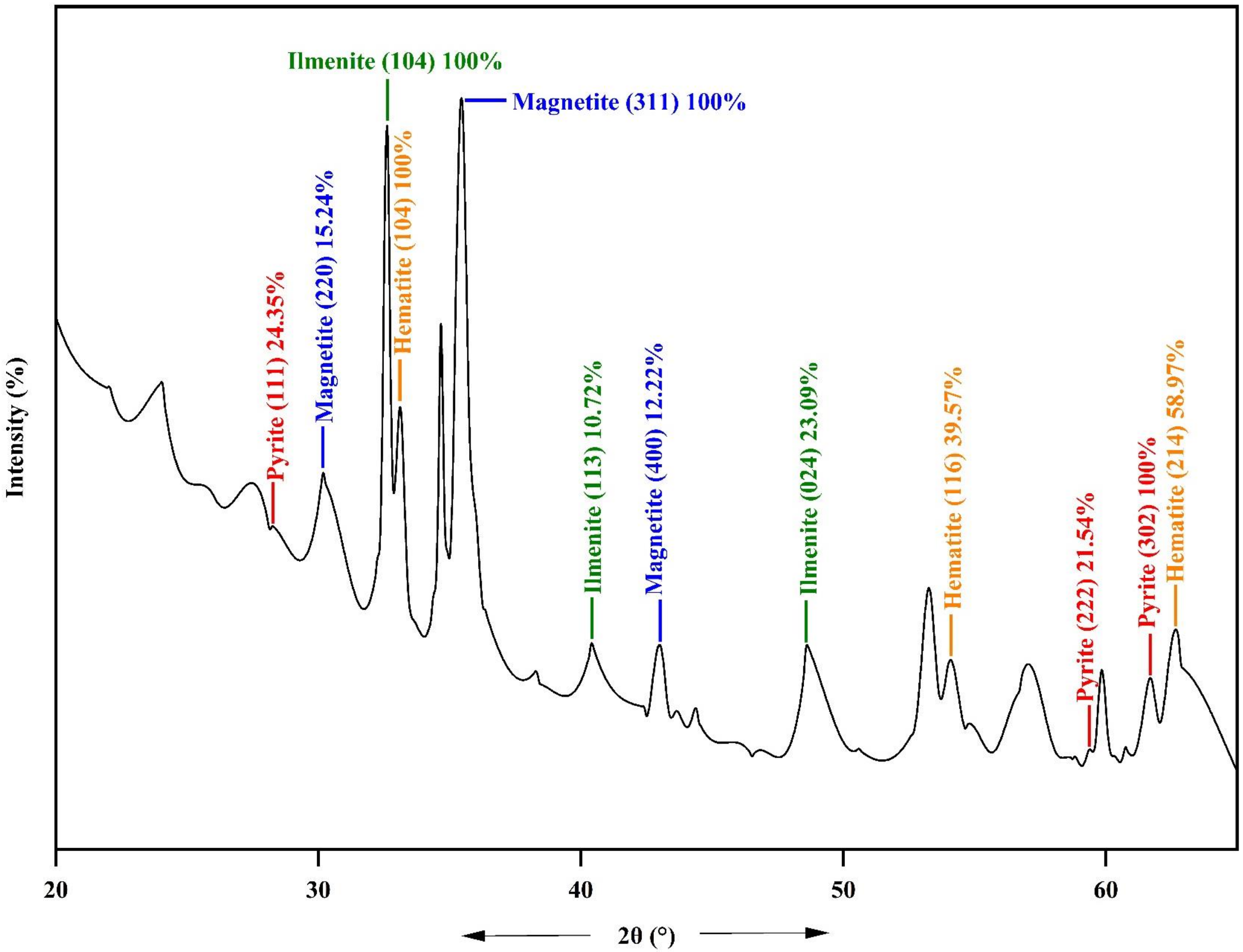

Figure 4.4 b. X-Ray Diffractogram of sample S2F3

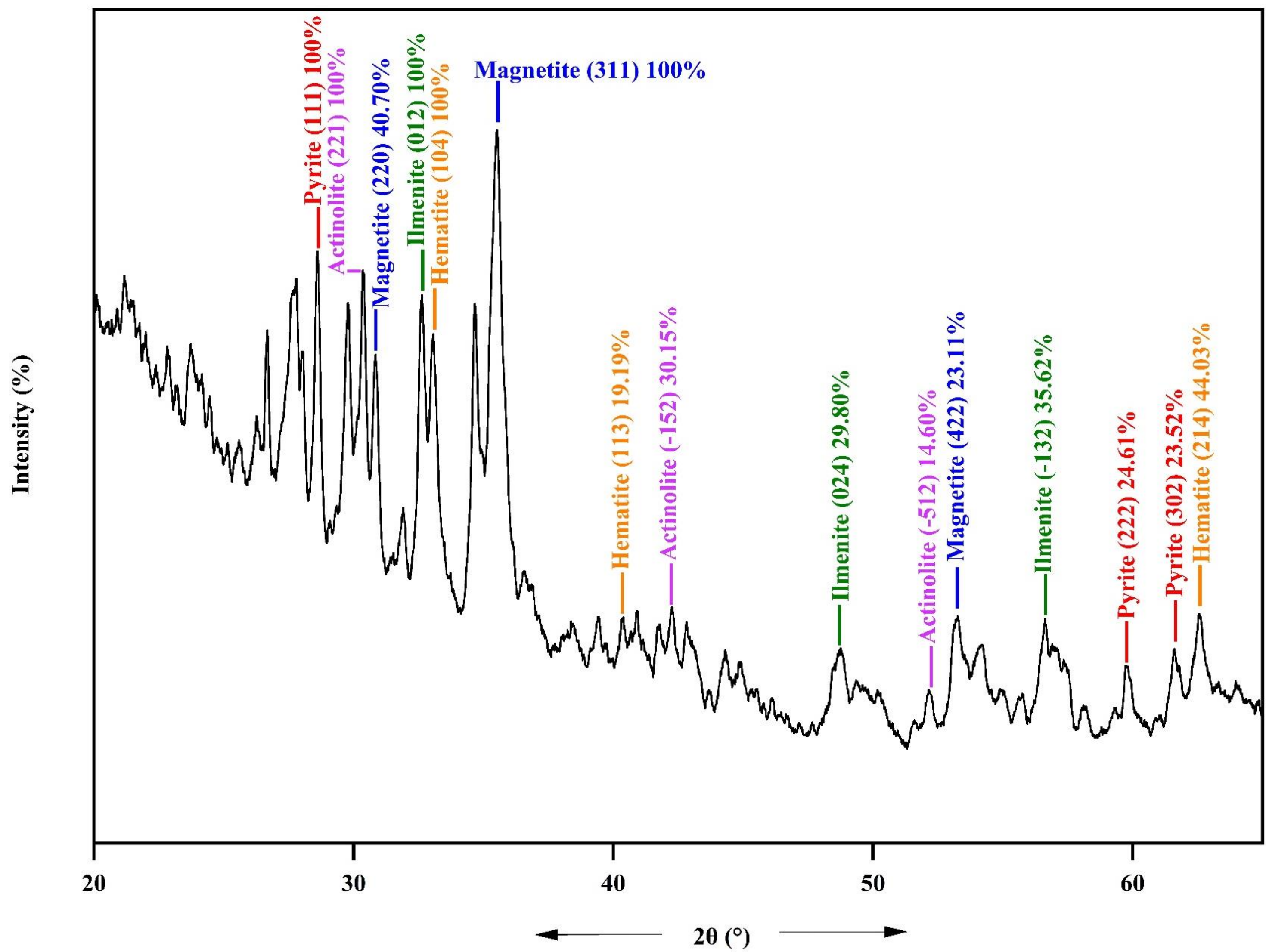

Figure 4.4 c. X-Ray Diffractogram of sample S3F3

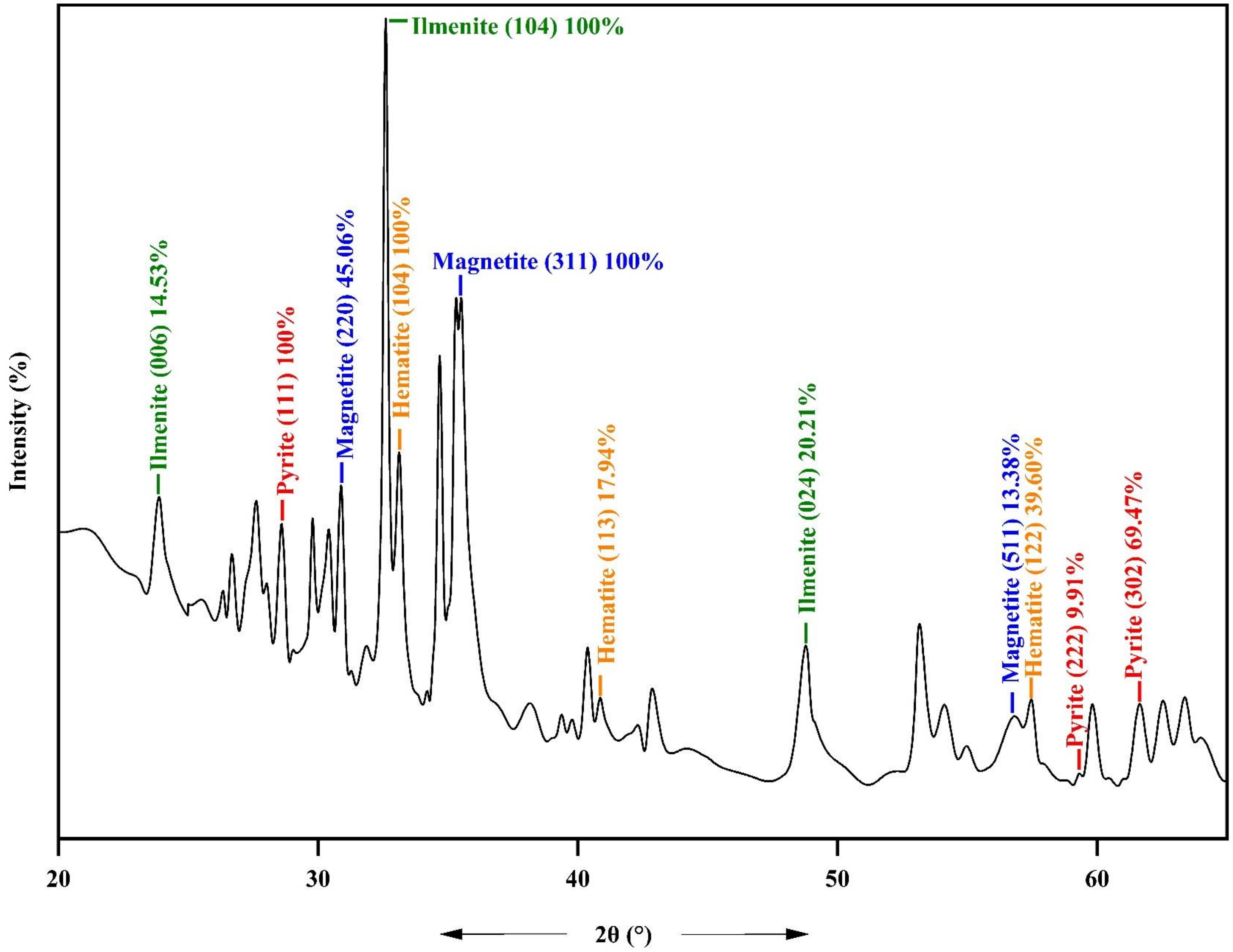

Figure 4.5 d. X-Ray Diffractogram of sample S4F3

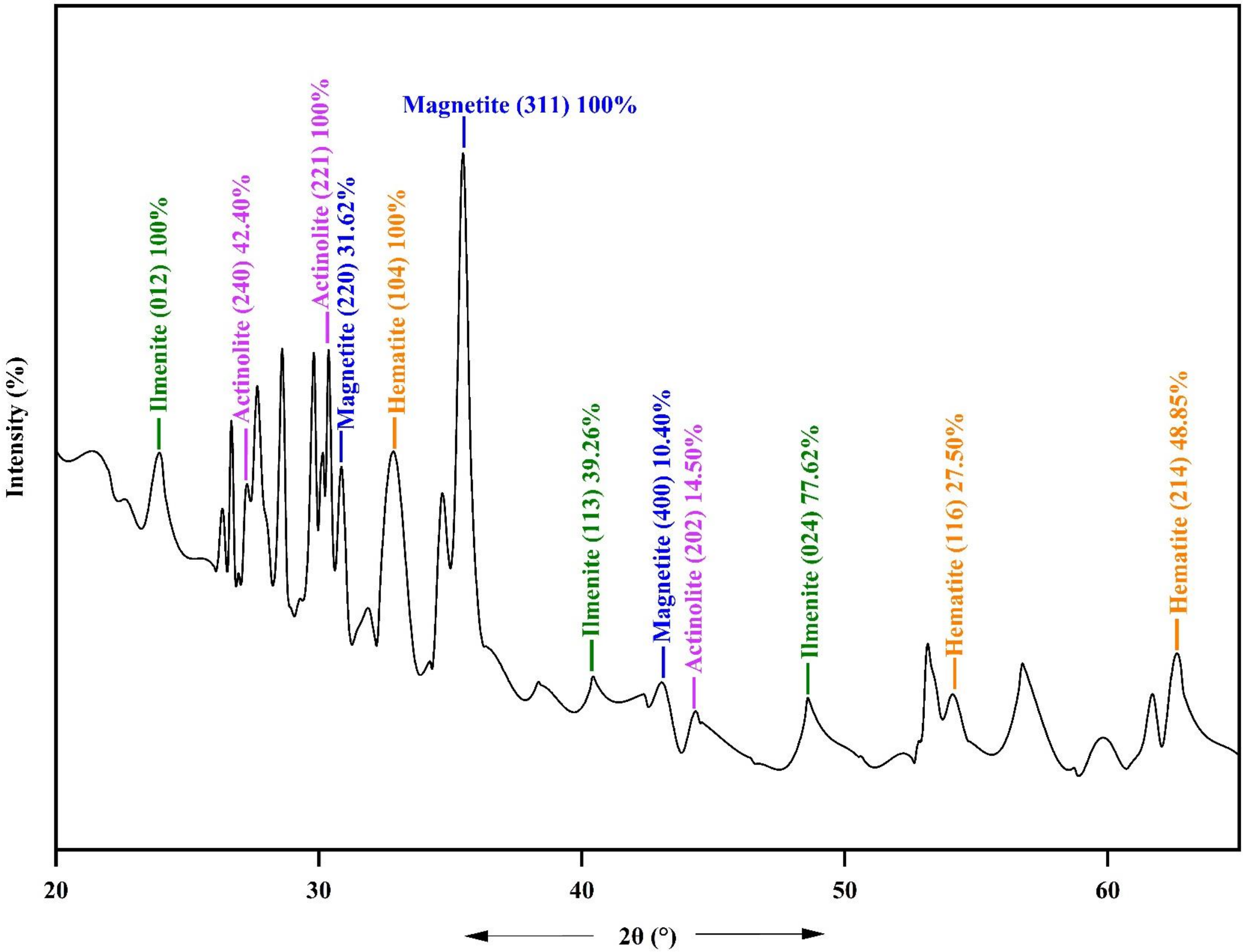

Figure 4.4 e. X-Ray Diffractogram of sample S5F3

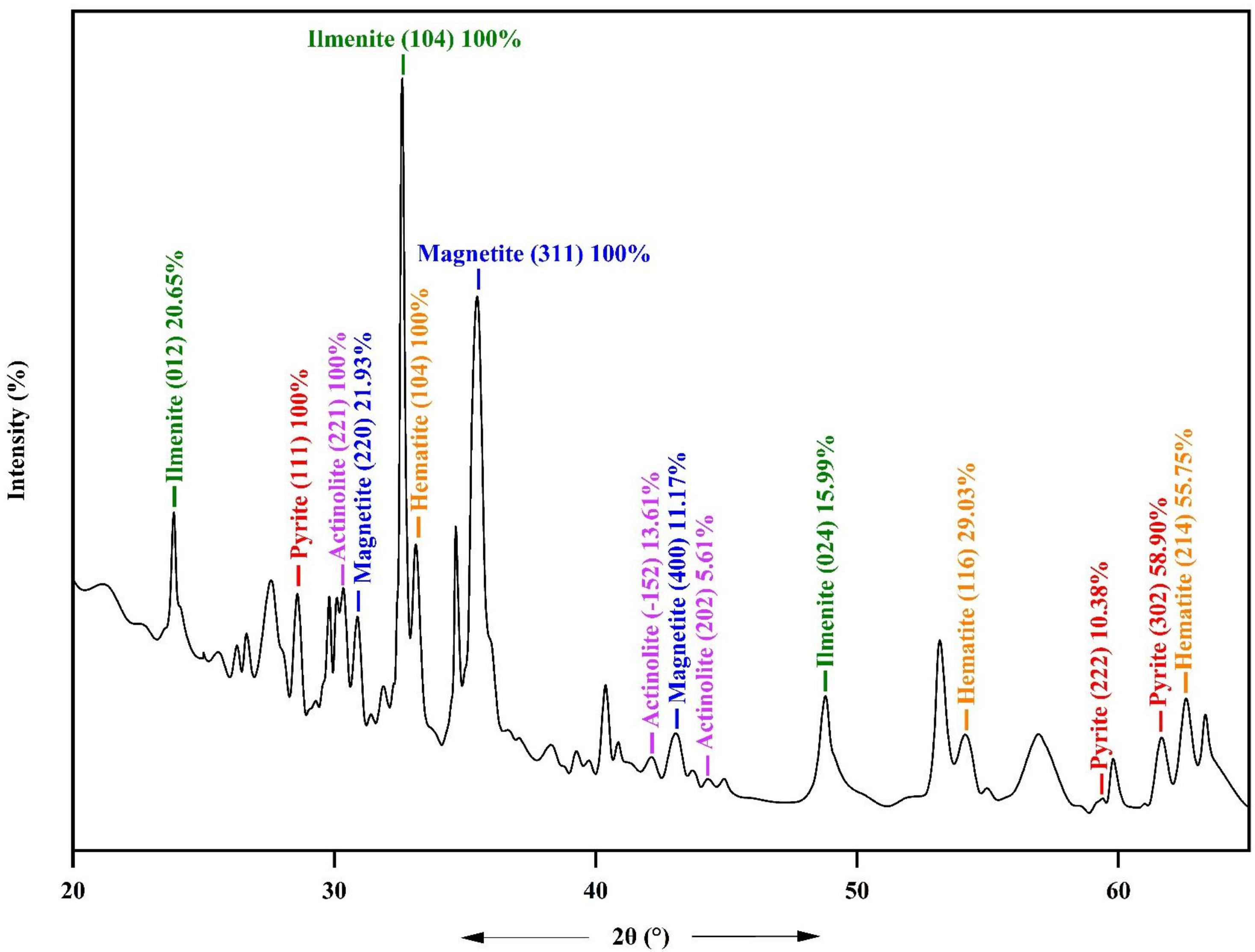

Figure 4.5 f. X-Ray Diffractogram of sample S6F3

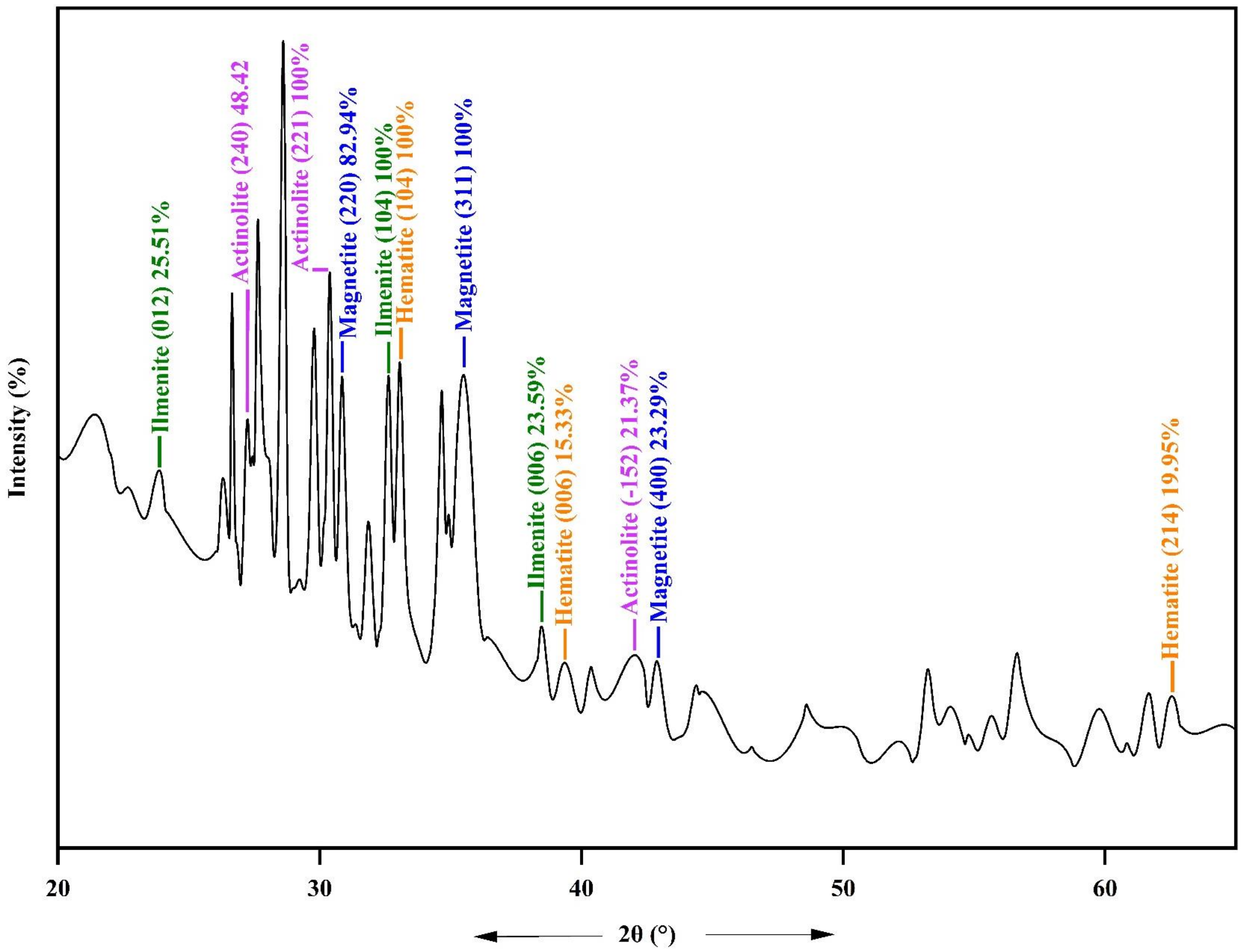

Figure 4.4 g. X-Ray Diffractogram of sample S7F3

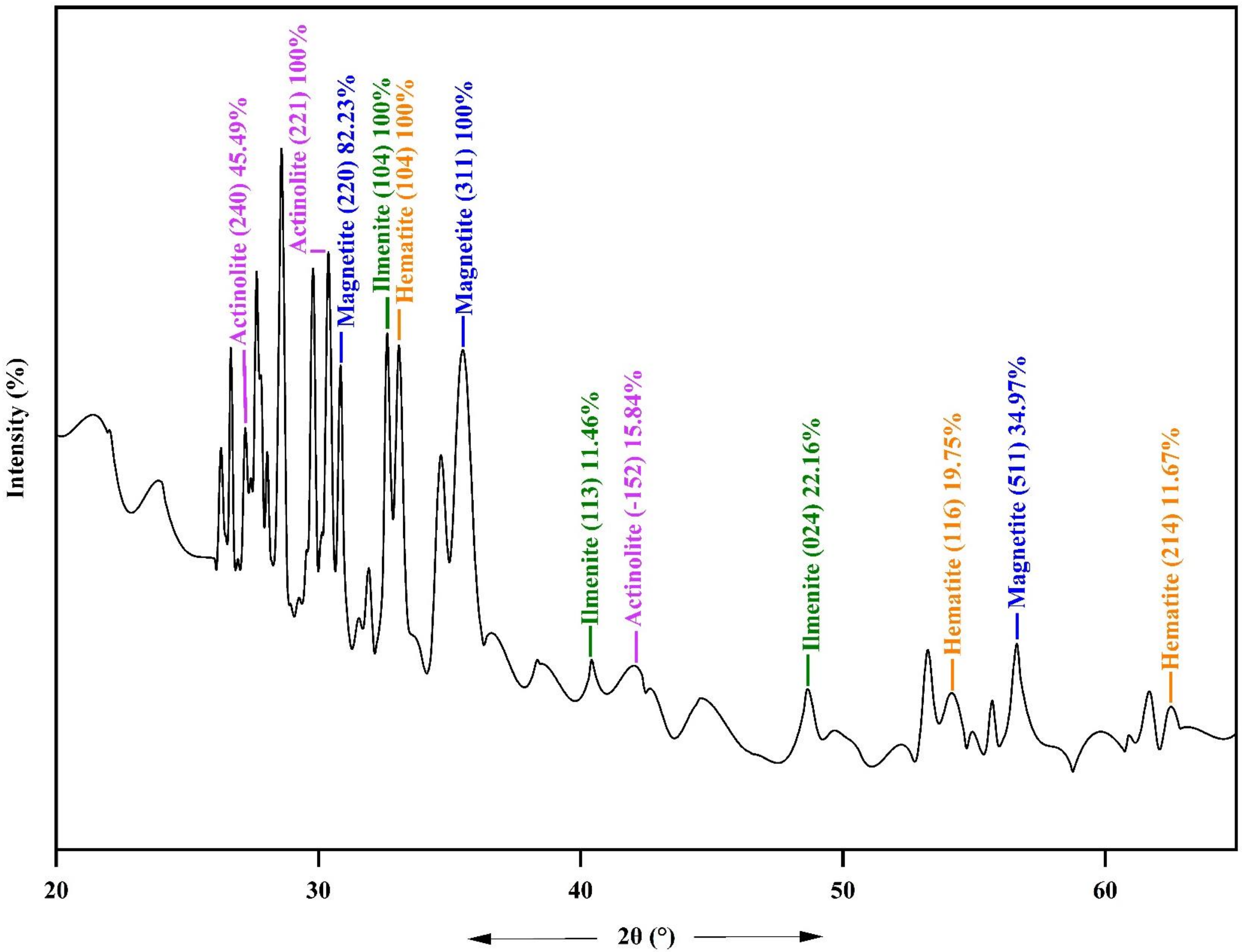

Figure 4.4 h. X-Ray Diffractogram of sample S8F3

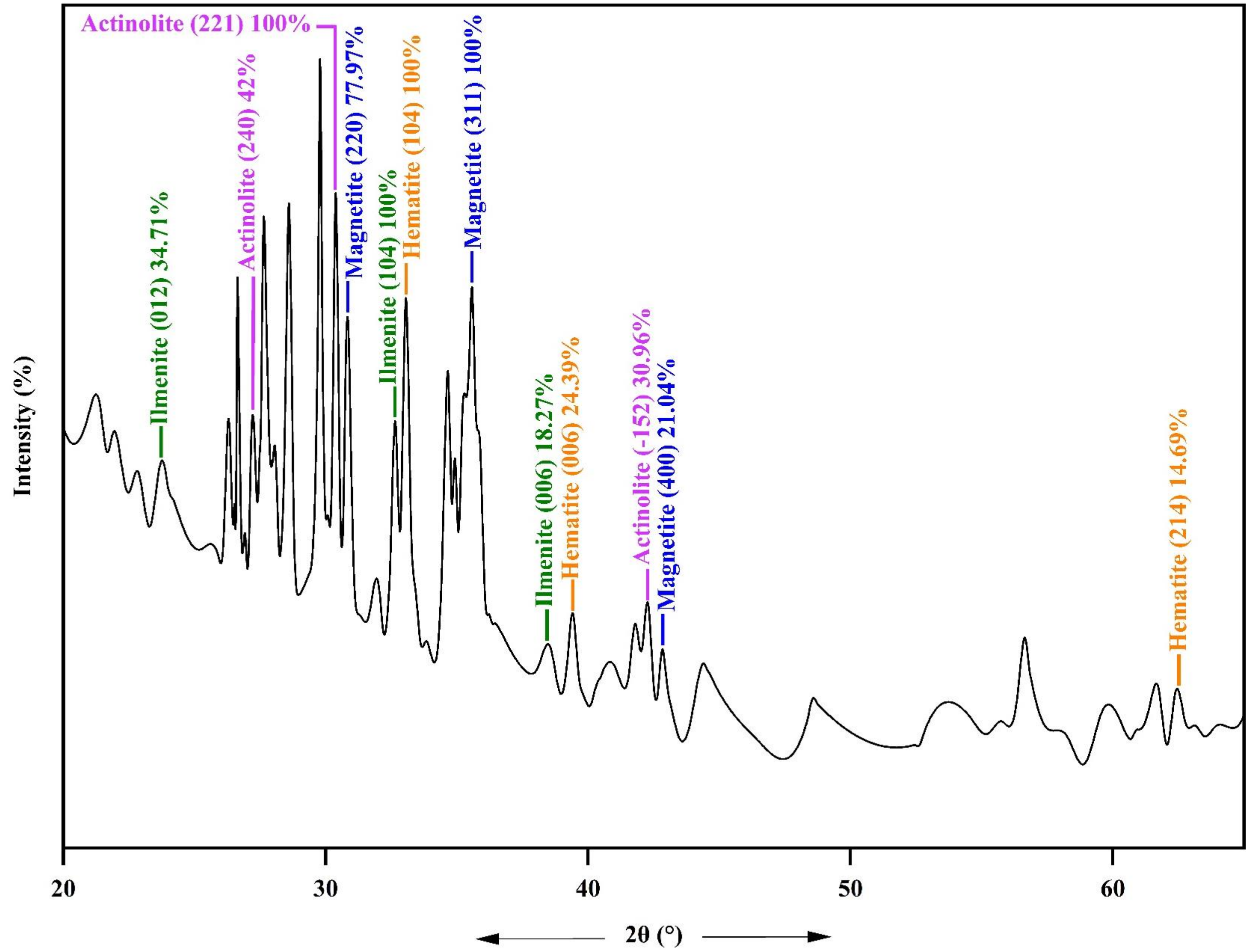

Figure 4.4 i. X-Ray Diffractogram of sample S9F3

Table 4.6 Minerals and their faces identified in the different analyzed samples (S1F3-S9F3)

Mineral	2θ	hkl	Formula
Actinolite	21.11	220	**$Ca_2(Mg, Fe)_5Si_8O_{22}(OH)_2$**
	27.24	240	
	30.38	221	
	42.17	-152	
	44.28	202	
	52.43	-512	
Ilmenite	23.87	012	**$FeTiO_3$**
	32.61	104	
	38.39	006	
	40.32	113	
	42.97	202	
	48.72	024	
	56.70	-132	
Hematite	33.11	104	**Fe_2O_3**
	39.37	006	
	40.93	113	
	54.12	116	
	57.49	122	
	62.60	214	
Magnetite	30.08	220	**Fe_3O_4**
	35.4	311	

	43.04	400	
	53.39	422	
	57.06	511	
Pyrite	28.58	111	**FeS_2**
	59.05	222	
	61.72	302	

4.5 NON-MAGNETIC MINERALS

The non-magnetic minerals identified from the sand samples are apatite, epidote, garnet, rutile, sillimanite, staurolite, tourmaline, and zircon. Apatite is yellow, elongated, and vitreous (Figures 4.5 a-c). Epidote grains are grass-green in colour, prismatic, and have a vitreous lustre (Figures 4.6 a-c). Garnet is cubic and is present in wide colour varieties including colourless, pale pink, orange, red and black. (Figure 4.7 a-h). Rutile is wine-red, prismatic and has an adamantine lustre (Figures 4.8 a-d). Sillimanite is colourless, greasy, and fibrous habit (Figures 4.9 a-b). Staurolite is dark reddish brown, columnar, elongated, has sub-vitreous lustre (Figures 4.10 a-b) and some grains show well developed conchoidal fractures. The grains of staurolite show well preserved habit. Tourmaline grains vary from colourless, greenish black to black and show prominent surface striations along the length of the grain (Figures 4.11 a-d). Zircon is colourless, yellow, orange, brown and some grains also show pale pink colour. The grains have adamantine lustre and exhibit a perfect tetragonal shape (Figure 4.12 a-e).

Figures 4.13 a-h show the distribution of each mineral in different samples (i.e. at different locations). Apatite is mostly common in all samples with the exception of S3 which is from the foreshore of Location B where it is rare. It is abundant at Location E in both, the foreshore and the backshore samples. Epidote is abundant at all locations except at the foreshore of Location B (sample S3). Garnet is rarely found in the sample from the sand spit (S1) while it is abundant in the backshore of location E (sample S9). It is common in all the other locations. Rutile is common to abundant in the backshore at all the locations while it is rarely found in the foreshore samples from all the locations. Sillimanite is abundant in samples S3 and S4. It is common in all the other samples. Staurolite concentrations vary between common and abundant at all the locations. Tourmaline is abundant is S3 and rare in S7. It is common in all the other samples. Zircon is absent in S1 and S7. It is abundant in S2 and highly abundant in S4. It is a common mineral in S6 and rare in the other samples.

Biotite and Muscovite are also present in the sand samples, but their concentrations cannot be commented on as not all their grains sink in bromoform. This is because most of their grains have a specific gravity lesser than that of bromoform (<2.88). Muscovite grains are colourless, platy and vitreous. Some of the grains of muscovite are stained yellowish to red. In foreshore samples the flakes are broken into small pieces. Biotite is dark brown and platy and show a pearly lustre.

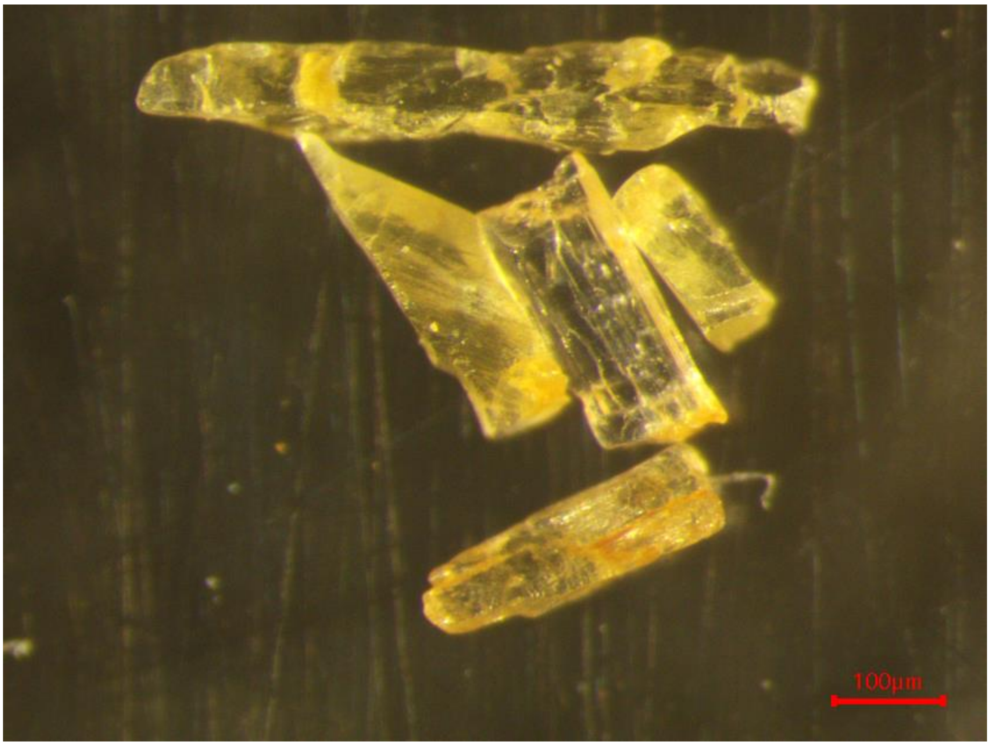

Figure 4.5 a. Photomicrograph of apatite grains

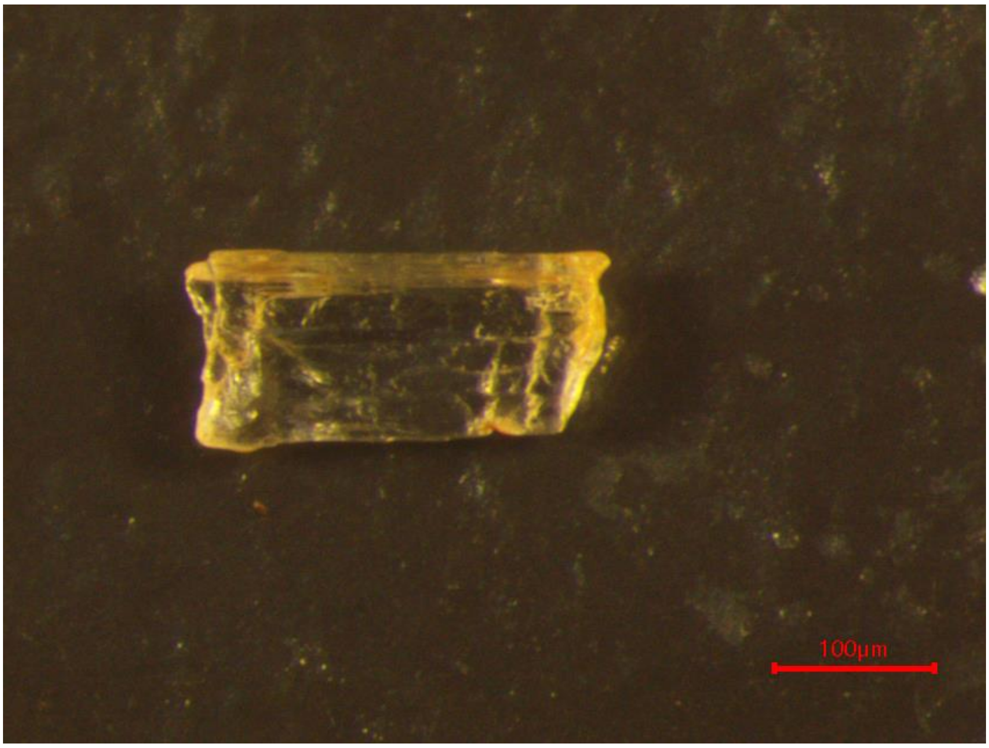

Figure 4.5 b. Photomicrograph of euhedral apatite

Figure 4.5 c. Photomicrograph of anhedral apatite

Figure 4.6 a. Photomicrograph of epidote grains

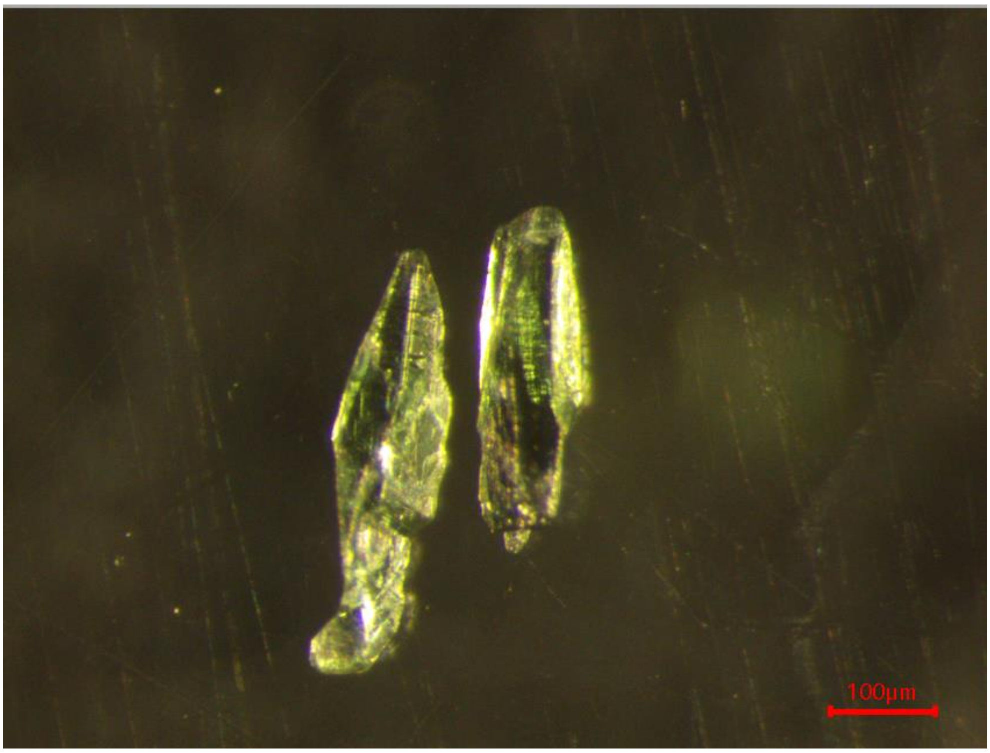

Figure 4.6 b. Photomicrograph of anhedral epidote grains

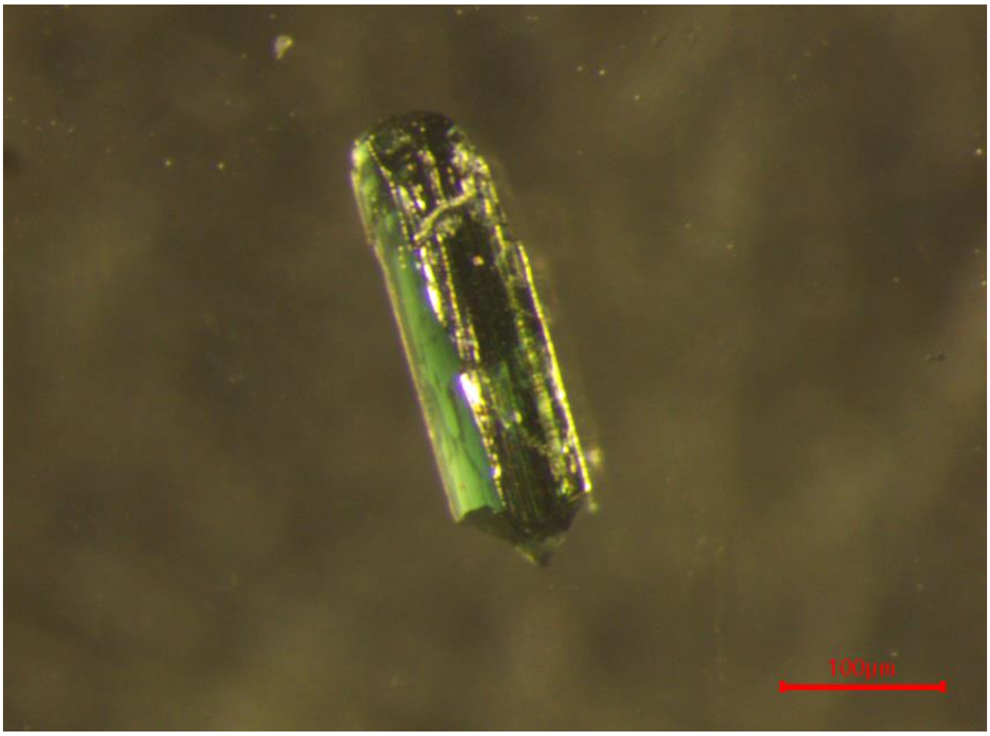

Figure 4.6 c. Photomicrograph of euhedral epidote

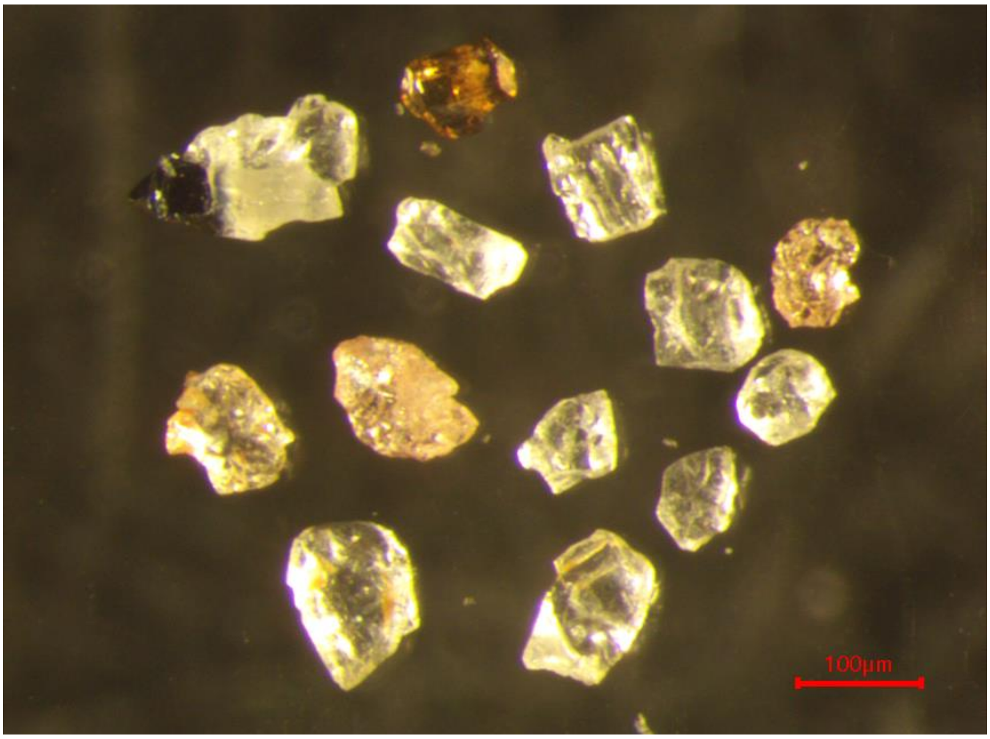

Figure 4.7 a. Photomicrograph showing different varieties of garnet from S9

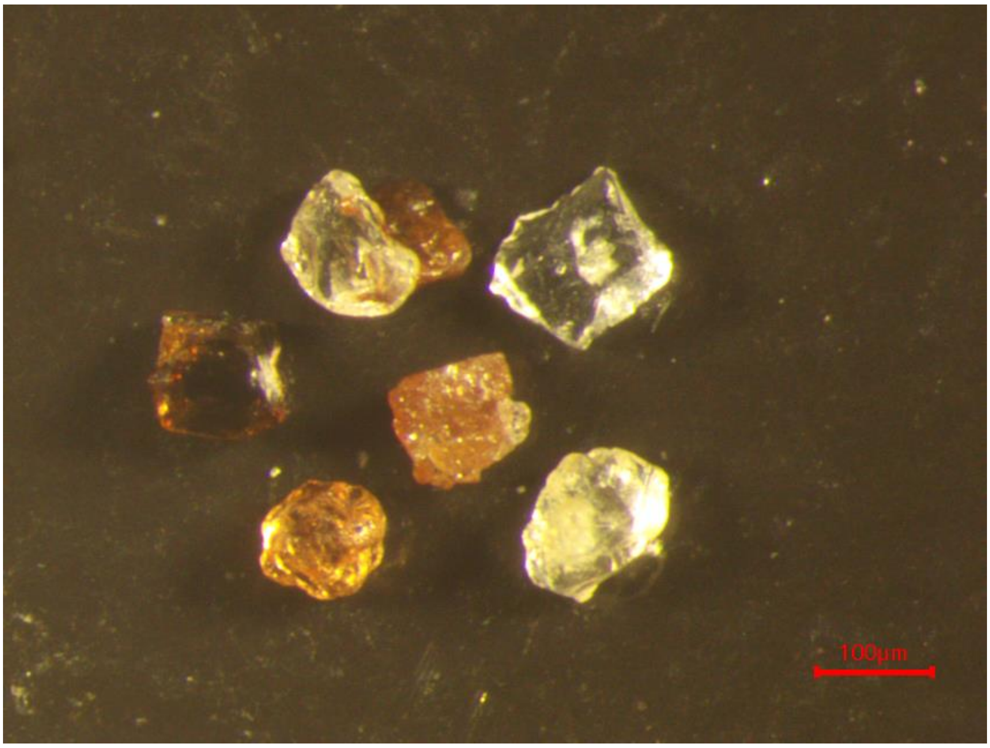

Figure 4.7 b. Photomicrograph showing different varieties of garnet

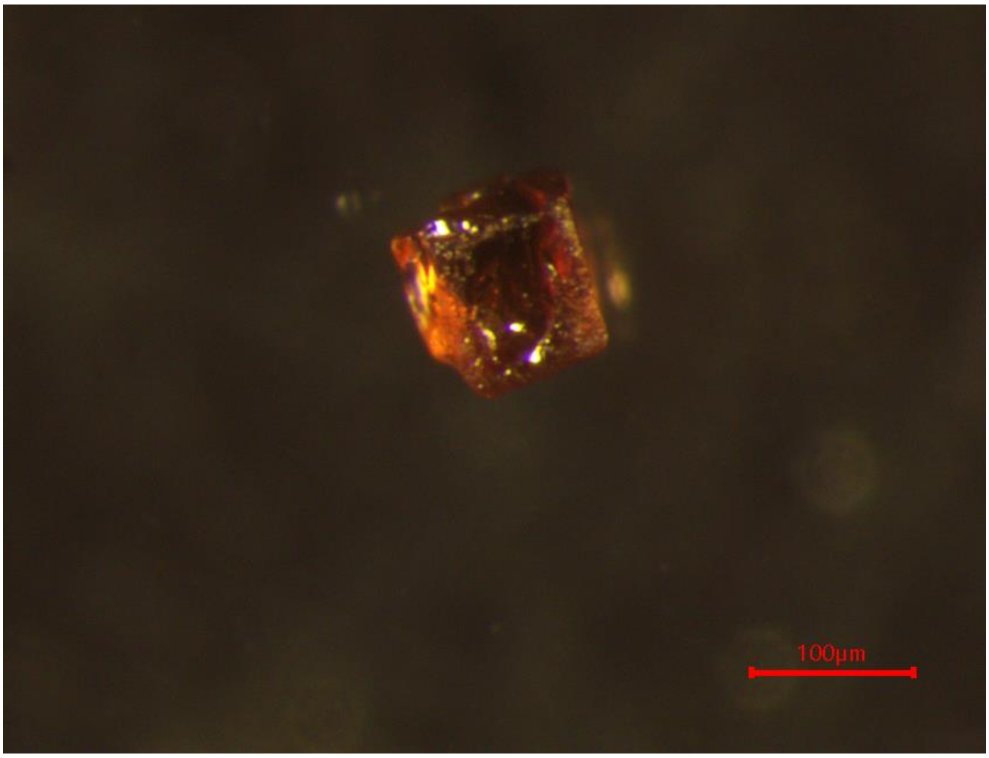

Figure 4.7 c. Photomicrograph of red coloured garnet from S2

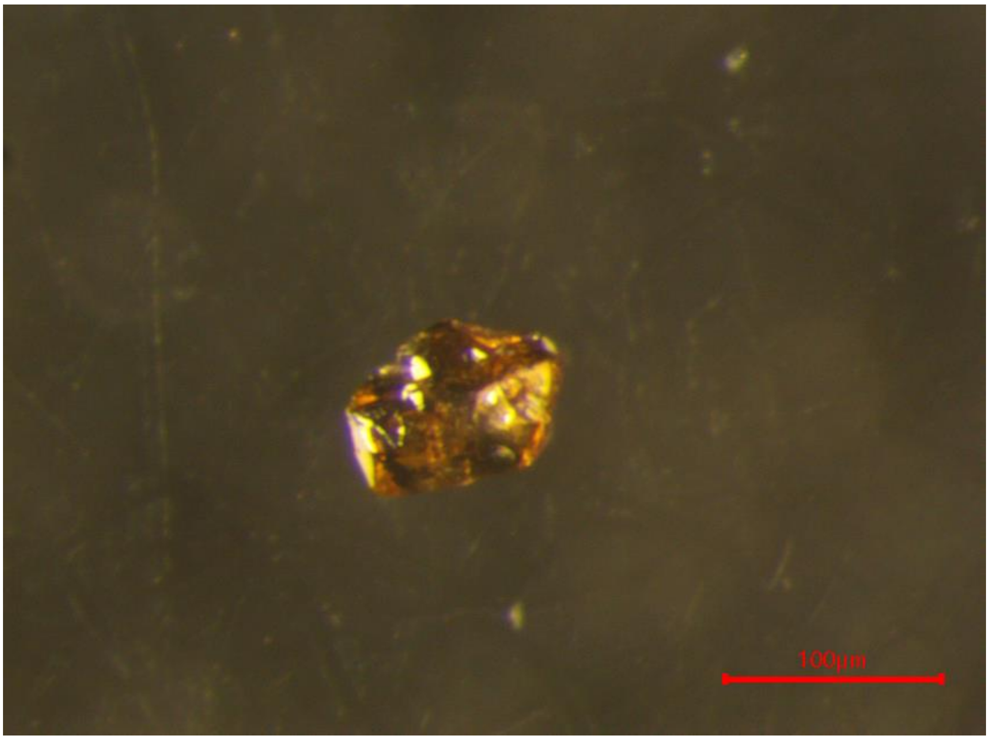

Figure 4.7 d. Photomicrograph of orange coloured garnet

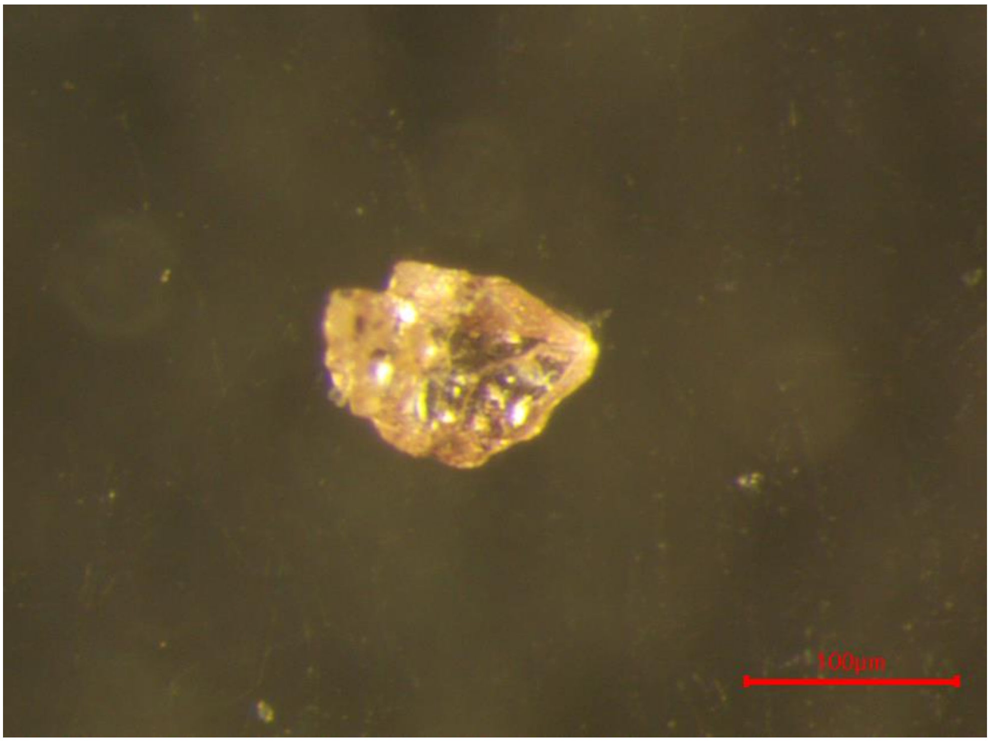

Figure 4.7 e. Photomicrograph of pale pink garnet grains

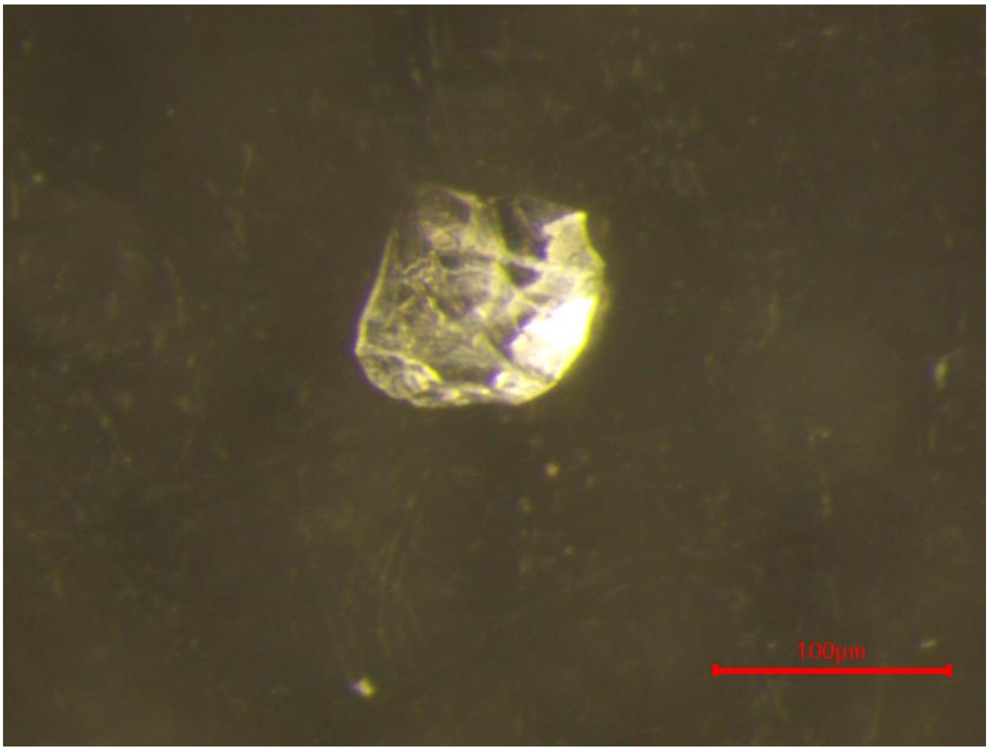

Figure 4.7 f. Photomicrograph of colourless garnet

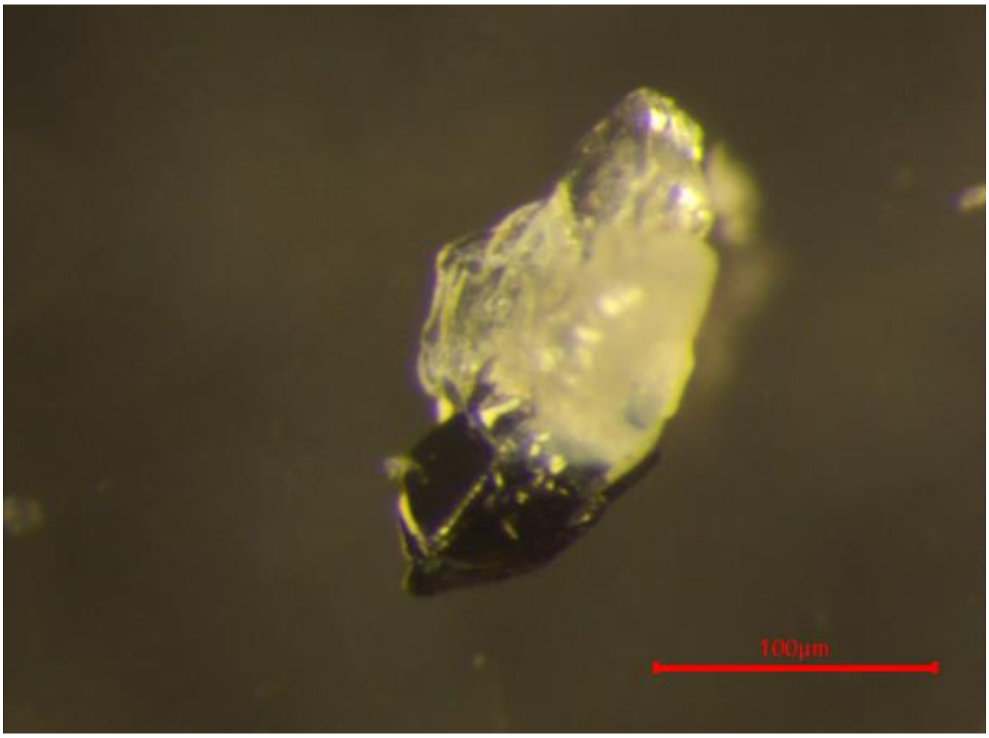

Figure 4.7 g. Photomicrograph of black garnet

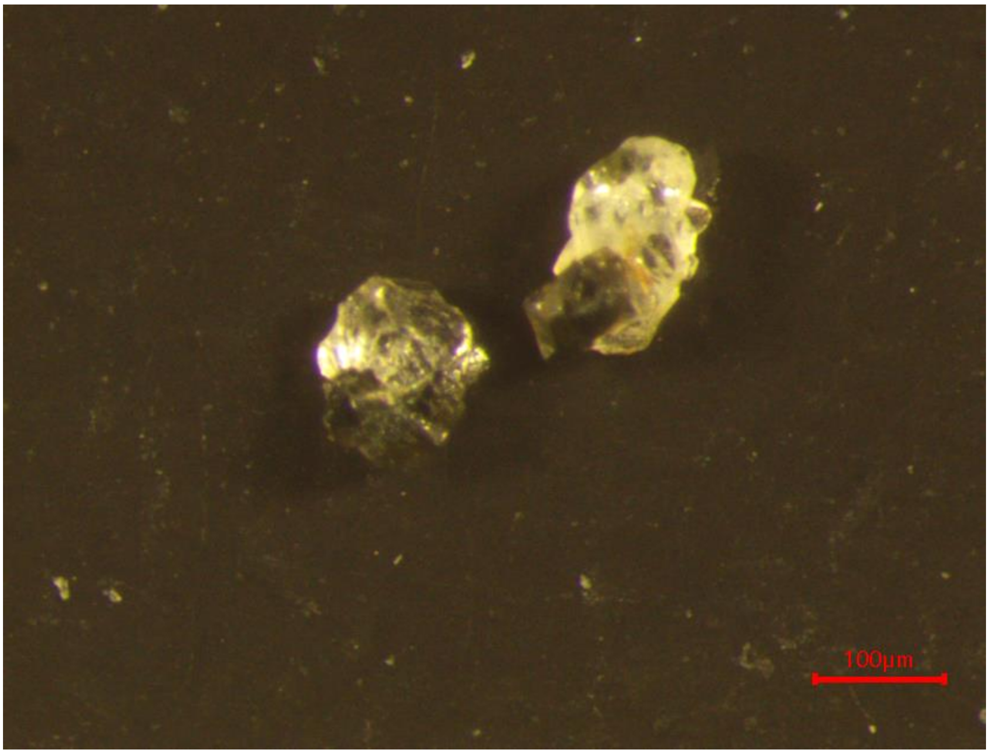

Figure 4.7 h. Photomicrograph of garnet grains from S8

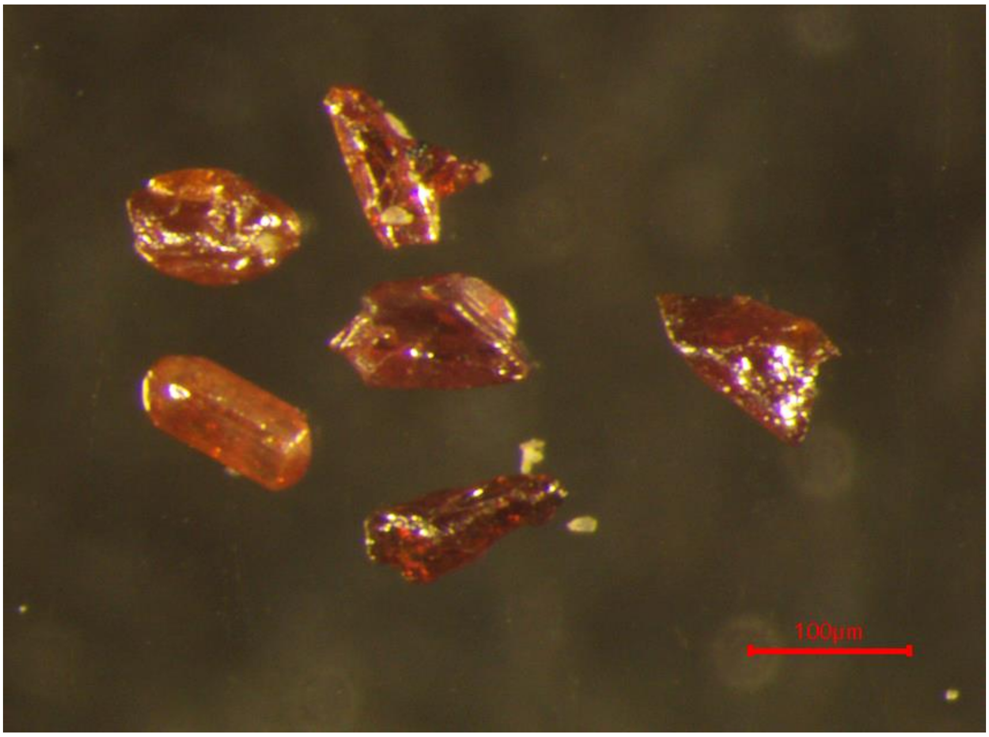

Figure 4.8 a. Photomicrograph of rutile grains

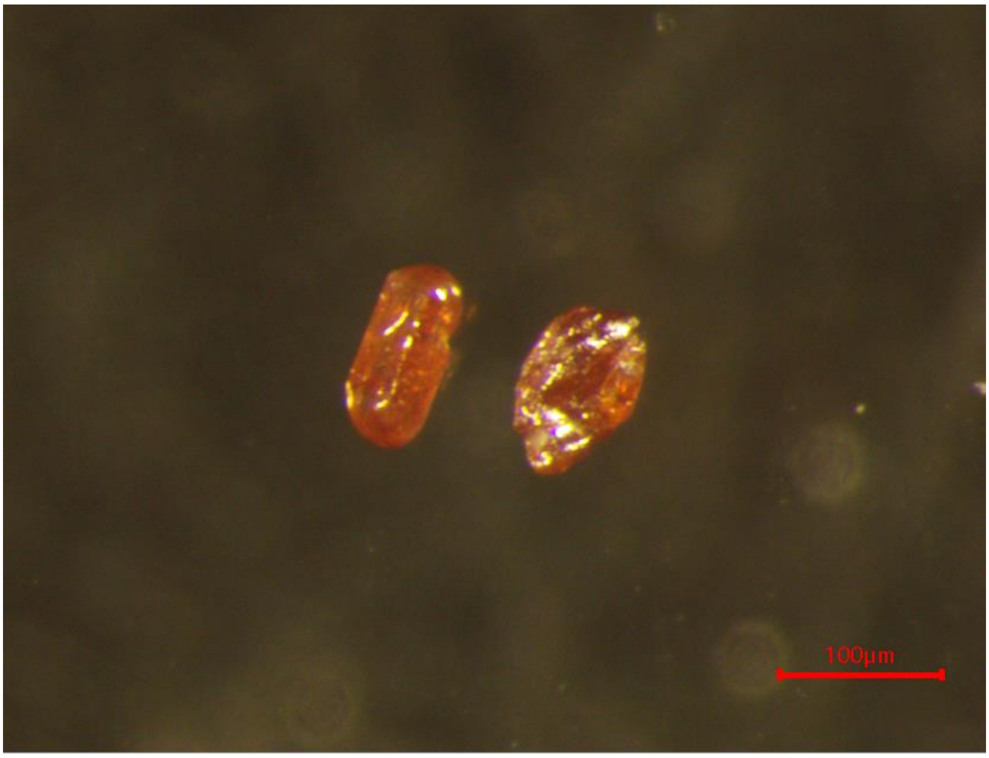

Figure 4.8 b. Photomicrograph of euhedral and anhedral rutile

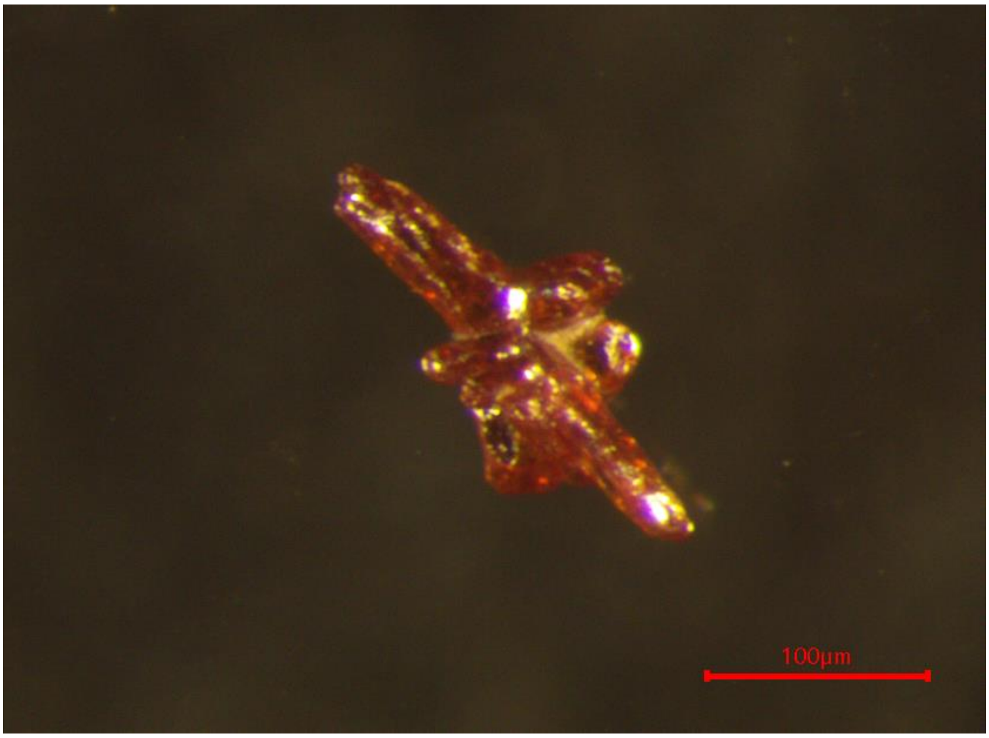

Figure 4.8 c. Photomicrograph of rutile from S5

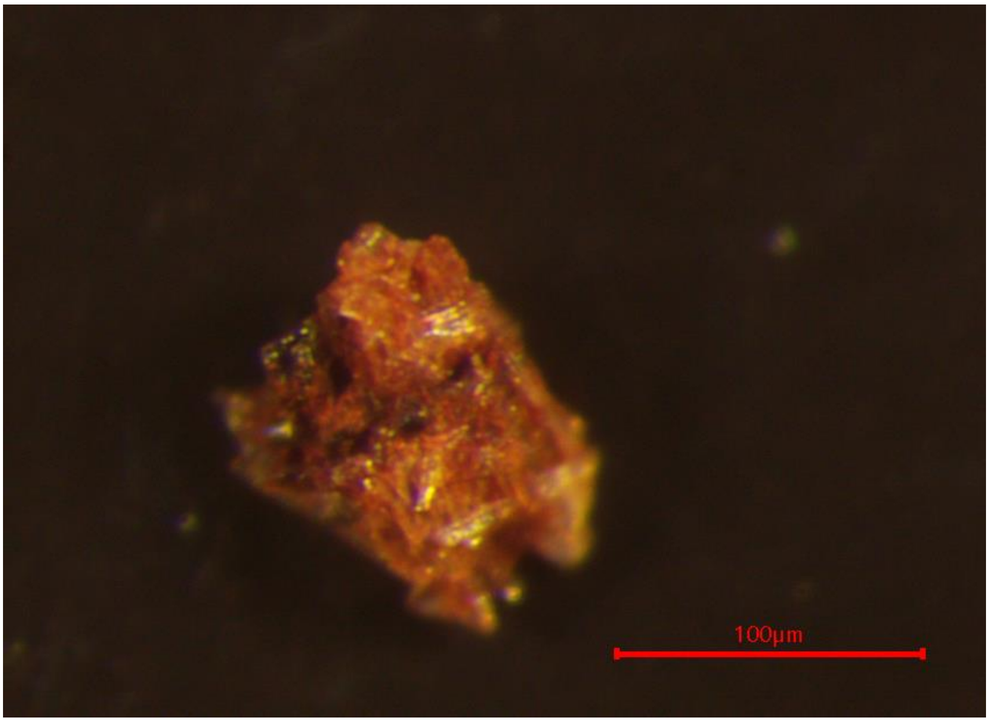

Figure 4.8 d. Photomicrograph of rutile from S8

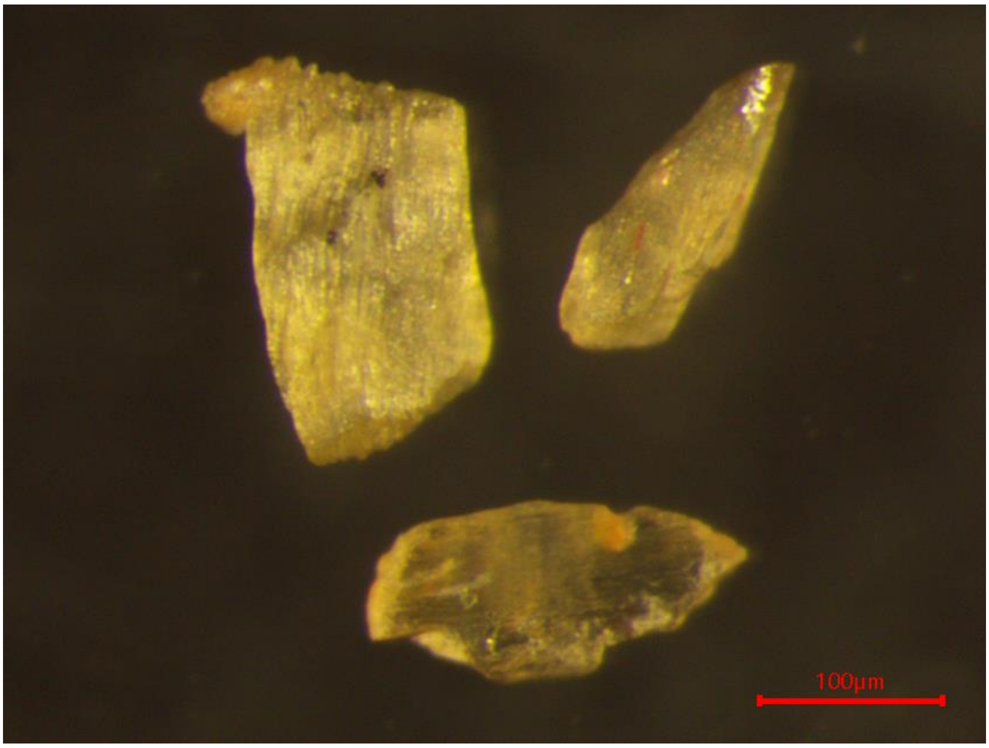

Figure 4.9 a. Photomicrograph of sillimanite grains

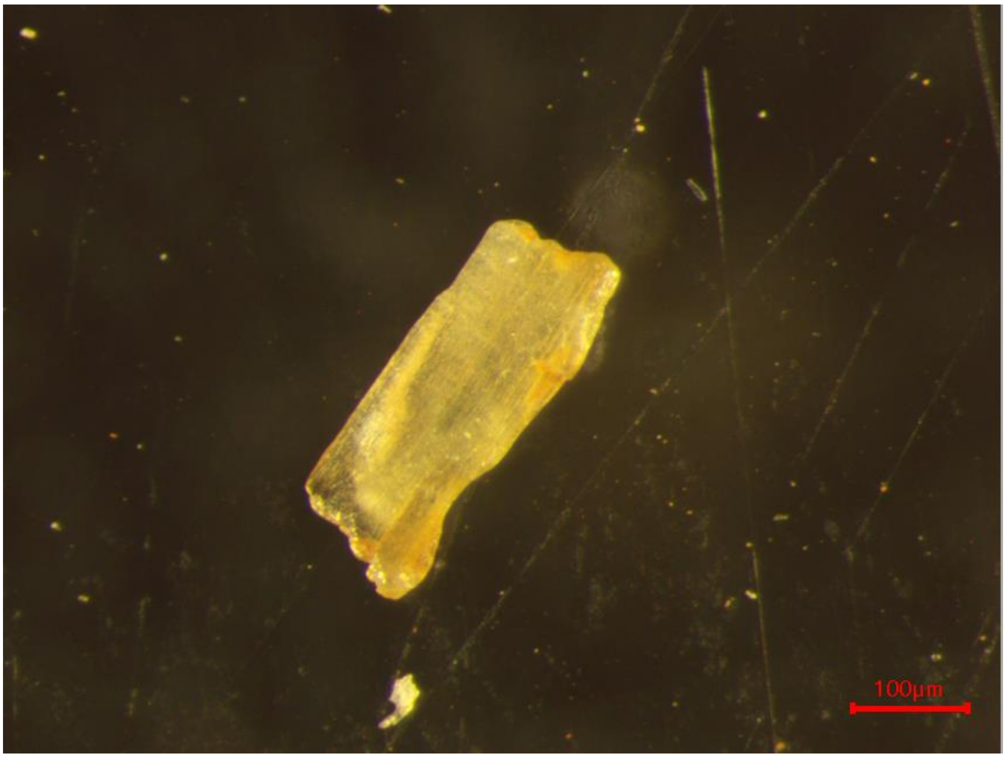

Figure 4.9 b. Photomicrograph of euhedral sillimanite

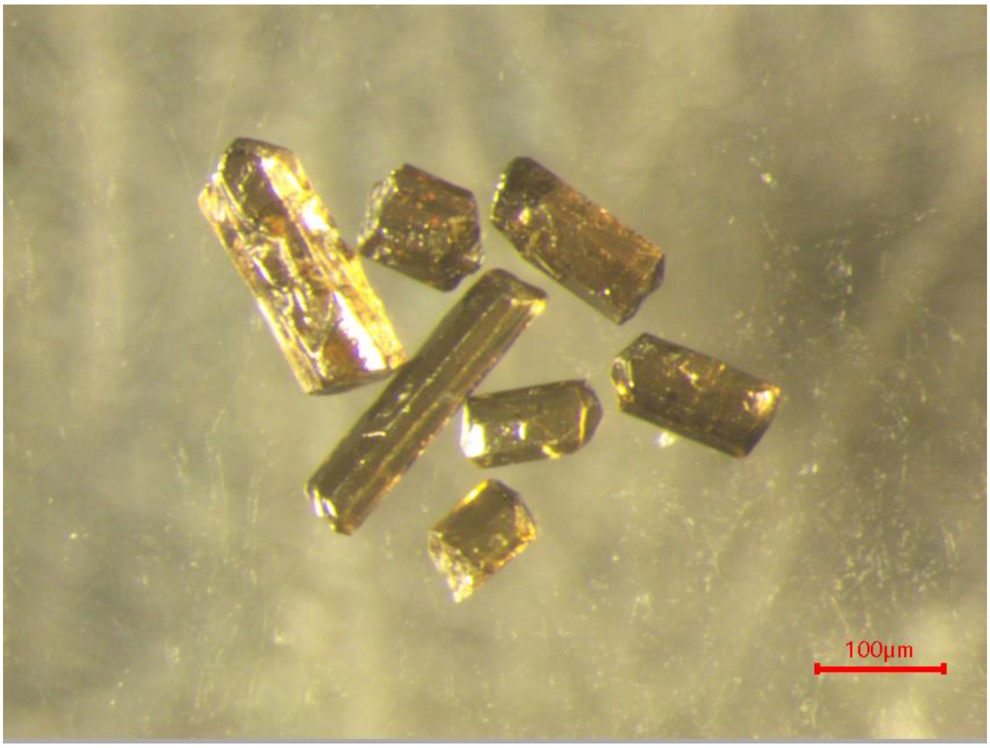

Figure 4.10 a. Photomicrograph of staurolite grains

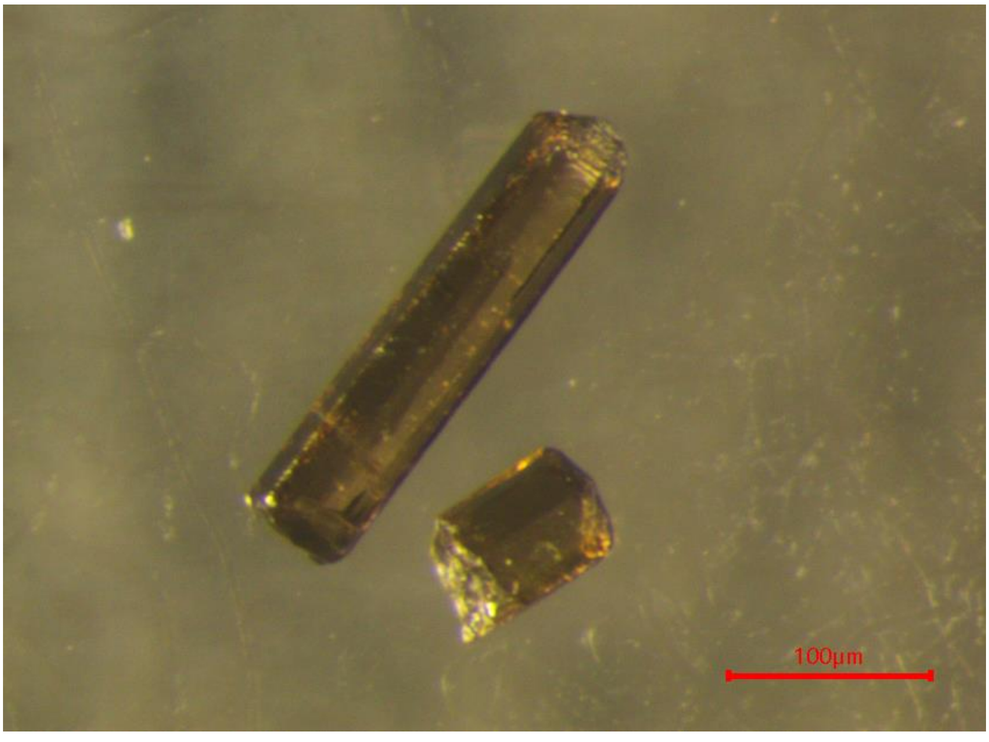

Figure 4.10 b. Photomicrograph of euhedral and anhedral staurolite grains

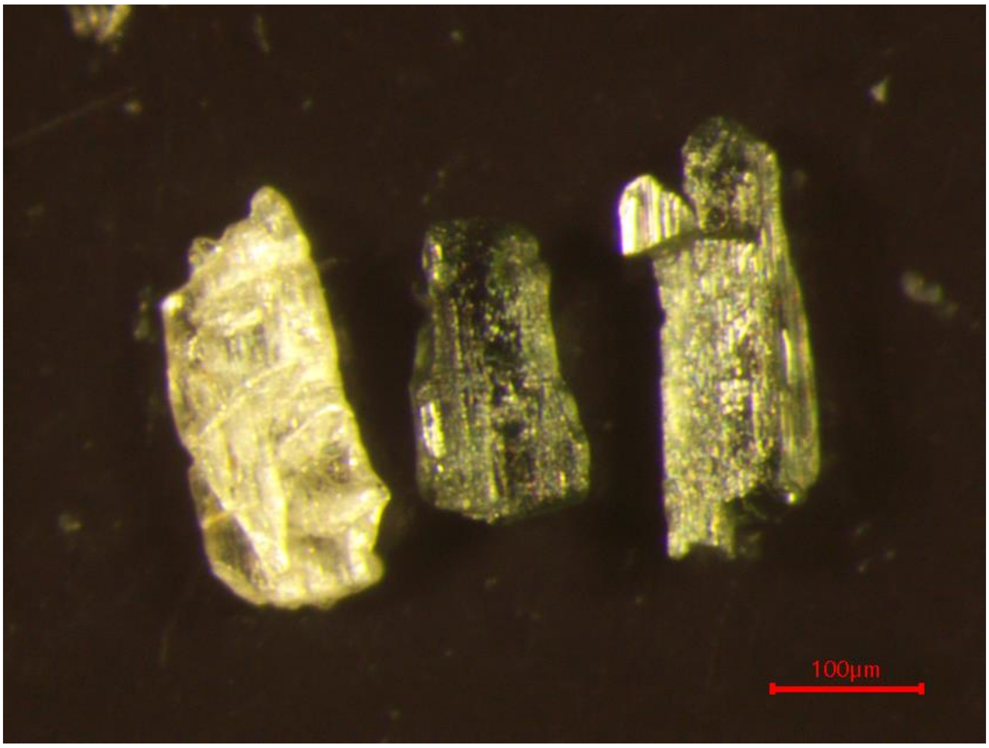

Figure 4.11 a. Photomicrograph of tourmaline grains

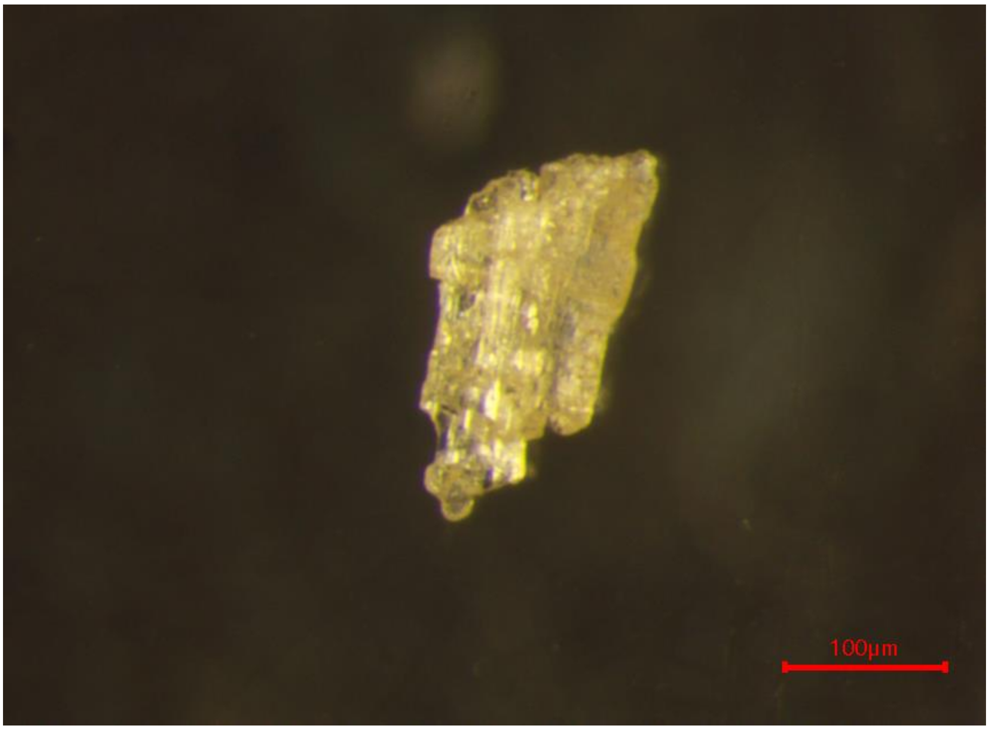

Figure 4.11 b. Photomicrograph of transparent tourmaline

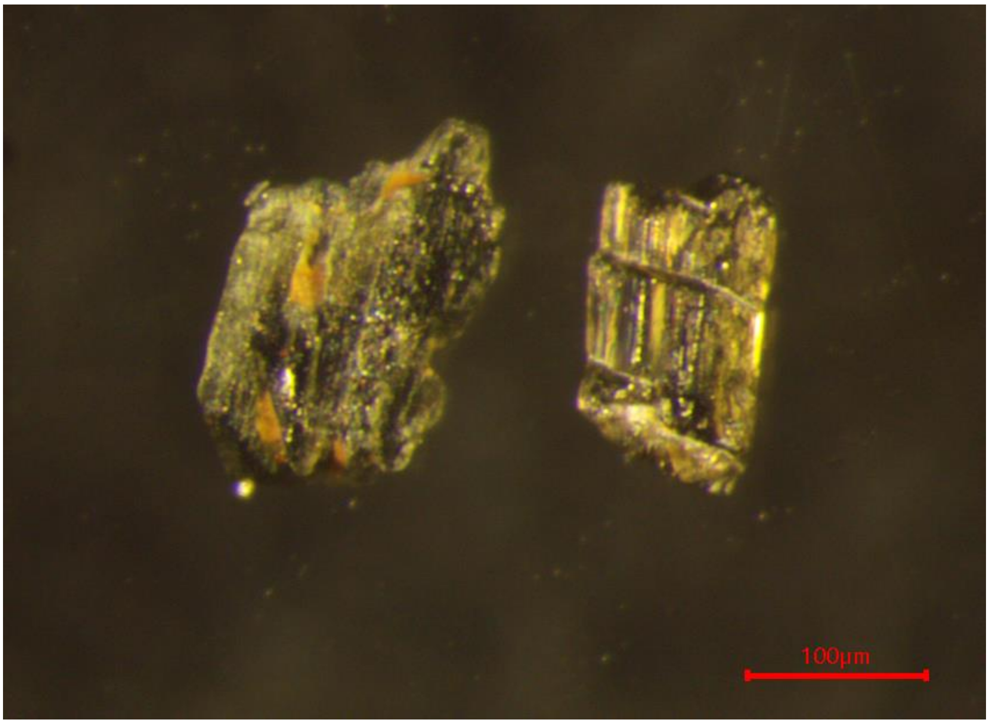

Figure 4.11 c. Photomicrograph of greenish-black tourmaline grains

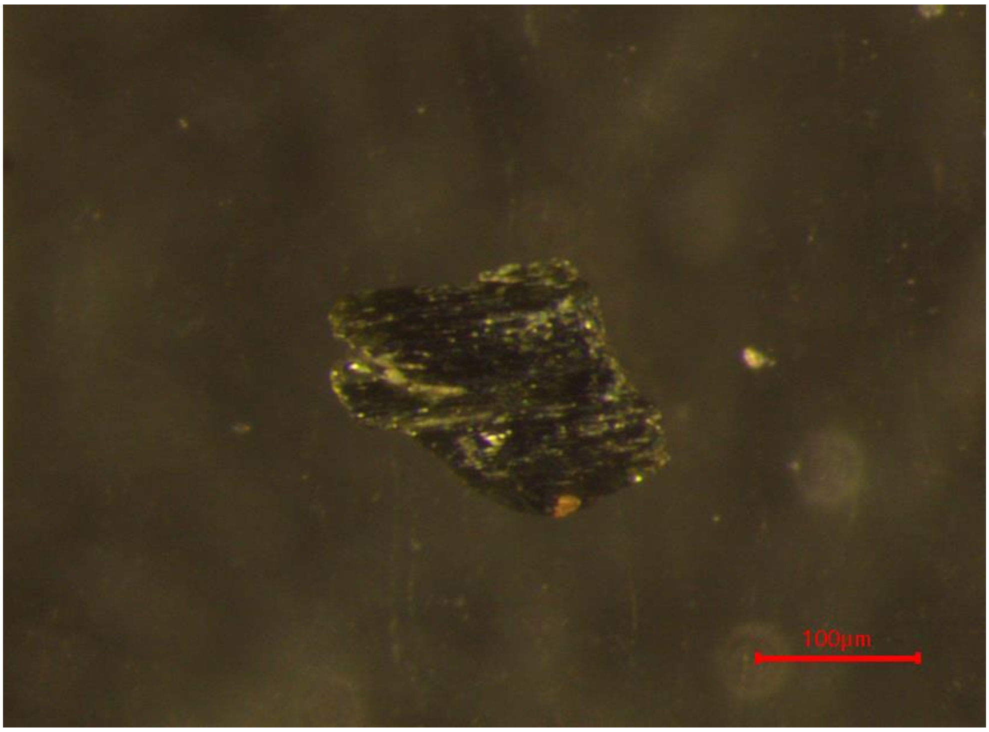

Figure 4.11 d. Photomicrograph of black tourmaline grain from S2

Figure 4.12 a. Photomicrograph of zircon grains from S4

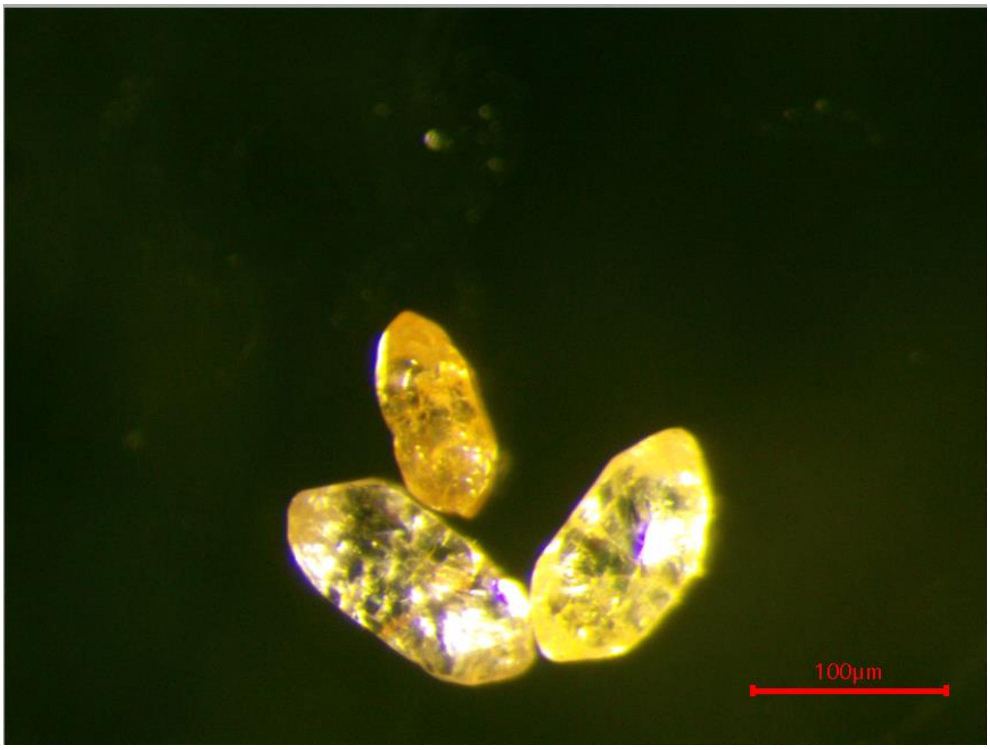

Figure 4.12 b. Photomicrograph of zircon grains from S2 in closeup

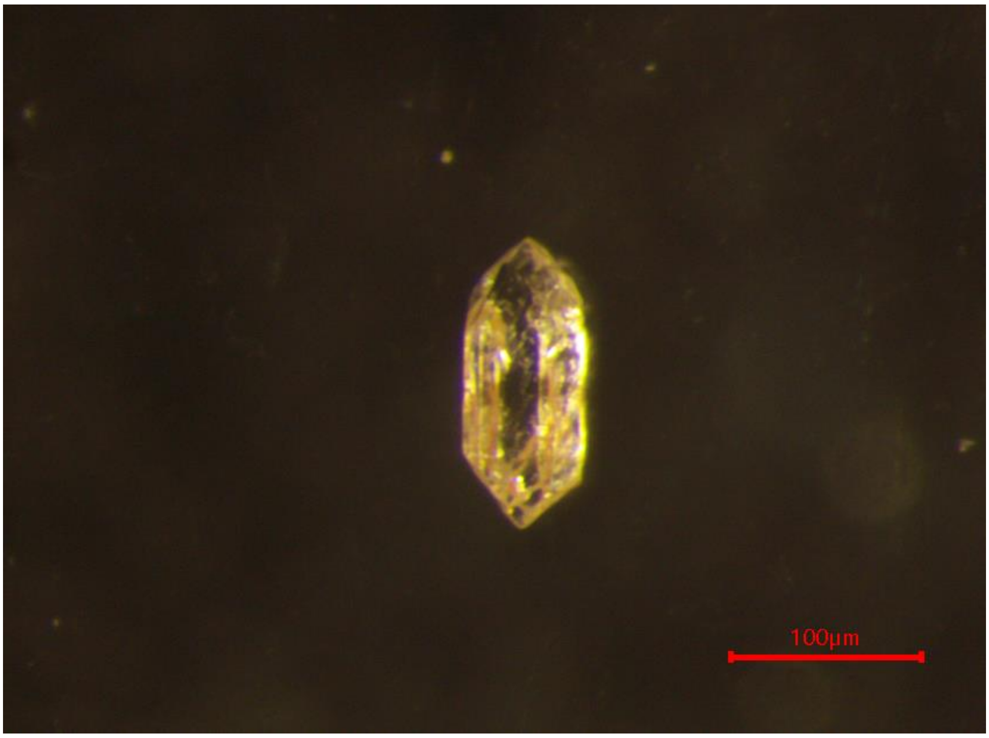

Figure 4.12 c. Photomicrograph of euhedral and colourless zircon grain

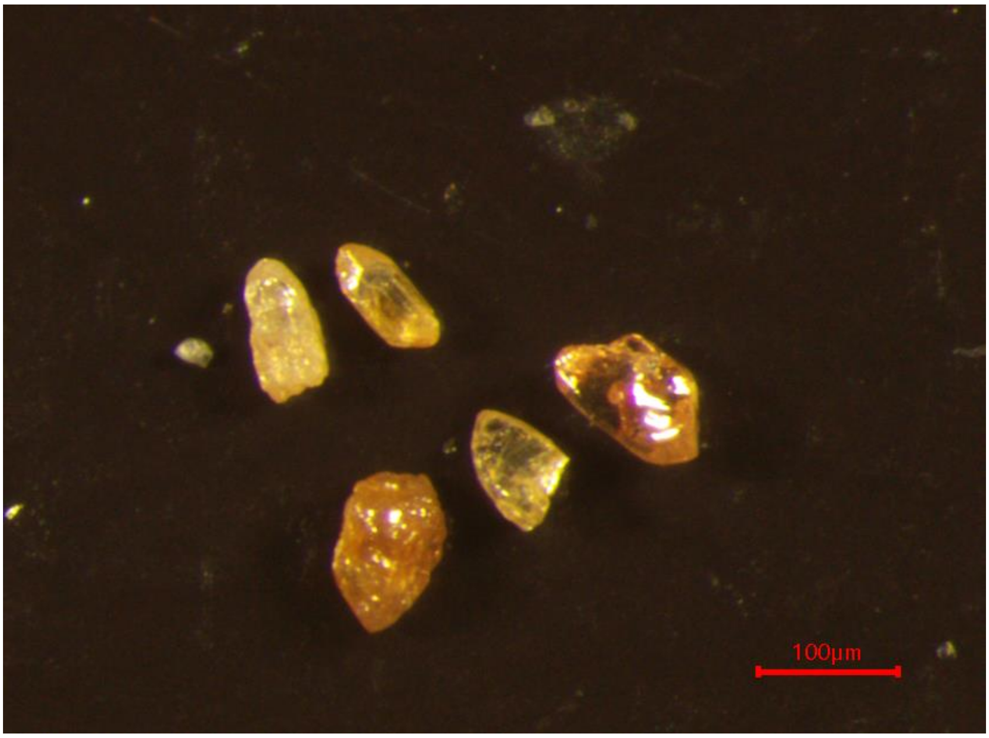

Figure 4.12 d. Photomicrograph of broken zircon grains

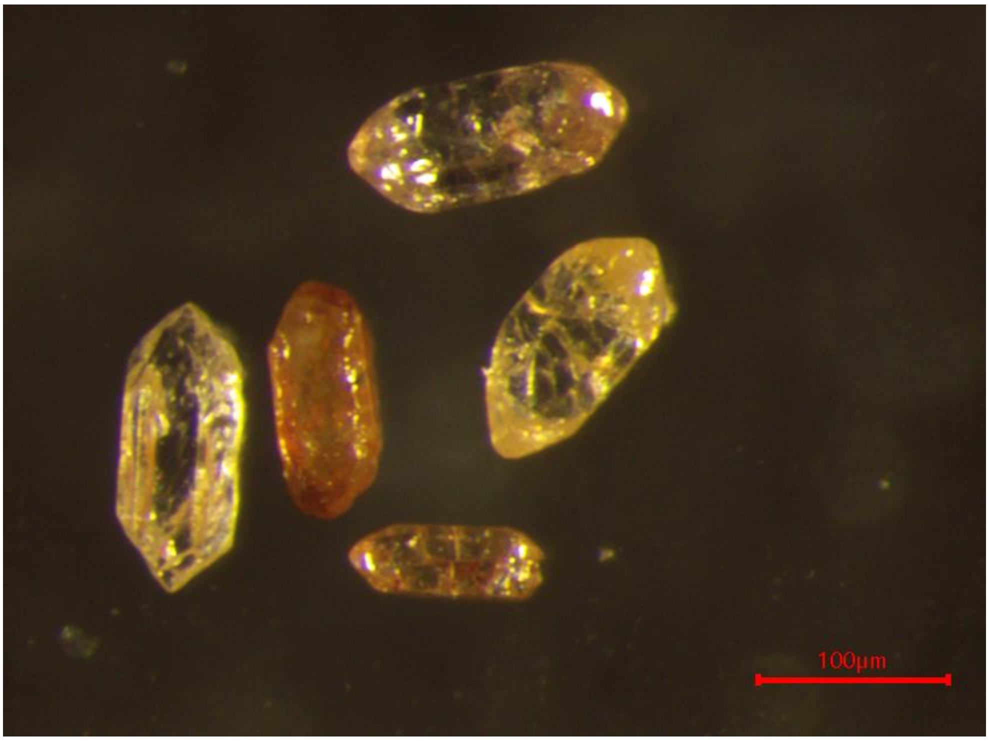

Figure 4.12 e. Photomicrograph of various coloured varieties of zircon grains (colourless, pale pink, pale yellow, orange, and brown)

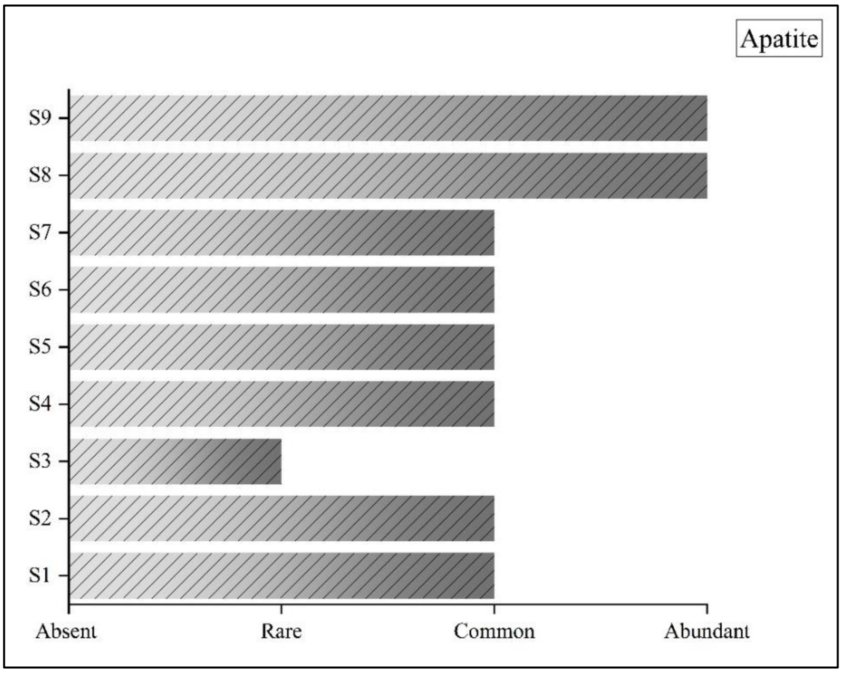

Figure 4.13 a. Abundance of apatite grains at different locations/ in different samples

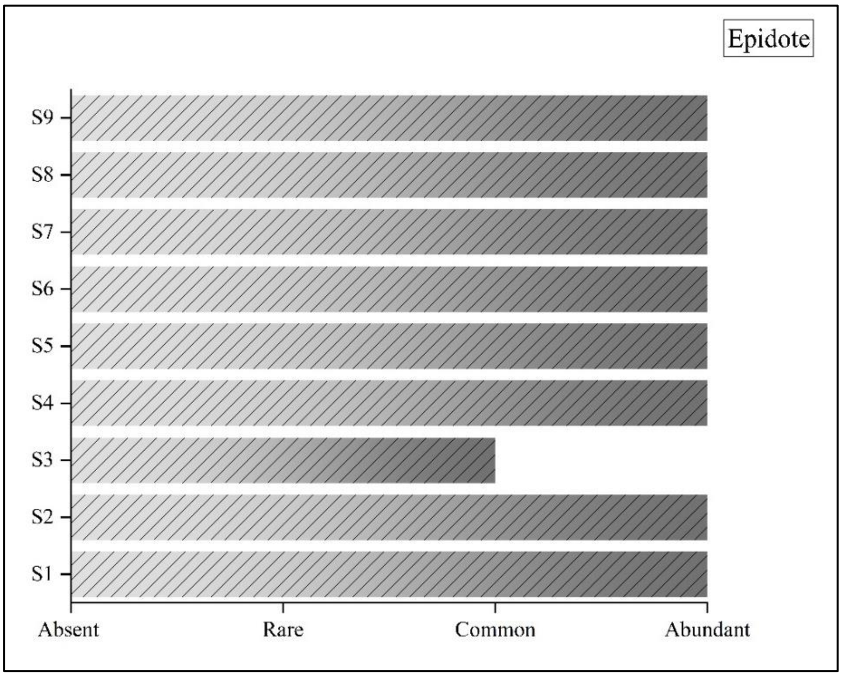

Figure 4.13 b. Abundance of epidote grains at different locations/ in different samples

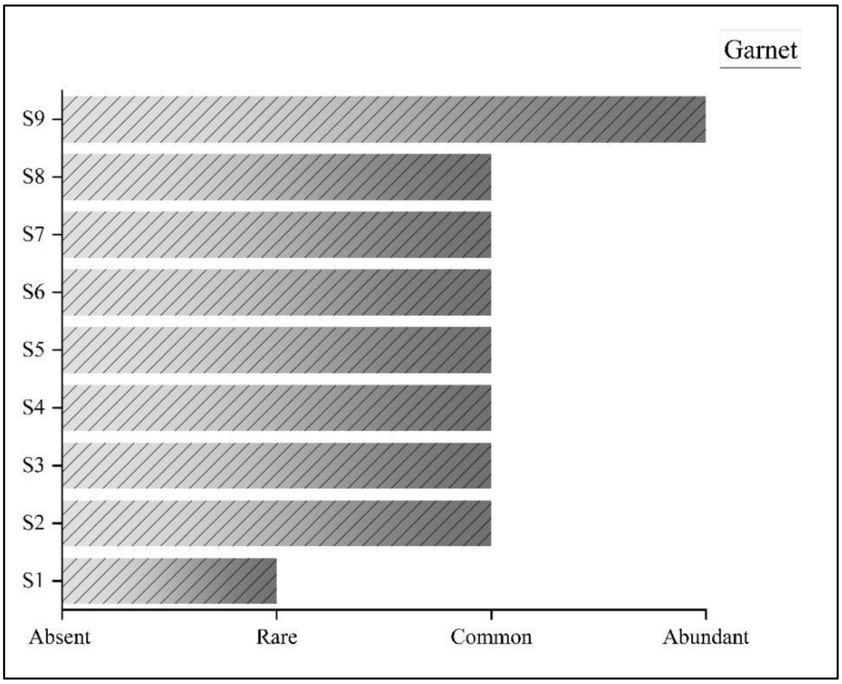

Figure 4.13 c. Abundance of garnet grains at different locations/ in different samples

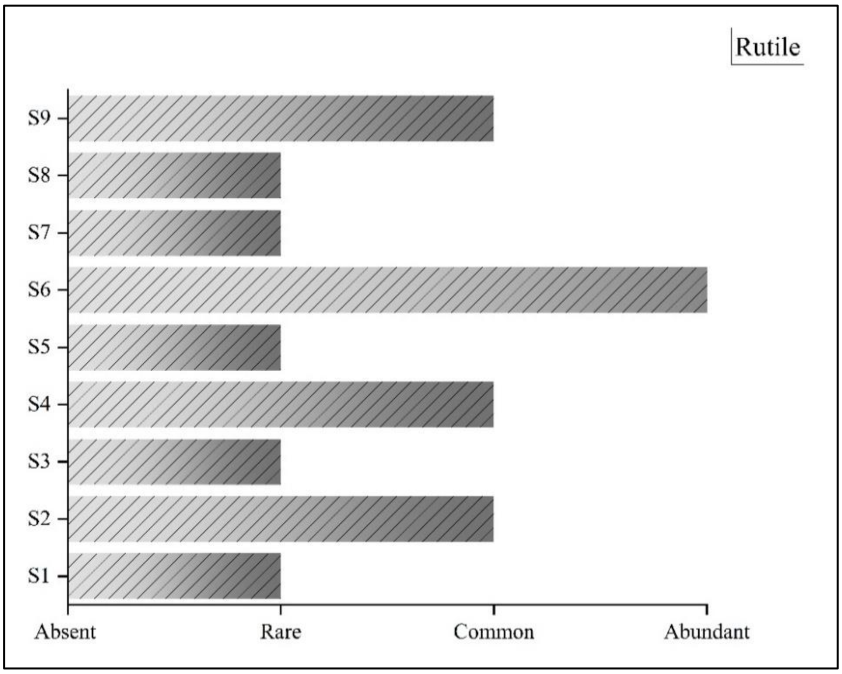

Figure 4.13 d. Abundance of rutile grains at different locations/ in different samples

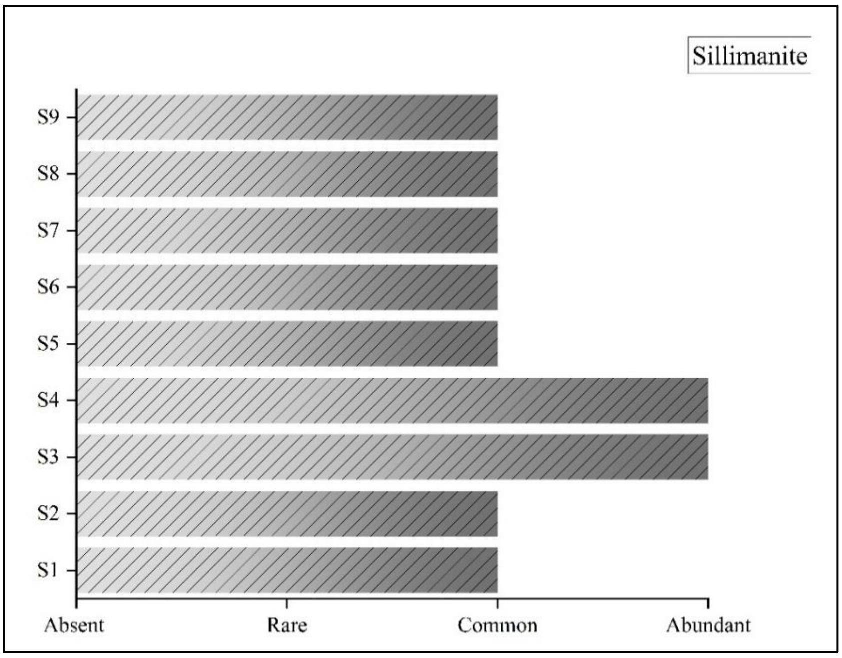

Figure 4.13 e. Abundance of sillimanite grains at different locations/ in different samples

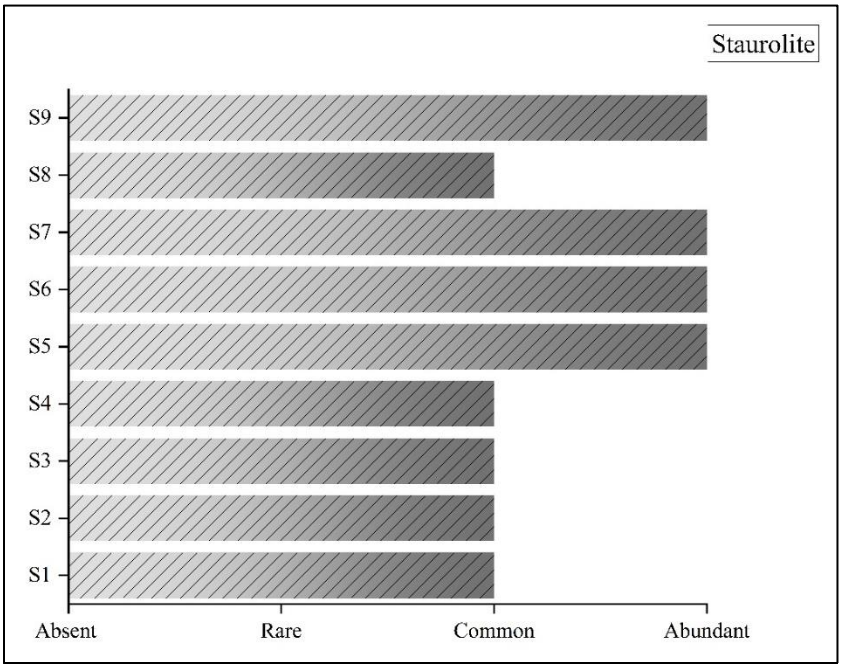

Figure 4.13 f. Abundance of staurolite grains at different locations/ in different samples

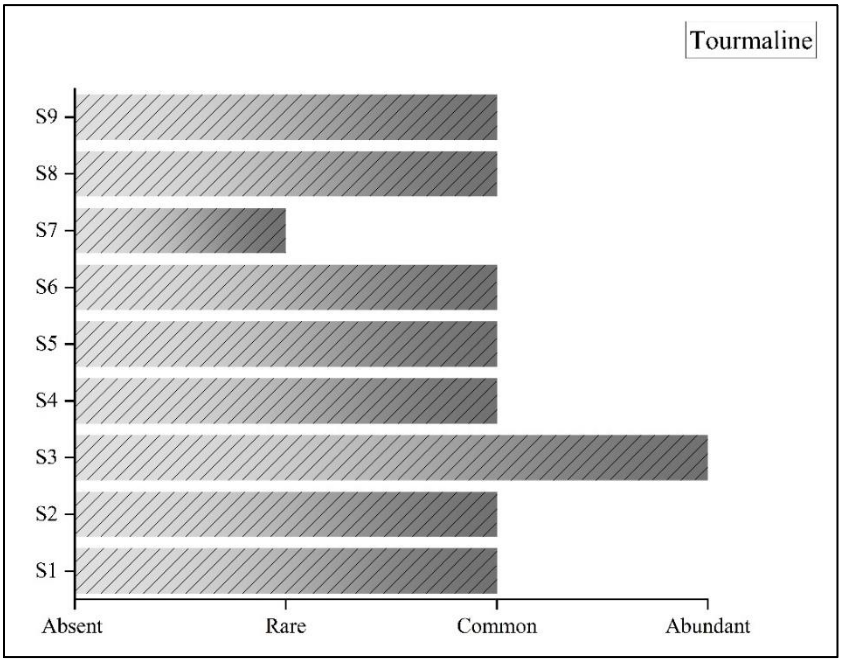

Figure 4.13 g. Abundance of tourmaline grains at different locations/ in different samples

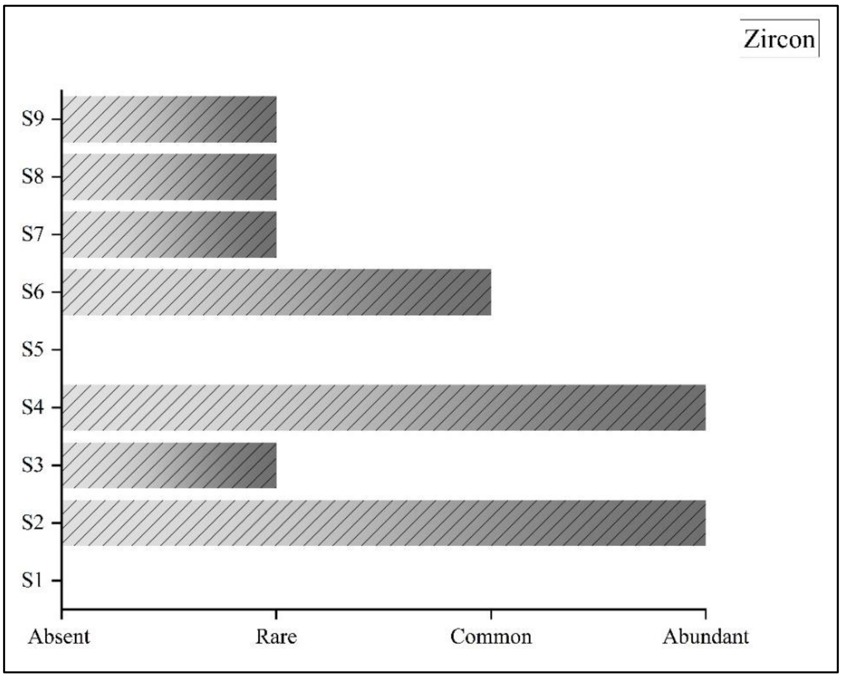

Figure 4.13 h. Abundance of zircon grains at different locations/ in different sample

DISCUSSION

CHAPTER 5: DISCUSSION

The loss in sediment weight after their treatment with HCl, KOH and H2O2 is due to the presence of $CaCO_3$ shells and cement, SiO_2 cement and organic matter. The maximum loss in the sediment weight is observed in sample S7. It was also observed that the sample consisted of high shell material. This may be due to high benthic production at that location and a high accumulation of organic and inorganic carbon in the foreshore region due to the absence of the backshore region at that location.

The dominant sand size in the sediments of Keri Beach is medium sand (500µm-250µm). Due to the process of selective sorting by the waves, the foreshore tends to have more coarser and lighter grains compared to the backshore which can be seen in the samples collected. The continuous swash and backwash lead to the washing away of lighter minerals towards the shoreline and thereby leading to the concentration of the heavy minerals in the calmer conditions of the backshore. Thus, backshore samples from each location have a higher concentration of fine sand and a lower concentration of coarse sand and are rich in heavy minerals. S1 has the highest concentration of coarse sand than in any other sample. This is because it is collected from the sand spit formed at the mouth of the Terekhol River. Sand spits usually consist of coarser sediments because as the river meets the sea at the mouth, its energy diminishes leading to the deposition of coarser material at the mouth while the finer material may still remain suspended in the water column and get transported further. Furthermore, sediments in backshore are dry and hence are light and therefore transported further backshore by the winds coming from the sea.

Since most of the heavy minerals are present in the rocks as accessory minerals, their concentration is much lower than the light minerals i.e. quartz and feldspar which are present in abundance in the rocks.

Magnetic minerals are abundant as compared to the non-magnetic minerals because magnetic minerals like magnetite and hematite tend to have higher densities than non-magnetic minerals. When sediment is transported by waves and currents, the denser magnetic minerals settle out more readily than lighter non-magnetic minerals, leading to their accumulation in beach placers and this process is known as density sorting. Due to the magnetic susceptibility of the magnetic minerals, they can also undergo the process of magnetic concentration and are hence abundant. The presence and dominance of any mineral in the placers also depends on the type of rocks present in the area and their chemical composition.

The minerals having higher specific gravity (Table 5.1) tend to show a higher concentration in the backshore. This explains the higher concentration of non-magnetic minerals like rutile and zircon in the backshore than in the foreshore. The presence of both fresh and altered grains signifies that there is a reworking of sediments and their residence for a considerable time in an oxidizing environment in the paleo-beaches. These sediments were then transported towards the shore with the increase in sea level in the Holocene period **(Gujar et al., 2021)**.

The heavy mineral suite suggests that the minerals have originated from a mixed source i.e. they are igneous, metamorphic, and sedimentary in origin. Table 5.2 shows the possible provenance of the identified minerals. Actinolite, epidote, garnet, hematite, ilmenite, magnetite, pyrite, rutile, sillimanite, staurolite, tourmaline and zircon are brought in by the river from the various rocks through which it flows. Apatite on the other hand is transported from the south via the longshore current which is locally in the north direction in the study area as reported by various authors. It is also confirmed by the growth of sand spit in the northern direction at the mouth of Terekhol River. The laterites present along the coast also contribute to hematite and magnetite.

Table 5.1 Specific gravity of heavy minerals

Mineral	Specific gravity
Actinolite	2.9-3.6
Apatite	3.2-3.4
Epidote	3.3-3.6
Garnet	3.65-3.84
Hematite	4.9-5.0
Ilmenite	4.3-5.5
Magnetite	4.9-5.2
Pyrite	5.0
Rutile	4.2-4.3
Sillimanite	3.24
Staurolite	3.65-3.77
Tourmaline	3.1
Zircon	4.4-4.8

Table 5.2 Minerals identified and their possible provenance **(Anon, 1976; Chari et al., 1975; Desai, 2018; Kelkar, 1959; Gadgil et al., 2019; Gokul et al., 1985; Gujar 1996; Gujar and Shrinivas, 1991; Gujar et al., 2010; Gujar et al., 2021, Gujar et al., 2022; Sahasrabudhe and Deshmukh, 1979; Sarkar and Soman, 1984)**

Mineral	Provenance
Actinolite	Schists and Amphibolites of Dharwar Group and Metabasalt of Vageri Formation
Apatite	Argillites and Metagreywackes of Sanvordem Formation
Epidote	Contact Metamorphic Rocks in Western Ghats and Metabasalt of Vageri Formation
Garnet	Schists of Dharwar Group
Hematite	Laterite exposed on the coast and BHQ of Bicholim Formation
Ilmenite	Deccan Trap Basalt
Magnetite	Laterite exposed on the coast, Deccan Trap Basalt and BMQ of Bicholim Formation
Pyrite	Argillites and Metagreywackes of Sanvordem Formation and Pyritiferous Carbonaceous Shale of Bicholim Formation
Rutile	Granites/Gneisses exposed in Sawantwadi, Sindhudurg
Sillimanite	Quartzites of Dharwar Group
Staurolite	Schists of Dharwar Group
Tourmaline	Granite and Pegmatite of Dharwar Group
Zircon	Quartzite and Pegmatite of Dharwar Group

CONCLUSION

CHAPTER 6: CONCLUSION

The study of heavy minerals from the beach sands of Keri, Goa, located on the west coast of India reveals that:

i. The dominant sand type in the study area is medium sand (500µm-250µm).

ii. The backshore samples have a higher concentration of fine sand and a lower concentration of coarse sand as compared to the foreshore samples.

iii. The backshore sediments have a higher concentration of heavy minerals as compared to the foreshore sediments.

iv. The highest concentration of heavy minerals (46.198%) is seen in the backshore sample (S6) of Location C while the lowest concentration (6.2024%) is seen in the sample collected from the sand spit (S1) at Location A.

v. The heavy mineral suite consists of actinolite, apatite, epidote, garnet, hematite, ilmenite, magnetite, pyrite, rutile, sillimanite, staurolite, tourmaline, and zircon.

vi. The minerals have originated from a mixed source i.e. from igneous, metamorphic, and sedimentary rocks. Actinolite, epidote, garnet, hematite, ilmenite, magnetite, pyrite, rutile, sillimanite, staurolite, tourmaline and zircon are brought in by the river while Apatite on the other hand is transported from the south via the longshore current. Hematite and Magnetite can also be in situ originating from the laterite outcrops present along the coast.

Since the study was carried out during the pre-monsoon period, the concentration of heavy minerals reported is comparatively less. It is believed that their concentration will be higher in the monsoon and post-monsoon periods and is therefore a promising site in Goa for sustainable exploitation in future.

REFERENCES

1. Ali, M. A., Krishnan, S., & Banerjee, D. C. (2001). Beach and inland heavy mineral sand investigations and deposits in India-an overview. Exploration and Research for atomic Minerals, 13, 1-21.
2. Anon. (1976) Geology of the Ratnagiri district,Maharashtra. Geol. Surv. India 125th Anniv. Publ., 1–8.
3. Chari, G. N., Marwar, S. A., Bobade, G. P., Kulkarni, G. A. and Bhagwatkar, D. A. (1975) Ilmenite, geology and mineral resources of Maharashtra. Directorate of Geology and Mining Government of Maharashtra, Nagpur, 341p.
4. Chavadi, V. C., & Nayak, G. N. (1990). Distribution of heavy minerals and provenance sediments in the beaches around Karwar, west coast of India.
5. Dessai, A. G. (2011). The geology of Goa Group: revisited. Journal of the Geological Society of India, 78(3), 233. https://doi.org/10.1007/s12594-011-0083-7.
6. Dessai, A. G. (2018). Geology and mineral resources of Goa. New Delhi publishers.
7. Dinesh, A. C., Shareef, N. M., Baraik, S., & Prasad, D. (2015). Occurrence of heavy minerals in coastal sediment of Daman-Dandi, Gujarat. Ind J Geosci, 69, 323-330.
8. Emery, K. O., & Noakes, L. C. (1968). Economic placer deposits of the continental shelf. Technical Bull. Economic Comission for Asia and Far East, UN, 1, 95-110.

9. Folk, R. L. (1968) Petrology of sedimentary rocks. Hemphill's, Austin, Texas, 182p.
10. Gadgil, R., Viegas, A., & Iyer, S. D. (2019). Structure and emplacement of the Coastal Deccan tholeiitic dyke swarm in Goa, on the western Indian rifted margin. Bulletin of Volcanology, 81(6), 1–19. https://doi.org/10.1007/s00445-019- 1297-6.
11. Gandhi, M. S., Gayathri, G. S., Panicker, M. V., & Paul, S. S. Sediment Properties and Provenance Study of Heavy Minerals Along Chinnavilai and Erayumanthurai Beach, South West Coast of India.
12. Ghosal, S., Agrahari, S., & Sengupta, D. (2022). Provenance studies on the heavy mineral placers along the coastal deposits of Odisha, eastern India. Journal of Palaeogeography, 11(2), 275-285.
13. Gokul, A. R., Srinivasan, M. D., Gopal Krishnan, K., & Vishwanathan (1985). Stratigraphy and structure of Goa. In Earth resources of Goa's development, Hyderabad (pp. 1–13). Geological Survey of India.
14. Gujar, A. R. and Srinivas, K. (1991) Contributions from coastal laterites to the nearshore placers of central west coast of India.Giorn. Geol., 53, 65–70.
15. Gujar, A. R. (1996) Heavy mineral placers in the nearshore areas of South Konkan Maharashtra: their nature of distribution, origin and economic evaluation. Unpubl. PhD Thesis, Tamil University, Thanjavur, 234p.
16. Gujar, A. R. (2007). Heavy mineral placers.
17. Gujar, A. R., Ambre, N. V., & Mislankar, P. G. (2007). Onshore heavy mineral placers of south Maharashtra, central west coast of India.

18. Gujar, A. R., Ambre, N. V., Mislankar, P. G., & Iyer, S. D. (2010). Ilmenite, magnetite and chromite beach placers from South Maharashtra, central west coast of India. Resource Geology, 60(1), 71-86.
19. Gujar, A. R., Ambre, N. V., Iyer, S. D., Mislankar, P. G., & Loveson, V. J. (2010). Placer chromite along south Maharashtra, central west coast of India. Current Science, 492-499.
20. Gujar, A. R., Iyer, S. D., Udayaganesan, P., Ambre, N. V., Mislankar, P. G., & Dhinesh, S. (2021). Nature, characterization and resource potential of littoral placer deposits of Goa, central west coast of India. Journal of Sedimentary Environments, 6(3), 359-380.
21. Gujar, A. R., Iyer, S. D., Prabhu, G. A., Mislankar, P. G., & Ambre, N. V. (2022). Multi-mineral potential of littoral placers of Sindhudurg District, Maharashtra, West coast of India. Environmental Earth Sciences, 81(5), 161.
22. Hegde, V. S., Shalini, G., & Kanchanagouri, D. G. (2006). Provenance of heavy minerals with special reference to ilmenite of the Honnavar beach, central west coast of India. Current Science (00113891), 91(5).
23. Kamble D. T., Gupta S. K. and Rai, R. P. (1987). Preliminary appraisal of different minerals inSindhudurg district, GSI Unpublished progressreport for FSP 1986-87.
24. Kelkar, K. V. (1959). On some Archean rocks in southern part of Ratnagiri district. J. Univ. Pune, 10, 85–101.
25. Komar, P. D. (1977). Beach processes and sedimentation.
26. Mitchell, W. A. (1975). Heavy minerals. In Soil Components: Vol. 2: Inorganic Components (pp. 449-480). Berlin, Heidelberg: Springer Berlin Heidelberg.

27. Morton, A.C. (1978). Heavy minerals. In: Sedimentology. Encyclopedia of Earth Science. Springer, Berlin, Heidelberg.
28. Müller, G. (1967). Methods in sedimentary petrology. Stuttgart E. Schwezerbartische Verlagsbuchandlung. pp. 233.
29. Nallusamy, B., Babu, S., & Suresh Babu, D. S. (2013). Heavy mineral distribution and characterisation of ilmenite of Kayamkulam—thothapally Barrier Island, southwest coast of India. Journal of the Geological Society of India, 81, 129-140.
30. Nayak, G. N. (1993). Beaches of Karwar: morphology, texture and mineralogy. Rajhauns Vitaran, Panajji.
31. Nayak, G. N. (1997). Grain size parameters and heavy minerals as indicators of depositional environment: A case study of beach sediments from Goa.
32. Nayak, B. (2011). Gold in the beach placer sands of Chavakkad-Ponnani, Kerala coast, India. Journal of the Geological Society of india, 78, 345-348.
33. Nayak, B., Mohanty, S., & Bhattacharyya, P. (2012). Heavy minerals and the characters of ilmenite in the beach placer sands of Chavakkad-Ponnani, Kerala Coast, India. Journal of the Geological Society of India, 79, 259-266.
34. Pradhan, A. (2016). State of India's rivers. For India Rivers week, Sandrop files. World Press.com, p. 23.
35. Reddy, K. S. N., Deva Varma, D., Dhanamjaya Rao, E. N., Veeranarayana, B., & Lakshmi Prasad, T. (2012). Distribution of heavy minerals in Nizampatnam-Lankavanidibba coastal sands, Andhra Pradesh, east coast of India. Journal of the Geological Society of India, 79, 411-418.

36. Sahasrabudhe, Y. S. and Deshmukh, S. S. (1979) The laterites of the Maharashtra State. Proc. Int. Seminar on Lateritization Processes, Oxford-IBH, New Delhi, 209–220.

37. Sarkar, P. K. and Soman, G. R. (1984) Heavy mineral assemblage from Konkan. Kaladgi sediments. Proc. Indian Geol. Cong.,Pune, 19–23.

38. Sen B., Jeere D. S., Fatima S., Ahmed S. (2012) Report on Specialized Thematic Mapping in Precambrian terrain in parts of Sindhudurg District, Maharashtra. Geological Survey of India.

39. Swaminath, J., Ramakrishnan, M. (Eds.), 1981. Early Precambrian supracrustals of southern Karnataka. Geological Survey of India, Memoir 112, 350.

40. Wentworth, C. K. (1922). A scale of grade and class terms for clastic sediments. The journal of geology, 30(5), 377-392.

41. https://chem.libretexts.org/Bookshelves/Inorganic_Chemistry/Map:_Inorganic_Chemistry_(Housecroft)/14:_The_Group_14_Elements/14.04:_Allotropes_of_Carbon/14.4A:_Graphite_and_Diamond_-_Structure_and_Properties

Accessed on 08th February, 2024.

42. https://www.gsi.gov.in/webcenter/portal/OCBIS

Accessed on 19th April, 2024.

43. https://mausam.imd.gov.in/

Accessed on 1st June, 2023.

44. http://prism.mit.edu/xray

Accessed on 1st February, 2024.

45. https://rruff.info/

Accessed on 18th January, 2024.

46. https://rruff.geo.arizona.edu/AMS/amcsd.php

Accessed on 9th April, 2024.

47. https://webmineral.com/

Accessed on 28th February, 2024.

48. https://www.mindat.org/

Accessed on 28th February, 2024.